MHD POWER GENERATION

RESEARCH, DEVELOPMENT AND ENGINEERING

Quarterly Progress Report
October to December 1977

The Montana Energy and MHD Research and Development Institute, Inc.

Post Office Box 3809
Butte, Montana 59701

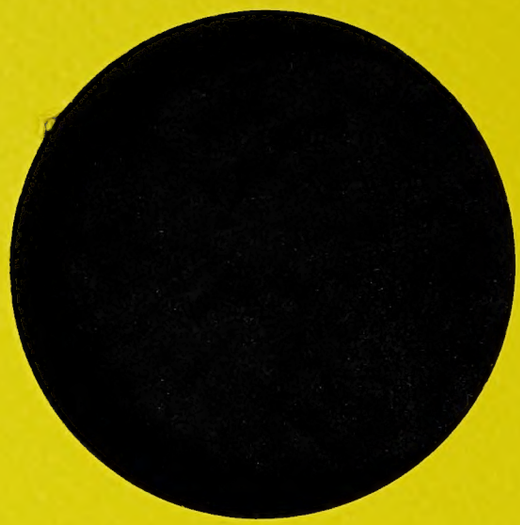

MHD
POWER GENERATION

RESEARCH, DEVELOPMENT AND ENGINEERING

Quarterly Progress Report
October to December 1977

THE MONTANA ENERGY AND
RESEARCH AND DEVELOPMENT INSTITUTE, INC.
P. O. Box 3809
Butte, Montana 59701

PREPARED FOR THE UNITED STATES
ENERGY RESEARCH AND DEVELOPMENT ADMINISTRATION

Under Contract No. E(49-18)-1811

TABLE OF CONTENTS

REPORT INTRODUCTION

During the fall of 1974, a major portion of Montana's scientific community formed a task force to initiate and aggressively pursue a broad-based program of research, development, and engineering in the field of open-cycle magnetohydrodynamics (MHD). This effort was based on the firm belief that MHD technology, although still early in its development and not fully proven as a practical generator of electric power, is the only non-nuclear, central station electric power generation technology with significant potential for greatly improved fuel efficiency and direct operation with coal. MHD also offers lower environmental impact and a reduced pollution signature. Associated with this high efficiency is the reduced consumption of water--a factor of importance to the semi-arid western regions.

This task force was incorporated into the Montana Energy and MHD Research and Development Institute (MERDI). MERDI is a not-for-profit Montana corporation with performing team members drawn from in-house staff and the research faculties of the Montana College of Mineral Science and Technology (MCMST) in Butte and the Montana State University (MSU) in Bozeman.

With the able and generously provided assistance and advice of the MHD research and development staff of the Avco Everett Research Laboratory in Everett, Massachusetts, MERDI researchers formulated a broad-scope research proposal to address the key technical problems currently recognized for MHD technology at both fundamental and practical levels. The Institute prepared a complete, unsolicited proposal that included a section on the design and construction of major MHD experimental facilities (Combustion Test Facilities, Engineering Test Facility). In November 1974, this proposal was submitted to the U.S. Energy Research and Development Administration (ERDA), now the Department of Energy.

Following an intensive and critical review of the proposal, ERDA awarded MERDI a contract in March 1975 for a portion of the MHD supporting science and technology tasks submitted in the original proposal. Work was divided among researchers at the performing elements (MCMST and MSU) on the basis of primary specialization and expertise. MCMST was assigned tasks relating to coal fuel supply, characterization, preparation, and handling--as well as MHD materials engineering. MSU tasks are related to science, heat transfer and mechanical engineering, and chemical and chemical engineering aspects of MHD technology. MERDI assumed responsibility for overall program management, environmental impact assessment of MHD facilities, and site selection studies of future MHD central station power plants.

Current Status

This report summarizes the work accomplished from October to December, 1977. While much of the material has been reported previously in monthly progress reports, this writing provides the opportunity to consolidate all results for each task and thus provide better insight into the work being

performed.

MERDI is continuing to increase its activities relating to the design and construction of DOE's MHD CDIF (the Component Development and Integration Facility). A summary of this work is presented in a separate volume of this report entitled "Engineering Management."

The basic contract (No. EF-77-C-01-2524) was extended to March 31, 1978. The original schedule called for a definitization target date of February 1, 1978. Indications reveal that this target date will not be met.

MERDI has been informed that contract EF-77-C-01-2524 will be extended for an additional six months, April 1, 1978 to September 30, 1978. The request for a proposal for this extension has not been received from the Department of Energy procurement division.

Characterization of Coal for Open-Cycle MHD Power Generation System

F. Diebold

ABSTRACT

X-ray fluorescence method development work for sulfur has been directed toward establishing a procedure utilizing the acid-bomb aqueous solutions. The current effort is to elucidate those parameters essential to generate a precipitate of $BaSO_4$ free of interfering cations from the acid-bomb solutions. Additionally, an effort has been initiated to identify the possible presence of gaseous sulfur compounds being lost from the O_2 combustion bomb.

The cold vapor atomic absorption spectrometric procedure for Hg in the coal samples which utilizes the acid-bomb solutions has been established. This procedure has been shown to be accurate, to exhibit a minimum precision of ± 6 percent relative standard deviation, and to exhibit sufficient sensitivity for the Rosebud coal samples. Examination of 15 Rosebud coal samples has revealed a range of 0.130 to 0.1933 ppm Hg.

The combustion train procedure, utilizing an automated Perkin Elmer 240 elemental analyzer, has been established for determining the O_2 content of the coal samples directly. This procedure is exhibited to be accurate and to have a precision of ± 6 percent relative standard deviation for the coal samples. All of the Dietz No. 2 and Rosebud seam channel samples have been analyzed for their O_2 content.

The photographic emission spectrographic procedure, utilizing the acid-bomb solutions, has been established for the major and selected trace metals. An intensive study has identified the contributions of each step to the overall precision and the selection of 15 mg of a densely packed matrix consisting of 2:1 graphite to Li_2CO_3, the Cahn microbalance for weighing the matrix, the predrying of the matrix, an arc gap of 4mm, an arc amperage of 8.1 amps, and a CO_2 pressure of 1.0 kg/cm^2 with a shield hole size of 5mm diameter.

I. OBJECTIVE AND SCOPE OF WORK

The primary objective of this program is the detailed characterization of typical Fort Union region coal to assess its applicability to and performance in direct, coal-fired MHD electrical generation systems. Accomplishment of this objective requires the selection of specific coal seams for study and development. It also necessitates a progressive sampling technique that permits three-dimensional chemical mapping of the seam as well as the development of suitable sample preparation and sample analysis

techniques. Resultant data will be compared and correlated with information obtained from a literature search and the mining companies. The goal is to provide the MHD process designer with the most comprehensive fuel engineering information available. The coal properties to be determined are as follows:

1) Btu, percent moisture, volatile matter, fixed carbon, ash, and S, H, C, O, N, Cl, and F content.

2) Major inorganic constituents of the coal ash: Al, Ca, Fe, K, Mg Na, Si, and Ti.

3) Trace elements of the coal ash: Ag, As, B, Ba, Be, Cd, Co, Cr, Cs, Cu, Ga, Hg, La, Li, Mn, Ni, P, Pb, Rb, Sb, Se, Sn, Sr, U, V, Zn, and Zr.

A secondary project objective involves a careful examination of potential environmental problems caused by the inorganic constituents of the coal. Special consideration will be given to the effects that each inorganic element has on air, soil, and water problems. This study will be coordinated closely with the work of the MHD environmental engineer as well as federal and state officials. It also will include a review of pertinent literature.

The analytical data generated by this work will be of immediate use in the interpretation of corrosion studies involving MHD preheater materials and experiments on coal drying. Coal properties certainly will affect the drying mechanics of western coals. Therefore, it will be important to ascertain the magnitude of coal property changes, such as Btu content, caused by drying and grinding. The data from the corrosion study of preheater materials eventually must be interpreted in terms of the actual Eastern Montana coal properties having the greatest potential for use in MHD power generation.

II. SUMMARY OF PROGRESS TO DATE

The following subtasks were undertaken during the period of October 1, 1977 to January 1, 1978:

Analytical Method Development
- Sulfur Method Development
- Atomic Absorption Method Development for Hg
- Oxygen Method Development
- Emission Spectrographic Solution Method Development

Coal Properties
- Generation of O_2 and Hg Content on Selected Fort Union Formation Coals

The development of an appropriate X-ray fluorescence procedure for sulfur has been directed toward an investigation of a sample preparation technique

capable of removing interferents. Currently, this work is involved with establishing criteria for the selective precipitation of $BaSO_4$ from the acid-bomb solutions. Additionally, studies have been initiated to identify the possible loss of gaseous sulfur from the O_2 bombs.

The establishment of the atomic absorption procedure for the analysis of Hg by a cold vapor technique utilizing acid-bomb solutions essentially is complete. The precision has been shown to be ±6 percent or ±10 percent (relative standard deviation) depending on the dilution factor. The accuracy has been checked and found to be well within the experimental precision of the accepted value. The storage of acid-bomb solutions has been shown to be free of Hg loss within one day and to exhibit relatively greater stability when stored in glass vessels instead of plastic. Hg concentrations have been determined in 15 selective Rosebud coal samples, and no concentration trends were indicated.

The investigation of the combustion-train procedure for directly determining the oxygen content of the coal samples has shown the procedure to be accurate and to exhibit a precision of approximately ±4 percent and ±6 percent (relative standard deviation), respectively, for acetanilide and coal. The O_2 concentration of all the Dietz No. 2 and Rosebud channel coal samples has been determined with the PE 240 combustion-train procedure.

The work on establishing the photographic emmission spectrographic procedure for major and trace metal analysis in acid-bomb solutions has been directed toward an intensive precision study and the selection of appropriate excitation conditions. The precision study has involved the elucidation of the contribution of the steps of matrix concentration, choice of balance, and matrix drying technique. Additional studies have identified the appropriate arc gap, amperage, CO_2 flow, and shield configuration.

III. DETAILED DESCRIPTION OF TECHNICAL PROGRESS

A. Sulfur Method Development

1. Work Accomplished

The current effort has been directed toward establishing a sample preparation technique that will remove the interferents in the X-ray fluorescence procedure. The procedure investigated utilizes acid solutions generated by the dissolution of coal samples in teflon digestion bombs. This study is still in progress and consists of experimentally investigating the parameters required for the selective precipitation of barium sulfate. The parameters being investigated are the pH, type of base, and volume of solution. The resulting precipitate, $BaSO_4$, is investigated via photographic emission spectrography.

2. Discussion

As noted in the October 1977 annual report to DOE, we have observed interferents in the X-ray fluorescence analysis of whole coal samples. These were illustrated to be the chemical combination of sulfur. Other investigators also have observed this interference effect as well as interference from other elements such as Fe and Ca (Kuhn, et al., 166th National American Chemical Society Meeting, August 1973; Berman and Ergun, United States Bureau of Mines Report Investigation 7124, 1968).

Based on these experiences, we have decided to investigate a sample preparation procedure that will result in only one chemical form of sulfur (i.e., sulfate) and the effective removal of the chemical interferents. An additional consideration is the efficiency of the total scheme for the analysis of the coal samples (i.e., the utilization of the same sample preparation technique for as many analytical procedures as possible). Thus, it appeared appropriate to investigate the parameters for the precipitation of BaO_4 from the aqueous solutions generated by the acid dissolution of the coal samples in teflon-lined bombs.

B. Atomic Absorption Method Development for Hg

1. Work Accomplished

The effort to establish the cold vapor atomic absorption (AA) spectrometric procedure for Hg utilizing the acid-bomb coal solutions has been directed toward determining the precision, accuracy, and storage time. The experimental precision of ±6 percent and +10 percent (relative standard deviation) was based on a Rosebud coal sample that had experienced dilution factors of 90:1 and 60:1, respectively. Fifteen samples of the National Bureau of Standards (NBS) 1632 coal sample were analyzed. The average of 0.114 ± 0.013 ppm compares well with the NBS certified value of 0.12 ± 0.02 ppm.

In addition, five aqueous solutions, which were generated by the acid dissolution of a Rosebud coal sample in teflon-lined bombs, were used for a study to ascertain the effect of storage time upon the Hg concentration. Two aliquots of each acid-bomb solution were diluted to different amounts, 100 ml and 10 ml. The 100 ml-dilution set of solutions was stored in Pyrex volumetric flasks, and the 10 ml-dilution set was stored in snap-cap plastic vials. The averages of each five solutions for each set per day are reported in Table 1.

2. Discussion

The cold vapor AA technique for Hg consists of reducing the Hg^{+2} ion in the acid-bomb solution to elemental mercury with stannous chloride; the Hg is swept into a quart window absorption cell placed in the optical path of a Hg hollow cathode lamp. This technique, as

noted above, is sufficiently precise and accurate and apparently is sufficiently sensitive for the Rosebud coal samples analyzed to date (see Table 3). The calibration curve illustrates a break in slope; thus, two linear concentration ranges are obtained between 0 and 10 ppb. In addition, our experience has been that the signal generated without background correction is significantly higher; thus, all data are generated with background correction.

The data in Table 1 indicates that the average Hg concentrations are beginning to decrease within a 24-hour period. In addition, the average Hg concentration is slightly lower in the solutions stored in the plastic vessels. Although some of these differences in concentration (time and vessel) are within one standard deviation, the data appears to indicate that the samples should be analyzed the same day as the acid-bomb solutions are generated and that the solutions be stored in the Pyrex volumetric flasks.

C. Oxygen Method Development

1. Work Accomplished

A method for directly determining the oxygen content of the coal was established. The procedure utilizes a Perkin Elmer Model 240 elemental analyzer equipped with an O_2 analyzer kit. The sample is pyrolyzed at 975°C under helium, which has been passed over platinized carbon. The oxygen in the coal sample is released as carbon monoxide in the gas stream, which is passed over elemental copper at 900°C and through a colorcarb scrubber. The thermal conductivity of the gas stream then is compared before and after scrubbing of the resulting carbon dioxide.

Twelve different NBS acetanilide (No. 1416) samples, twelve benzoic acid primary standard samples, and twelve samples of an eastern Montana coal (air-dryed) were analyzed for their O_2 content to ascertain the experimental precision. Table 2 illustrates these precision data.

2. Discussion

The automated procedure exhibits a sufficient precision and apparent accuracy for discerning differences within and between Fort Union formation coal seams (see Tables 4 and 5). Some electronic and mechanical problems have occured occasionally with the PE 240 elemental analyzer; this has contributed to some disappointment with the anticipated speed of C-H-N-O analysis with this instrumental procedure. The larger precision of the coal sample indicates an approximate ±2 percent due to sample inhomogeneity. It should be noted that this same approximate value was observed during the C-H-N method development. Although we were able to reproduce the accepted values for the acetanilide and benzoic acid standards, it is our opinion that

the coal sample preparation (i.e., the ASTM air drying step) requires further study with respect to its effect on not only the O_2 but also the C-H and N content of the coal.

D. Photographic Emission Spectrographic Metal Method Development

1. Work Accomplished

The work initiated during the last quarter on establishing the photographic emission spectrographic method for metals in the acid-bomb aqueous solutions has been continued. The recent work has been directed toward elucidating the contribution of various matrix concentrations, choice of balance, and various matrix drying techniques upon the overall analytical precision.

The matrix concentration experiments were conducted by varying the ratio of graphite: to Li_2CO_3 and the density of the packing of the matrix data generated is too voluminous to present here. It will suffice to note that the intensity ratios and intensities of the analytical lines and background were tabulated for each of these experimental parameters. The effects of the Roller-Smith torsion balance and the Cahn micro-balance used to measure the mass of the matrix was ascertained from a number of appropriate experiments. In order to determine the effect of the drying mode, experiments were conducted in which the matrix was either dried or not dried prior to being loaded into the electrodes.

In addition to these precision studies, experiments have been conducted to determine the appropriate excitation conditions. These experiments were designed to determine the effects of varying the arc gap, the arc amperage, the magnitude of CO_2 flow, and the shield hole size. The precision of the element: background intensity ratios, "burnability" of the sample, and burn time were recorded for each individual variation of these parameters.

2. Discussion

The intensity ratio data generated by the matrix concentration experiments indicate that better precision, sensitivity, and lower background intensity are associated with increasing concentration of graphite in the matrix. This effect continues until CN band intensity becomes excessive. The density of the packing of the matrix does not appear to affect the precision, sensitivity, and background levels significantly, but the good correlation of element intensities with that of lithium makes high density packing of the matrix preferable. In addition, the good correlation of element intensities with matrix in the high density matrix packing is also desirable. Thus, the best set of matrix conditions are 15 mg of high densely packed 2:1 ratio of graphite to lithium carbonate.

The data generated from the balance experiments indicate that the precisions associated with the Roller-Smith and the Cahn balances are not observed appreciably in the overall analytical precision of the intensity ratios. Due to the ease of achieving and maintaining calibration, the Cahn microbalance is preferred. Finally, the data generated from the drying experiments indicates that the overall precision can be improved significantly by drying the matrix at 95°C for one hour prior to putting it in the electrodes.

The experimental data generated by individually varying the arc gap, the arc amperage, CO_2 flow, and shield hole size results in the following interpretation. The variation in arc gap appears to have little effect on the precision of the intensity ratios. For the reasons of burn symmetry, good Li precision, and lower arc flickering, the 4mm arc gap is preferred. The amperage is observed to affect the precision of the intensity ratios significantly and seems to affect the background intensity more than that of the line intensity. At this arc gap, the minimum overall precision in the intensity ratios is obtained at 8.1 amps arc current. It has been observed that the most appropriate CO_2 pressure is a function of the size of the hole in the alumina arc shield. Both of these parameters appear to have a significant effect on the detection limits and precision. The optimum conditions are a 5mm diameter hole in the shield and a 1.0 kg/cm^2 CO_2 pressure.

These studies described herein and conducted during the previous quarter essentially have exhausted the possible experimental conditions that have to be optimized for the photographic E.S. analysis of the acid-bomb solutions. The only remaining step is the use of the densitometer, and this study will be delayed until this solution procedure is adapted to the ARL densitometer.

E. Characterization of Fort Union Formation Coal

1. Work Accomplished

The Hg concentration of 15 selective Rosebud seam channel samples has been determined and is presented in Table 3. In addition, the O_2 concentration of all of the Dietz No. 2 seam and Rosebud seam channel samples were determined. These data are presented in Tables 4 and 5.

2. Discussion

The Hg concentrations are plotted (Figure 1) as a function of the position in the Rosebud coal seam. Although there are only a few data points, there does not appear to be any observable vertical or horizontal concentration trend.

Table 6 illustrates the horizontal average of the C-H-N-O concentrations for each depth within the Dietz No. 2 and the Rosebud coal seams, and it is difficult to discern any concentration trends. The discrepancy of the sum of the ash, C, H, N, and O from the mass of the coal sample could be explained by the moisture content. The correct interpretation

of the problems associated with this summation is not possible at this time because we do not know the moisture content of the air-dried sample and the effect of the technique of ASTM air-drying upon the hydrogen concentration and the summation noted in Table 6.

IV. CONCLUSIONS

The results to date in establishing a reliable total sulfur method that coordinates well with the other analytical procedures we are setting up have been somewhat disappointing. The initial results with the O_2-bomb sample preparation, which would coordinate well with the Btu determination procedure, appeared to indicate a loss of sulfur. To substantiate this observation, we are proceeding with a detailed examination of the bomb-vent gases. The X-ray fluorescence procedure utilizing whole coal, although promising due to the limited sample preparation, has been observed to be accompanied with numerous interferences. It is our opinion that if we can remove these interferents by precipitating a sulfate from the acid-bomb solutions, the X-ray fluorescence procedure will coordinate well with this acid-bomb sample preparation technique used for emission and absorption analysis of the metals.

It is our conclusion that the cold vapor AA method for Hg in the coal samples is a valid procedure and coordinates well with the acid-bomb sample preparation technique. We intend to continue this effort for As and Se utilizing the same acid-bomb solutions.

The automated combustion-train procedures for C-H-N-O essentially are established in our laboratory. The mechanical and electrical problems with the rebuilt PE 240 probably will be solved gradually, and it is apparent that the small sample size does not create a serious sampling error. The issue that still must be resolved is the elucidation of the effect the ASTM air-drying procedure has upon these C-H-N-O and other results.

It is our opinion that the procedure for trace metal analysis via the photographic emission spectrograph utilizing the acid-bomb solutions has been pushed to its limit of precision and sensitivity. The remaining area of investigation will be to apply this solution technique to the old ARL E.S. quantometer, which will serve to reduce the analysis time. But due to a large number of trace elements still not being detected by either spectrograph, it is most imperative that the plasma-source spectrograph be purchased.

TABLE 1
Storage Time and Vessel Study

Elapsed Time (Hrs)	100 ml Set		10 ml Set	
	Avg. Values	% Remaining	Avg. Values	% Remaining
0	.122 ± .010	100.0	.118 ± .008	100.0
24	.116 ± .005	95.1	.114 ± .005	96.6
48	.110 ± .007	90.2	.108 ± .008	91.5
72	.098 ± .008	80.3	.094 ± .009	80.5

TABLE 2
Accuracy and Precision of O_2 Procedure

	Acetanilide	Benzoic Acid	Coal Sample
Mean % O_2	11.84	26.6	17.28
Standard Deviation	± 0.53	± 0.62 (±2.3%)	± 1.0 (±6.0%)
Accepted Value	11.84	26.20	

TABLE 3
Hg Concentration in Rosebud Coal Seam

Sample No.	Concentration (ppb)
1-E	.130
-D	.143
-C	.128
-B	.153
-A	.116
6-E	.180
-D	.193
-C	.180
-B	.178
-A	.170
11-E	.158
-D	.173
-C	.113
-B	.148
-A	.133

TABLE 4
O_2 Concentration in Dietz No. 2 Coal Seam
(Trip I)

Sample	% Oxygen	Sample	% Oxygen	Sample	% Oxygen
1 A	20.02	1 B	19.88	1 C	21.13
2 A	19.19	2 B	20.16	2 C	19.60
3 A	19.87	3 B	20.10	3 C	19.90
4 A	19.82	4 B	19.81	4 C	20.02
5 A	19.80	5 B	19.61	5 C	17.68
6 A	23.37	6 B	19.54	6 C	19.16
7 A	19.20	7 B	19.64	7 C	18.90
8 A	19.99	8 B	19.64	8 C	19.23
AVG.	20.16	AVG.	19.80	AVG.	19.45

Sample	% Oxygen	Sample	% Oxygen
1 D	19.06	1 E	18.62
2 D	17.09	2 E	18.86
3 D	18.41	3 E	18.61
4 D	19.89	4 E	18.21
5 D	19.62	5 E	19.73
6 D	19.05	6 E	19.88
7 D	19.28	7 E	17.19
8 D	18.40	8 E	16.76
AVG.	18.85	AVG.	18.48

(Trip II)

Sample	% Oxygen	Sample	% Oxygen	Sample	% Oxygen
1 A	19.30	1 B	19.82	1 C	19.43
2 A	19.78	2 B	18.92	2 C	20.40
3 A	18.50	3 B	18.92	3 C	19.98
4 A	18.60	4 B	18.38	4 C	21.36
5 A	20.41	5 B	19.47	5 C	19.35
6 A	19.02	6 B	19.23	6 C	20.78
7 A	18.99	7 B	20.81	7 C	20.60
8 A	18.53	8 B	20.70	8 C	19.75
9 A	18.83	9 B	19.47	9 C	20.09
AVG.	19.11	AVG.	19.52	AVG.	20.19

TABLE 4
(Trip II)
Cont.

Sample	% Oxygen	Sample	% Oxygen
1 D	20.55	1 E	19.55
2 D	20.73	2 E	19.20
3 D	19.63	3 E	19.86
4 D	19.83	4 E	20.37
5 D	20.62	5 E	20.49
6 D	20.52	6 E	19.52
7 D	19.75	7 E	19.68
8 D	19.71	8 E	19.75
9 D	19.73	9 E	20.33
AVG.	20.12	AVG.	19.86

TABLE 5
O_2 Concentration in Rosebud Coal Seam

Sample	% Oxygen	Sample	% Oxygen	Sample	% Oxygen
1 A	18.01	1 B	18.46	1 C	18.11
2 A	18.39	2 B	18.24	2 C	17.75
3 A	17.96	3 B	17.60	3 C	10.66
4 A	19.17	4 B	17.95	4 C	17.21
5 A	18.99	5 B	19.54	5 C	18.80
6 A	19.52	6 B	18.09	6 C	18.22
7 A	17.61	7 B	17.84	7 C	17.86
8 A	18.50	8 B	17.80	8 C	19.34
9 A	22.19	9 B	18.00	9 C	17.95
10 A	18.23	10 B	17.80	10 C	16.27
11 A	21.41	11 B	18.02	11 C	17.64
AVG.	19.09	AVG.	18.12	AVG.	17.26

Sample	% Oxygen	Sample	% Oxygen
1 D	18.13	1 E	17.00
2 D	18.14	2 E	17.42
3 D	18.16	3 E	17.25
4 D	17.40	4 E	17.08
5 D	18.01	5 E	16.69
6 D	17.54	6 E	18.14
7 D	17.82	7 E	18.36
8 D	17.48	8 E	17.47
9 D	17.84	9 E	17.54
10 D	17.79	10 E	16.12
11 D	17.02	11 E	16.68

TABLE 6
C-H-N-O Concentration Averages

Dietz No. 2 Coal Seam (Trip I)

AVG.	Ash	C	H	O	N	TOTAL
Sample A	8.87	57.53	4.50	20.16	1.65	92.71
Sample B	5.65	56.54	4.02	19.80	1.65	87.66
Sample C	6.88	58.25	3.83	19.45	1.64	90.05
Sample D	6.11	55.89	3.90	18.85	1.52	86.27
Sample E	5.00	57.26	3.99	18.48	1.52	86.05

TOTAL AVG. 88.55

Dietz No. 2 Coal Seam (Trip II)

AVG.	Ash	C	H	O	N	TOTAL
Sample A	10.53	51.29	4.23	19.11	1.39	86.55
Sample B	7.43	51.58	4.22	19.52	1.37	84.12
Sample C	6.76	57.28	4.17	20.19	1.50	89.90
Sample D	6.09	60.73	4.73	20.12	1.38	93.05
Sample E	6.54	52.57	4.48	19.86	1.40	84.85

TOTAL AVG. 87.69

Rosebud Coal Seam

AVG.	Ash	C	H	O	N	TOTAL
Sample A	11.68	54.92	4.14	19.09	.89	90.82
Sample B	9.34	55.37	3.17	18.12	.84	86.84
Sample C	12.59	53.09	3.55	17.26	.83	87.32
Sample D	11.13	58.98	4.12	17.76	.78	92.77
Sample E	12.76	57.79	3.68	17.25	.82	92.30

TOTAL AVG. 89.99

Figure 1. Mg Concentration in Rosebud Coal Seam

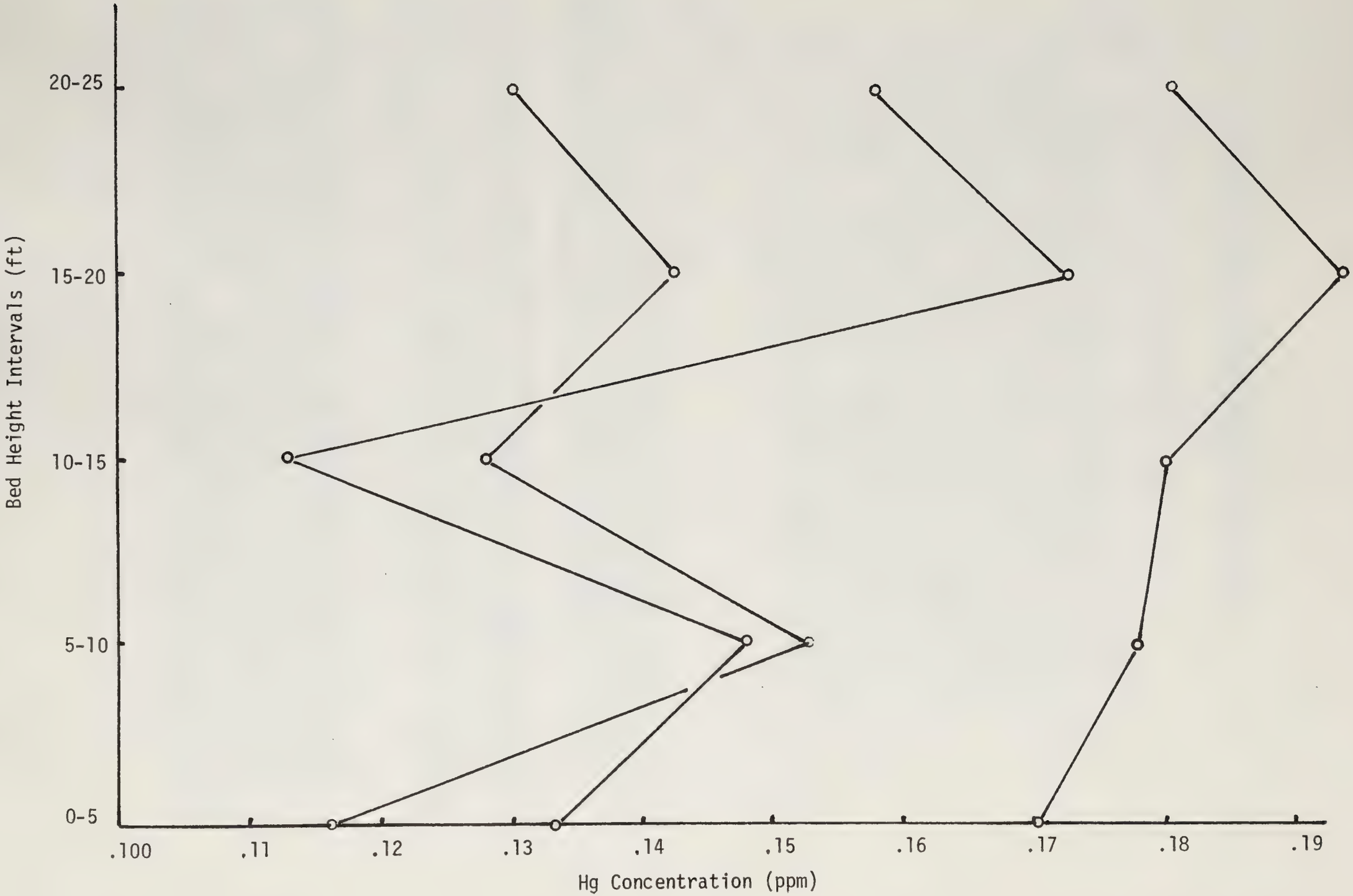

Corrosion Studies of MHD Preheater Materials

W. Callister

ABSTRACT

Slag and slag-seed corrosion tests have continued on a number of different refractory ceramic materials at elevated temperatures in order to investigate the corrosion behavior and mechanisms. The influence of several experimental parameters has been examined using the dipping corrosion test. Tests have been conducted using both air and simulated combustion atmospheres on alumina, spinel, and chrome-spinel materials; in all cases, corrosion was less in the combustion atmosphere. The presence of K_2SO_4 seed can either increase or decrease corrosion depending on the material and seed concentration. Corrosion is accelerated with increasing temperature, and this enhancement depends on the material. Alteration of the slag composition by corrosion products decreases the corrosiveness of the slag. Slag corrosion mechanisms should be investigated by using dipping, rotating rod, and rotating disc techniques at both room and elevated temperatures.

I. OBJECTIVE AND SCOPE OF WORK

The primary objective of this task is to characterize the behavior of potential MHD preheater materials under the following conditions: a) in gaseous atmospheres simulating the MHD preheater environment, b) at elevated temperatures to 3100°F (1700°C), c) for exposure periods up to 500 hours, and d) while being exposed to a slag that contains potassium.

Experimental systems will be constructed to permit dynamic or static corrosion tests at temperatures up to 3100°F and for periods of time up to 500 hours. The design will include the capability of passing the desired gas mixture into the furnace chamber containing the slag-immersed sample. Gaseous environments will include air and a simulated combustion atmosphere whose composition will be in accord with NBS computations for air combustion of seeded coal.

Synthetic slags and seed-slags will be prepared. Initial tests will begin with a simple four-component slag to provide very basic engineering data. Further tests will employ more complex systems to include the addition of a potassium seed. These compositions will be representative of slags resulting from the combustion of typical coals found in the United States. The slag compositions appearing in the preheater region may be quite different than the starting coal slag. Therefore, synthetic slags will be prepared to duplicate compositions of condensed products resulting from the combustion of coal at the University of Tennessee Space Institute's MHD combustion facility.

During corrosion tests, the slag will be sampled periodically to determine compositional changes (especially in potassium content) and changes by the dissolution of refractory constituents.

The candidate materials to be tested will be high purity, single crystal, or dense polycrystalline materials to include Al_2O_3 and MgO. Prior to exposure, sample materials will be characterized with respect to chemical composition, microstructure, density, and open porosity.

After the high temperature exposure to the slag, the refractory samples will be recovered and dimensional changes recorded. Metallographic and microprobe investigations will be made so that corrosion mechanisms may be ascertained.

This quarter's efforts have been devoted to the following: 1) finding a reliable method of making chemical analyses on pre- and post-corrosion slags; 2) performing corrosion tests on a variety of refractory materials in order to examine the influence of ambient atmosphere, temperature, seed, dipping rate, and slag composition alteration on corrosion behavior; 3) looking into the possibility of examining fluid-mechanical parameters in the slag and their influence on corrosion; and 4) ordering components and equipment for the creep apparatus.

II. SUMMARY OF PROGRESS TO DATE

Slag and slag-seed corrosion tests have continued on a variety of refractory ceramic materials using the reciprocating dipping test. Tests have been made in the simulated combustion atmosphere, and corrosion results can be compared with ones made in air. The influence of other experimental parameters on corrosion include seed concentration, alteration of slag composition by corrosion products, temperature, and rate of dipping.

A technique has been developed to chemically analyze slag and slag-seed compositions, which should produce reliable and reproducible results. It is being compared with analyses made by other laboratories.

Materials characterization has continued with respect to microstructural examination. The effort has centered around the characterization of new materials and of materials which have experienced corrosion.

Because of recommendations made by the review team which visited recently, we have redirected our corrosion effort slightly: first, to look into the mechanisms and modes of corrosion in the molten slag-seeds with respect to fluid-dynamic phenomena; and second, to attempt to make some correlation between our laboratory corrosion tests and those in FluiDyne's simulated preheater.

Because of funding uncertainties, we only recently have begun ordering equipment with which to conduct the creep-corrosion tests.

A renewal proposal has been prepared for a 30-month period beginning April 1978.

III. DETAILED DESCRIPTION OF TECHNICAL PROGRESS

A. Work Accomplished

Work has continued in trying to find a reliable and reproducible technique for making chemical analyses on both pre- and post-corroded slags and slag-seeds. It is felt that such a technique has been found, and slag specimens have been sent to the other facilities capable of making analyses so that reliability of these tests may be ascertained.

Corrosion tests have continued on materials which fall into several general classifications: 1) single crystals, including alumina, magnesia, and magnesia-alumina spinel; 2) a fully dense and polycrystalline alumina; 3) materials which are high purity and contain very little porosity, including two different aluminas, magnesia, two magnesia-alumina spinels, and mullite; and 4) materials which are commercially available from refractory companies, most of which are polyphase, and contain spinel, corundum, periclase, and/or chromia phases.

A survey has begun on the influence of the various experimental parameters on the corrosion behavior of some of these materials. Tests have been conducted to determine the influence of both air and the simulated combustion atmosphere on the corrosion of several materials, as well as seed (K_2SO_4) concentration, dipping rate, temperature, and the alteration of slag composition by corrosion products.

Microstructural investigations have continued on both pristine and corroded specimens. The polishing technique which is used in preparing specimens for examination has been refined. We presently are in the process of developing methods to thermally etch some of our polycrystalline and dense specimens. Our SEM with X-ray dispersive optics is now operational, and we are working with it to develop some facility for microstructural examinations.

The ordering of equipment and supplies to be used for the creep study has commenced.

B. Discussion

All corrosion tests this past quarter were performed using the dipping test in which the ½-inch diameter cyclindrical specimen is translated vertically into and out of the slag bath. Only one type of slag has been used: the synthetic four-component slag (which composition is representative of a Montana Rosebud coal).

During this quarter, corrosion runs were commenced in the simulated combustion atmosphere which contains a mixture of N_2, CO_2, and H_2O gases. Data has been collected for sapphire, dense and polycrystalline alumina, single crystal and polycrystalline spinel, and a commercial chrome-spinel material (the material which is designated as material A and characterized in a previous report[1]). This data is reported in Table I and was taken at 1550°C and a dipping rate of 25 cycles per minute. Both time and slag-seed

compositions were variable for these materials, as is noted in the table.

In all cases, the volume percent corrosion was less in the combustion atmosphere than in air. This difference was rather dramatic for the commercial chrome-spinel material, in both seeded and unseeded slags.

As noted in previous reports, there can be an influence of seed concentration on the corrosion behavior of refractory materials. Table II presents corrosion data for several different materials in both unseeded and seeded slags which illustrate this effect. For fully dense and polycrystalline alumina, it appears that the presence of K_2SO_4 can either increase or decrease the corrosion. At 1500°C in air after 16 hours, the corrosion in unseeded slag is 52.1 volume percent while for slag and 15 percent K_2SO_4, it is 66.1 volume percent. On the other hand, after an 8-hour corrosion exposure in air at 1550°C, the respective volume percent corrosion values in unseeded slag and slag with 30 percent K_2SO_4 added are 57.8 and 53.8. Another high purity alumina material which is not fully dense experienced a rather dramatic corrosion increase after adding 15 percent K_2SO_4--34.4 versus 50.0 volume percent corrosion.

Two commercial materals also were tested, a chrome-spinel (previously designated as material A) and a chrome-alumina (or material B); both were corroded at 1550°C in air for 24 hours and in both an unseeded and a 15 percent K_2SO_4 slag-seed. The chrome spinel corroded slightly less in the slag-seed, whereas the chrome alumina corroded slightly more.

A mullite material which is of reasonably high purity and close to being theoretically dense also was examined. Its corrosion decreased slightly when 15 percent K_2SO_4 was added at 1550°C and after a four-hour exposure.

The influence of temperature on the corrosion behavior of several materials is being investigated, while other experimental variables are being held constant. Tests have been made between 1500°C and 1600°C on polycrystalline but not fully dense spinel and alumina, and also on a commercial magnesia-chrome, which has been previously designated as Material D. These results are presented in Figure 1 as the logarithm of a corrosion rate versus the reciprocal of the absolute temperature. The corrosion rate is the volume percent corrosion divided by the time of the test. Since the testing time was different for each material, comparisions of the corrosion behavior of these materials cannot be made. As expected, the amount or rate of corrosion increases with increasing temperature in all cases, and it appears that the spinel increases the greatest amount. For the polycrystalline alumina and in the unseeded slag, tests at both 1550°C and 1600°C were made for two different corrosion times, four and six hours. There appears to be a slight difference in temperature dependence for these two times.

We investigated how alteration of the slag composition by corrosion products influenced the corrosion rate of mullite and an alumina material.

The tests were performed by immersing a pristine sample in a slag, removing the sample, and then corroding another pristine sample of the same material in this slag which then was altered in composition by corrosion products from the first specimen. This procedure was repeated three more times using the same slag each time and a new pristine sample and then comparing the volume percent corrosion of each specimen. The data is tabulated in Table III for both the alumina and the mullite; it may be noted that in both cases the volume percent corrosion decreases as the slag became more contaminated.

A final experimental parameter which was investigsted is the influence of dipping rate on the rate of corrosion. A series of tests was performed on an alumina material for 6 hours at 1550°C in an unseeded slag at rates of 3, 25, and 100 cycles per minute; the resultant data is presented in Table IV. There appears to be, perhaps, a slight corrosion decrease in going from 3 to 25 cpm; but in going from 25 to 100 cpm, there is a dramatic increase in volume percent corrosion. Apparently, over some ranges of dipping rate, there can be a substantial corrosion enhancement by an increase in rate.

It has been observed that a heat treatment of specimens prior to corrosion can have an influence on the corrosion behavior. Corrosion tests were made on several mullite samples for 4 hours in unseeded slag at 1550°C in air. One test was made on a pristine, as-received sample, while two other tests were performed on the same starting material which had been heat treated at 1550°C for 24 and 48 hours in just air. The pristine material experienced approximately 57 volume percent corrosion, while the other specimens corroded 70 and 73.2 percent, respectively, after the 24- and 48-hour anneals. Apparently, the pre-corrosion heat treatment makes this material more susceptible to corrosion. As a consequence, we are annealing some specimen materials and then performing a microstructural examination in order to determine what, if any, microstructural changes occur due to the annealing.

It has been necessary to purchase the dense and polycrystalline alumina specimens from another supplier. Therefore, we felt it was necessary to compare the corrosion behavior and microstructure of these materials from the two different sources. A comparison of the corrosion data is in Table V for two different times and seed concentrations and 1550°C in air. In one case, the amount of corrosion is about 10 percent lower in the new material; in the other, it is about 5 percent higher. We are in the process of comparing grain sizes and compositions of the two materials to see if either might have an influence on the difference in corrosion behavior. We feel that the discrepancies are beyond just experimental uncertainties.

The Department of Energy review team, which visited in November 1977, made several recommendations for this task. One specific recommendation was that we conscientiously pursue our investigation into fluid mechanical aspects of the slag corrosion mechanisms. Consultation was made with

Dr. Harry Townes of the Department of Mechanical Engineering at Montana State University, who is involved with the MHD slag flow, air preheater facility there. The following presents the assessment, after this consultation, of what kinds of corrosion tests can and should be used to uncover the mechanisms of corrosion, what information can be gleaned from the tests, and the advantages and disadvantages of each.

Our current tests employ the dipping rod technique. The advantages include 1) a high degree of reproducibility of the corrosion data; 2) rotating-rod corrosion tests produce exaggerated corrosion at the slag-air interface, and the dipping tests permit extension of this interface over a region of the dipped specimen; 3) simulation of slag replenishing on actual MHD preheater refractory surfaces; and 4) control of slag layer thickness by the rate of withdrawal of the specimen from the slag bath. The main disadvantage of this technique is that it is possible that the dominant corrosion mechanism may be different in the actual preheater environment. For example, electrochemical and/or surface effects may be more pronounced in our tests than in the actual preheater.

Initial corrosion tests were the rotating rod type exclusively. Results were disappointing due to the lack of reproducibility, both with respect to corrosion rates and the general shape of the corroded specimen. However, tests of this type have been used widely in corrosion investigations; and this test is more applicable to the study of the effects of shear forces and fluid velocity profiles on corrosion-erosion mechanisms.

The disadvantages of the rotating-rod test are as follows: 1) this test may not reproduce the corrosion mechanism that would be seen in the preheater; 2) fluid mechanical parameters cannot be solved analytically without substantial effort by a super-fluidynamic specialist; and 3) shear flows are altered very easily by small changes in specimen geometry and specimen rotation (e.g., eccentric rotation) and physical properties of the slag such as viscosity.

One test commonly used in dissolution measurements is the rotating disc method in which dissolution is measured across a rotating face. There are several advantages to this technique: 1) fluid flow patterns have been solved exactly within certain experimental constraints; 2) requirements of sample volume are minimized; and 3) diffusion coefficients of dissolution (the rate at which a sample corrodes) have been measured using well-characterized slags. The disadvantages include 1) our test geometry (specimen and crucible sizes) may preclude direct use of existing mathematical solutions; 2) tests are short-term, probably less than an hour's duration (because of tests being conducted at elevated temperatures, the exact corrosion time at temperature may be difficult to determine); 3) MHD slags and slag-seeds are not characterized well enough to directly measure diffusion coefficients; and 4) commercial materials may not be conducive to tests by this method because of surface roughness effects which may not be possible to totally eliminate.

Corrosion testing should be directed toward experiments which replicate the type of corrosion which would be experienced in an acutal preheater environment. Unfortunately, preheater environmental parameters are lacking at present. Therefore, we feel that it is the responsibility of this task to provide a variety of tests and data from which scaling factors for actual refractory preheater corrosion may be determined.

We currently are designing room temperature tests to conveniently study various corrosion parameters. These will be fluid media which have physical properties at room temperature which are the same as the slags at elevated termperatures.

For the dipping test, two distinct and different tests will be utilized. The first will be to map the fluid flow at the sample-air-fluid interface. The second will use ionically and non-ionically bonded samples in both polar and non-polar solutions. The corrosion mechanism at elevated temperatures will be inferred from the specimen shapes resulting from these room temperature tests.

The reasons for utilizing the rotating rod tests at room temperature are as follows: 1) to empirically solve fluidynamic parameters; 2) to decide which experimental and geometrical parameters can be varied with utilization of solutions of the first reason; and 3) as with the dipping test, to relate room and elevated temperature corrosion mechanisms.

For rotating disc tests at room temperature, we want to determine if the existing analytical solutions can be applied to high temperature rotating disc tests in slags. If utilization is possible, they will be used. Furthermore, room temperature tests will indicate the degree of corrosion which may be tolerated before the rotating disc model breaks down. This will allow us to determine maximum corrosion times for high temperature tests.

Continued effort will be devoted to relating our tests to the actual preheater environment. This will be accomplished by the correlation of results with both Montana State University and FluiDyne Corporation, both of whom are conducting tests in prototype MHD preheaters. This will be carried out to provide corrosion scaling factors for all three of these test types (ours, MSU's, and FluiDyne's) on a variety of refractory materials.

C. Work Forecast

During the ensuing quarter, corrosion studies will continue on single crystals, polycrystalline, and commercial materials at elevated temperatures in order to explore the influence of the various experimental parameters on the corrosion behavior. Tests to be conducted at room temperature (as outlined in this report) will be designed and initiated.

Examination of the microstructure of both pristine and corroded materials will continue in an effort to discover the corrosion processes in the refractory itself.

The ordering of components and equipment for the creep study will continue, and the assembly of this system will commence.

IV. CONCLUSIONS

The following have been concluded from this quarter's work:

1) For alumina, magnesia-alumina spinel, and chrome-spinel materials, the amount of corrosion is less in the simulated combustion atmosphere than in air. The difference is significant for the commercial chrome-spinel.

2) It appears that the presence of K_2SO_4 seed in the slag can either increase or decrease the corrosion, depending on material and the seed concentration.

3) Increasing the temperature increases the amount of corrosion of several materials. The degree of corrosion increase with temperature is different for various materials.

4) Alteration of slag composition with corrosion products decreases the corrosiveness of the slag for mullite and alumina materials.

5) It appears that increasing the rate of dipping produces an increase in the amount of corrosion.

6) Slag corrosion mechanisms can be investigated by performing several types of tests (dipping, rotating rod, and rotating disc) at elevated temperatures. Tests also should be performed at room temperature using solutions which replicate the properties of the slag at high temperatures and also sample materials which are soluble in these solutions.

TABLE I

Tabulation of Volume Percent Corrosion in Both Air and Simulated Combustion Atmosphere for Several Materials; the Test Temperature was 1550°C, and Dipping Rate was 25 Cycles Per Minute.

Material	K_2SO_4 Content (Wt.%)	Time (Hrs)	Volume % Corrosion	
			Air	Combustion Atmosphere
Sapphire	0	4	27.8	25.4
Dense, Polycrystal Alumina	15	6	54.1	46.7
Single Crystal Spinel	15	6	61.3	41.6
Polycrystal Spinel	0	4	49.0	33.6
Chrome-Spinel (Material A)	0	48	14.2	8.1
Chrome-Spinel (Material A)	15	24	8.7	0

TABLE II
Tabulation of Volume Percent Corrosion in Unseeded and Seeded Slags for Various Refractory Materials; the Dipping Rate for the Tests Was 25 Cycles Per Minute

Material	T(°C)	Time (Hrs)	Volume Percent Corrosion	
			Unseeded	Slag + 15% K_2SO_4
Dense Alumina	1500	16	52.1	66.1
Dense Alumina	1500	8	57.8	53.8*
Alumina	1550	6	34.4	50.0
Chrome Spinel (A)	1550	24	10.7	8.7
Chrome Alumina (B)	1550	24	31.3	34.7
Mullite	1550	4	56.8	53.6

*Slag + 30% K_2SO_4

TABLE III

Tabulation of Data for Polycrystalline and Nearly Dense Mullite and Alumina Showing the Influence on Corrosion of Corrosion Products. Tests were made in Unseeded Slag, in air, at 1550°C, and at a dipping rate of 25 cpm.

MATERIAL	Slag Corrosion Time Prior to Test (HRS)	Slag Corrosion Time Prior to Test (HRS)	Slag Corrosion Time Prior to Test (HRS)	Slag Corrosion Time Prior to Test (HRS)
	Volume Percent Corrosion	Volume Percent Corrosion	Volume Percent Corrosion	Volume Percent Corrosion
MULLITE	0	4	8	12
	57.6	50.0	42.0	33.1
ALUMINA	0	6	12	18
	32.2	25.4	22.5	19.9

TABLE IV
Tabulation of Dipping Rate and Volume Percent Corrosion Data For a Polycrystalline Alumina, at 1550°C, for 6 Hours, and in an Unseeded Slag.

Dipping Rate (cpm)	Volume Percent Corrosion
3	37.2
25	34.4
100	71.4

TABLE V
A Comparison of the Corrosion Behavior of a Fully Dense and Polycrystalline Alumina from Two Different Manufacturers. Tests Were Conducted in Air, at 1550°C, and at a Dipping Rate of 25 cpm.

Corrosion Time (HR)	K_2SO_4 Conc. (Wt.%)	Volume Percent Corrosion	
		Original Material	Latest Material
8	0	57.8	52.1
6	15	51.1	54.1

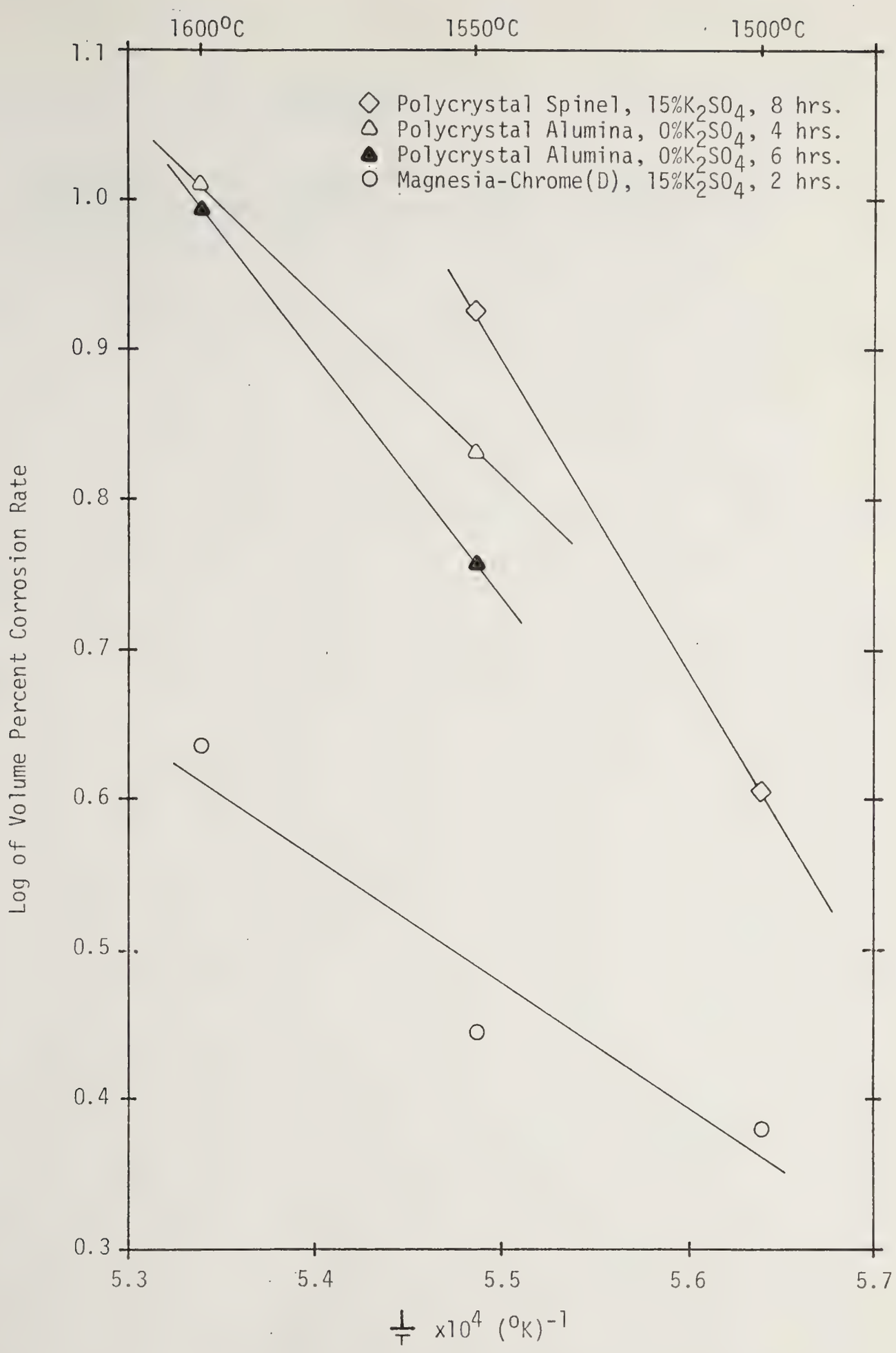

Figure 1. Plot of the logarithm of the volume percent corrosion rate versus the reciprocal of the absolute temperature for polycrystalline spinel and alumina, and for a commercial magnesia-Chrome, in air and at a dipping rate of 25 cpm.

REFERENCE

1. Annual Report, MHD Power Generation Research, Development and Engineering, Montana Energy and MHD Research and Development Institute, October 1977

Preparation of Coals for Utilization in Direct Coal-Fired MHD Generation

G. Ziesing

ABSTRACT

During this contract period, we completed a test program aimed at characterizing the fluidization properties of Rosebud coal in a 6-inch column at ambient temperature. This work has demonstrated the relationship between coal particle size, fluidization velocity, bed porosity, and a fraction factor to be of the form

$$f_F = \frac{C}{\varepsilon^n N_{Re}} ,$$

where C and n are constants, f_F is a fluidization friction factor, and N_{Re} is a particle Reynolds number. This result shows that fluidization of Rosebud coal occurs as a result of viscous drag forces, and that turbulence is not a predominant mechanism in bed support.

The assembly of the small-scale continuous drying system is still in progress. The major pieces of equipment are expected to be erected by the end of January. A full-time project engineer has been hired to coordinate this phase of the task.

I. OBJECTIVE AND SCOPE OF WORK

During the contract period April 1, 1975 to September 30, 1976, five thermal drying methods were examined at vendor facilities for demoisturizing Rosebud (Colstrip, Montana) coal to various moisture levels. Analysis of the collected vendor data indicated that nearly 83 percent of the total energy required to prepare Rosebud coal for MHD combustion is consumed in drying the coal from 25 to 5 percent moisture and that only 5.5 percent is consumed in pulverizing the coal from 3 inches x 0 to 0.003 inches x 0. If drying energy is to be supplied by heating the drying gas, it is quite immaterial whether the coal is dried first and then pulverized, pulverized first and then dried, or dried and pulverized simultaneously. However, if drying energy is to be supplied by sensible heat of waste gases, as proposed for large-scale MHD power generation, then the order in which the coal is prepared may become important because in this situation, grinding energy assumes a major operating cost. The energy to pulverize Rosebud (Colstrip, Montana) coal was found to decrease with decreasing coal moisture content based on standard Hardgroove grindability tests and vendor tests in a 10-inch roller mill. Therefore, to economize on operating costs, it appears advisable to dry the coal prior to pulverization when recycling waste heat, preferably by crushing the coal to minus 0.1-inch, drying the coal in a fluidized bed dryer, and then pulverizing the coal to final combustion size.

Fluidization was found to be a viable process for drying Rosebud coal to low moisture levels. Although vendor tests demonstrated the feasibility of the drying method, the tests did not shed much light on the behavior of Rosebud coal in the fluidized state, on the influence of processing variables, or on the heat and mass transfer phenomenon associated with the drying process. To obtain engineering data of this nature, the contractor has initiated a program to construct a small-scale continuous fluidized-bed dryer of and associated equipment capable of handling up to several hundred pounds of coal per hour and from which experimental drying data can be collected to predict drying performance over a range of operating conditions. The experiments will measure drying rates, the equilibria between the dried coal moisture content and the off-gas humidity, heat and mass transfer coefficients, and entrainment losses for variable drying conditions and will include the effect of coal feed rate, inlet drying temperature, inlet drying gas humidity, drying gas mass flow rate, and coal particle size on these parameters. A benefit of operating the drying system in steady-state is that personnel of Task D will be able to sample the dryer off-gases for analysis of organic volatiles which are lost during demoisturization of Rosebud coal. Analysis of the data will lead to a better understanding of the mechanism of drying the coal to low moisture levels and the interrelationships among the operating and design variables in achieving various coal moisture levels.

II. SUMMARY OF PROGRESS TO DATE

A test program has been completed in which five size fractions of Rosebud coal have been examined in a 6-inch fluidization column using orifice plates of 3, 5, 7, and 9 percent open area. The experimental fluidization data have been correlated using a friction factor, bed porosity, and a particle Reynolds number. Prediction of fluidization behavior is satisfactory.

Progress on assembly of the small-scale continuous fluidization drying system has not been as rapid as expected due to in-house problems related to modification of a working area for the system.

Identification of mass spectra data of organic volatile matter (Dr. Beuerman) obtained during the previous quarter continued.

III. DETAILED DESCRIPTION OF TECHNICAL PROGRESS

A. Batch Fluidization Studies

1. Work Accomplished

During the past nine months, we operated a six-inch plastic fluidization column in an attempt to arrive at some quantitative means of characterizing the fluidization of Rosebud coal. We have conducted this work at ambient temperature on fractions of coal

ranging in size from 6x8 mesh to 20x28 mesh using orifice plates varying in open area from 3 to 9 percent. This range of open areas corresponds to values reported in the literature for commercial coal dryers.

The fluidization tests are carried out in the apparatus shown in Figure 1. A variable-speed fan delivers air to the fluidization column through a capillary tube calming section. A calibrated orifice-plate flow meter serves to meter the flow of air. Prior to data collection, a sample of coal is fluidized in the column for 60 minutes to attain constant weight. This conditioning period lowers the moisture content of the coal from 20 percent to 7 to 12 percent, depending on the particle size. The coal also experiences size reduction during the conditioning period. After moisture and particle size equilibria are attained, the air flow is reduced slowly to zero to allow the coal to form a packed bed. The height of the static bed is recorded. Air flow is resumed then, and pressure drop measurements are taken at various points in the column. This procedure is repeated using a higher air flow rate until 8 to 10 sets of data have been collected. A typical set of data for five sizes of coal are summarized in Table 1 for an orifice plate of 5 percent open area.

Columns 1 through 4 list the superficial velocity (i.e., the air flow velocity in the empty column), pressure drop across the bed, unit pressure drop across 1 inch of the bed adjacent to the orifice plate, and bed height, respectively. Columns 5 through 8 list the mass velocity, the particle Reynolds number, the calculated bed porosity (or voidage), and the bed expansion ratio. Data similar to those in Table 1 have been collected for nine other orifice plates.

2. Discussion

A fluidization curve depicts the relationship between the pressure drop across a bed of particulate solids and the flow velocity. Generally, the pressure drop is correlated with the particle Reynolds number defined as

$$N_{Re} = \frac{\rho_f V_s D_p}{\mu} \qquad (1)$$

where ρ_f = fluid density, lb/ft^3
V_s = superficial velocity, ft/sc
μ = fluid viscosity, lb/ft-sec
D_p = particle size, ft.

In our tests, D_p is the geometric mean diameter of the coal fraction determined after completion of the fluidization test.

The fluidization curve appears as shown below on log-log coordinates.

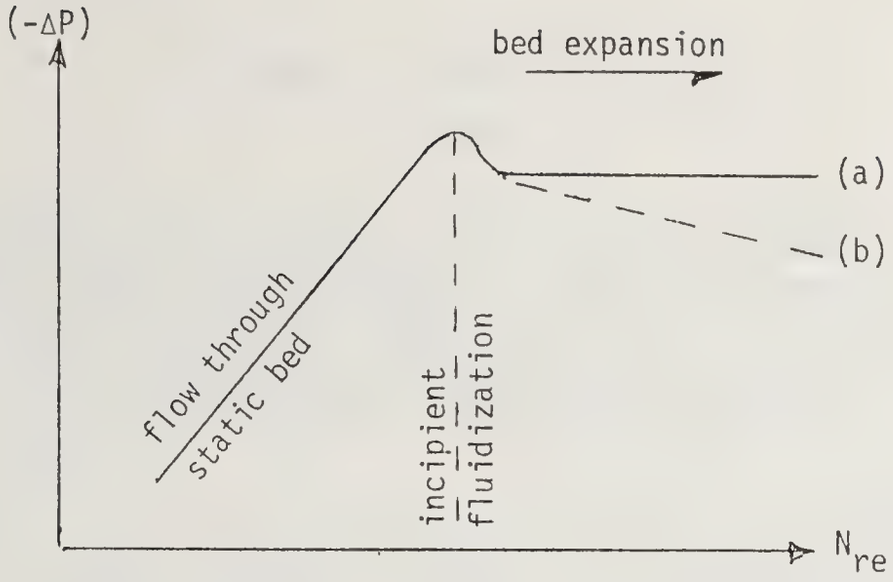

The inclined portion of the curve represents flow through the packed bed. The slope for this portion of the curve varies from 1 for laminar flow to 2 for turbulent flow. With a slight increase in pressure drop, the bed expands and becomes fully fluidized. Depending on the characteristics of the particles and the distribution of the fluid in the column, the pressure drop across the bed may remain constant with increasing flow, curve a, or the pressure drop may decrease with increasing flow, curve b. For fluidization along curve a, bed expansion increases the bed voidage sufficiently to keep ΔP constant. Curve b is characteristic of excessive bed expansion. The former process, curve a, is termed particulate fluidization, while the latter process is termed aggregative fluidization. Aggregative fluidization is accompanied by spouting and slugging and is a condition caused by the flow of gas bubbles through the solids.

The fluidization curves for the 5 percent open area orifice plate are shown in Figure 2. The curves are similar in appearance except that they are translated either along the x-axis to lower Reynolds number with decreasing particle size or, for a given particle

size, they are translated vertically along the y-axis with increasing bed load (i.e., compare curves a, b, and c for 1.3, 2.5, and 3.8 pounds of coal, respectively). The inclined portion of each curve, representing air flow through the static bed, varies in slope from 2.3 for the coarse size fractions to about 1 for the fine size fractions. Fluidization occurs when the bed pressure drop equals the weight of coal per unit area, i.e., when

$$\Delta P_{Bed} \simeq \frac{g}{9c} \frac{W_{coal}}{A_{bed}} , \ lb_f/ft^2 \qquad (2)$$

and corresponds to the region in the vicinity of the peak in each curve. The calculated bed ΔP's (Equation 2) are listed in Table 1 and shown in Figure 2 as arrows along the y-axis. Comparison between the calculated and measured ΔP's (Table 2) suggest that the ratio of the static bed height to the column diameter markedly affects the equivalence of the two pressure drops. The data indicate that coincidence of the two pressure drops occurs when the static bed height exceeds 1.5 times the column diameter.

Table 2 also summarizes the flow conditions at incipient fluidization. When the incipient superficial velocity is plotted against Reynolds number in Figure 3, a linear relationship is obtained on log-log coordinates, indicating that the minimum fluidization velocity is proportional to the mean size (D_p) of the coal particles raised to the 0.43 power, i.e.,

$$V_{s,min} \propto D_p^{0.43} . \qquad (3)$$

As the fluidization velocity is increased past the incipient fluidization point (Figure 2), the bed pressure drop gradually diminishes for all coal size fractions tested. This behavior confirms visual observations that Rosebud coal fluidizes in an aggregative or spouting manner, an effect noted for all orifice plates tested. Because of the spouting nature of the fluid bed, accurate measurement of the expanded bed height was not possible. This is shown in Figure 4, in which the bed expansion ratio (i.e., the ratio of the expanded bed height to the static bed height)--column 8 of Table 1--is plotted against Reynolds number for the 5 coal fractions. It is seen from Figure 4 that above a certain Reynolds number, the plotted points lie above the extrapolated straight line curve. Since most of the points fall on the straight line at low Reynolds number, we assume that the expansion ratio is a linear function of Reynolds number over the entire fluidization curve.

Based on this assumption, we have calculated bed porosities for those points in Figure 4 which depart from the extrapolated curve. These results are reported in column 7 of Table 1.

Following the correlation procedure of Lewis, Gilliland, and Bauer (Industrial and Engineering Chemistry, Vol. 41, No. 6, p. 1104, 1949), we calculated the fluidization friction factor, f_F, defined by

$$f_F = \frac{4gD_p\,(\rho s-\rho f)}{3\,V_s^{\,2}\,\rho f} \qquad (4)$$

where g = 32.2 ft/sec^2
D_p = mean size of the coal fraction, ft
ρs = coal density, lb/ft^3
ρf = air density, lb/ft^3
V_s = superficial velocity, ft/sec

and the particle friction factor, C_D, taken from published curves for spherical particles, both based on the particle Reynolds number defined by equation 1; and we plotted the bed porosity, ε, against the ratio C_D/f_F in Figure 5. The points in Figure 5 are seen to be correlated quite satisfactorily by a straight line with a slope of 0.163, viz.,

$$\varepsilon \propto \left[\frac{C_D}{f_F}\right]^{0.163}$$

or

$$f_F \propto \varepsilon^{-6.16} \quad . \qquad (5)$$

It is important to note that the straight line in Figure 5 extends to a bed porosity of 1 when C_D/f_F equals 1. When the friction factor is multiplied by the bed porosity raised to the 6.16 power and plotted against the particle Reynolds number in Figure 6, most of the data fall along a straight line of negative slope equal to 1. The data points which do not fall along the line correspond to the finer coal fractions, 14x20 and 20x28 mesh, in the vicinity of incipient fluidization and appear anomalous. The curve in Figure 6 may be expressed by

$$f_F = \frac{88}{\varepsilon^{6.16}\,N_{Re}} \qquad (6)$$

which has the form of the particle friction factor Reynolds number correlation for viscous flow. That is, the support of the coal particles in the fluid bed is due to simple viscous drag. Rearranging Equation 6 to

$$V_s = 0.49 \frac{D_p^2 (\rho s - \rho f) \varepsilon^{6.16}}{\mu} \qquad (7)$$

shows that the fluidization velocity is directly proportional to the square of the particle diameter, the particle density, and the bed porosity raised to the 6.16 power and inversely proportional to the fluid viscosity.

The correlations in Figures 5 and 6 make it possible to predict the batch fluidization characteristics of Rosebud coal. For example, given a batch of coal of mean particle size equal to 0.003 feet, a fluidization velocity of 3 ft/sec, and density of 73 lb/ft^3, the calculated Reynolds number is 45. From Equation 4, the friction factor is 17; and from Figure 6, $f_F \varepsilon^{6.16}$ equals 2. Hence, the bed voidage is

$$\varepsilon = \left[\frac{2}{17}\right]^{\frac{1}{6.16}} = 0.704,$$

a value which lies between 0.655 and 10x14 mesh coal (0.0035 ft) and 0.725 for 14x20 mesh (.0025 ft) coal shown in Table 1. In view of the difficulty in making accurate bed porosity measurement, we feel the above correlation satisfactorily describes the behavior of Rosebud coal in a spouting fluid bed.

B. Fluidization Drying

Efforts continued to assemble the small-scale continuous drying system. Some progress has been made in modifying the laboratory area in the basement of the Metallurgy Building to accommodate the equipment and to comply with codes. For example, bids have been received to erect a concrete wall to isolate the drying system from the remainder of the laboratory space. However, since the responsibility for this work lies outside of Task C, we are unable to expedite the contracting of this work.

Mr. Bryce Rhodes has been hired as full-time project engineer. He is a chemical engineer with considerable expertise in process engineering. With his full attention to the coal drying study, we hope to regain momentum in accomplishing our task goals.

C. Organic Volatile Matter

1. Work Accomplished

A study of the mass spectra data from fractions eluting from the gas chromatographic column interface continues.

2. Discussion

The eluting fractions appear to be a mixture of organics and subject to only minor interpretations. The presence of at least two unknown sulfur compounds was noted, and a search of known mass spectra was made to find a comparable spectra. Work also included obtaining the spectra of known compounds that are suspected to be present in the volatile matter. This background is needed before further identification can be established.

Gas chromatographic response factors for a variety of known and suspected volatile components were established. These are necessary to relate the area of the chromatograph with the amount of volatile matter giving the response. This is background material for future use.

D. Work Forecast

1. Batch Fluidization Studies

Analyses similar to those presented in the discussion currently are underway for the other orifice plates and will be completed during the next quarter. We also will examine other correlation methods, such as those suggested by Leva.

2. Fluidization Drying

The major pieces of machinery (i.e., bag house, humidifier, blowers, and piping) are scheduled to be emplaced by the end of January.

3. Organic Volatile Matter

During the next quarter, work will continue on the identification of organic volatile matter.

IV. CONCLUSIONS

Using orifice plates of low open-area (viz., 3 to 9 percent), we found that Rosebud coal fluidizes in an aggregative manner. That is, the coal does not fluidize homogenously, and the bed has the physical appearance of spouting. This characteristic appears to be related to the passage of

the fluidizing gas as large bubbles through the bed. Evaluation of experimental fluidization data suggest that the coal particles are suspended during fluidization by viscous drag forces, a result which is surprising in view of the spouting nature of the bed. The influence of the orifice plate open-area is not known at this time, pending evaluation of the other experimental data sets.

TABLE 1
Batch Fluidization Data for Rosebud Coal in 6-Inch Column
at Ambient Temperature Using a 5 Percent Open Area Orifice Plate

	(1) V_s, ft/sec	(2) ΔP_{Bed}, lb_f/ft^2	(3) ΔP_{unit}, lb_f/ft^2	(4) L, ft	(5) G, lb/ft^2-hr	(6) N_{Re}	(7) ε	(8) le
	1.78	2.44	1.09	0.232	390	52	0.561	1.00
Test 209	2.29	4.41	1.82	0.232	501	67	0.561	1.00
6x8 mesh	2.90	6.18	2.86	0.243	635	85	0.580	1.047
D_p = 0.0058 ft	3.71	6.39	2.49	0.255	812	109	0.600	1.099
ρ_f = 0.0608 lb/ft^3	4.38	6.18	2.49	0.261	959	128	0.610	1.125
μ = 0.04334 lb/ft-hr	4.91	6.23	2.34	0.267	1073	144	0.616	1.151
Wgt = 584.2 gm	5.40	6.18	2.34	0.288	1183	158	0.646	1.241
ΔP_{Bed},calc'd = 7.8 lb_f/ft^2	5.55	5.92	2.18	0.313	1215	163	0.674	1.349
	7.19	5.35	2.23	0.332	1573	211	0.693	1.431
Test 309	0.83	0.99	0.52	0.214	180	20	0.531	1.00
8x10 mesh	1.48	3.74	1.56	0.214	321	37	0.531	1.00
D_p = 0.0050 ft	1.95	6.54	2.65	0.218	422	49	0.540	1.019
ρ_f = 0.0603 lb/ft^3	2.42	7.11	3.12	0.232	526	61	0.568	1.084
μ = 0.0432 lb/ft-hr	3.11	6.49	2.54	0.248	676	78	0.596	1.159
Wgt=593.7 gm	3.67	6.60	2.49	0.258	796	92	0.611	1.206
ΔP_{Bed},calc'd = 7.9 lb_f/ft^2	4.58	6.39	2.33	0.263	995	115	0.619	1.229
	5.21	6.39	2.23	0.288	1131	131	0.652	1.346
Test 409	1.11	3.01	1.40	0.228	246	20	0.549	1.00
10x14 mesh	1.49	5.82	2.80	0.228	330	27	0.549	1.00
D_p = 0.0035 ft	1.87	7.06	2.60	0.248	414	34	0.585	1.088
ρ_f = 0.0616 lb/ft^3	2.30	6.13	2.75	0.275	510	41	0.626	1.206
μ = 0.0431 lb/ft-hr	2.67	6.44	2.54	0.281	592	48	0.634	1.232
Wgt = 570.5 gm	3.09	6.44	2.49	0.298	684	56	0.655	1.307
ΔP_{Bed},calc'd = 7.6 lb_f/ft^2	4.96	5.35	2.08	0.387	1099	89	0.734	1.697
	7.98	5.09	1.92	0.569	1770	143	0.819	2.496

TABLE 1 (Cont.)

	(1)	(2)	(3)	(4)	(5)	(6)	(7)	(8)
	V_s, ft/sec	ΔP_{Bed}, lb_f/ft^2	ΔP_{unit}, lb_f/ft^2	L, ft	G, lb/ft^2-hr	N_{Re}	ε	l_e
Test 901	.757	2.03	0.31	0.417	164	13.4	0.515	1.00
10x14 mesh	1.035	6.96	1.30	0.417	223	18.3	0.515	1.00
D_p = 0.00357 ft	1.30	12.20	2.44	0.417	281	23.0	0.515	1.00
ρ_f = 0.0600 lb/ft^3	1.78	13.81	2.91	0.457	384	31.6	0.558	1.096
μ = 0.0435 lb/ft-hr	2.68	14.49	2.55	0.526	579	47.5	0.616	1.261
Wgt = 1121.3 gm	4.69	13.66	2.39	0.746	1013	83.1	0.729	1.789
ΔP_{Bed}, calc'd = 15.0 lb_f/ft^2	8.14	12.46	1.97	0.959	1758	144	0.789	2.30
Test 509	0.79	3.12	1.45	0.228	172	10.1	0.567	1.00
14x20 mesh	1.50	5.92	2.91	0.230	284	16.6	0.571	1.009
D_p = 0.0025 ft	1.84	6.18	2.70	0.274	400	23.4	0.640	1.202
ρ_f = 0.0606 lb/ft^3	2.20	6.54	2.54	0.295	480	28.0	0.665	1.294
μ = 0.04284 lb/ft-hr	3.04	6.02	2.60	0.359	662	39	0.725	1.575
Wgt = 542.5 gm	4.89	5.71	2.23	0.492	1064	62	0.799	2.158
ΔP_{Bed}, calc'd = 7.3 lb_f/ft^2	6.64	5.14	2.08	0.671	1447	85	0.853	2.943
	7.89	4.31	1.97	0.833	1709	100	0.881	3.659
Test 609	0.82	4.57	1.92	0.228	180	8.4	0.587	1.00
20x28 mesh	1.51	6.08	2.44	0.278	333	15.4	0.661	1.219
D_p = 0.0020 ft	1.94	6.39	2.44	0.323	427	20	0.709	1.417
ρ_f = 0.0612 lb/ft^3	2.30	6.13	2.49	0.361	507	23.5	0.739	1.583
μ = 0.0431 lb/ft-hr	3.77	5.92	2.08	0.498	831	39	0.811	2.184
Wgt = 518.4 gm	5.88	5.19	2.03	0.792	1295	60	0.881	3.474
ΔP_{Bed}, calc'd = 6.9 lb_f/ft^2	6.83	4.21	1.92	0.896	1504	70	0.895	3.93

TABLE 2
Incipient Fluidization Data for 5 Percent Open Area Orifice Plate

Size Fraction	D_p, ft	ΔP, lb_f/ft^2 Calculated	ΔP, lb_f/ft^2 Measured	$\Delta P_{measured}/\Delta P_{calc}$	L_{static}/D_{column}	N_{Re}	V_s ft/sec	1_e	ε
6x8	0.0058	7.8	6.5	0.833	0.464	95	3.2	1.07	0.590
8x10	0.0050	7.9	7.1	0.899	0.428	60	2.4	1.06	0.558
10x14a	0.0035	7.6	7.0	0.921	0.456	31	1.9	1.07	0.578
10x14b	0.0036	15.0	14.5	0.976	0.834	31	1.9	1.07	0.547
10x14c	0.0036	23.1	23.0	0.996	1.27	31	1.9	1.07	0.541
14x20	0.0025	7.3	6.4	0.877	0.456	21	1.65	1.09	0.603
20x28	0.0020	6.9	6.4	0.928	0.456	14	1.4	1.05	0.607

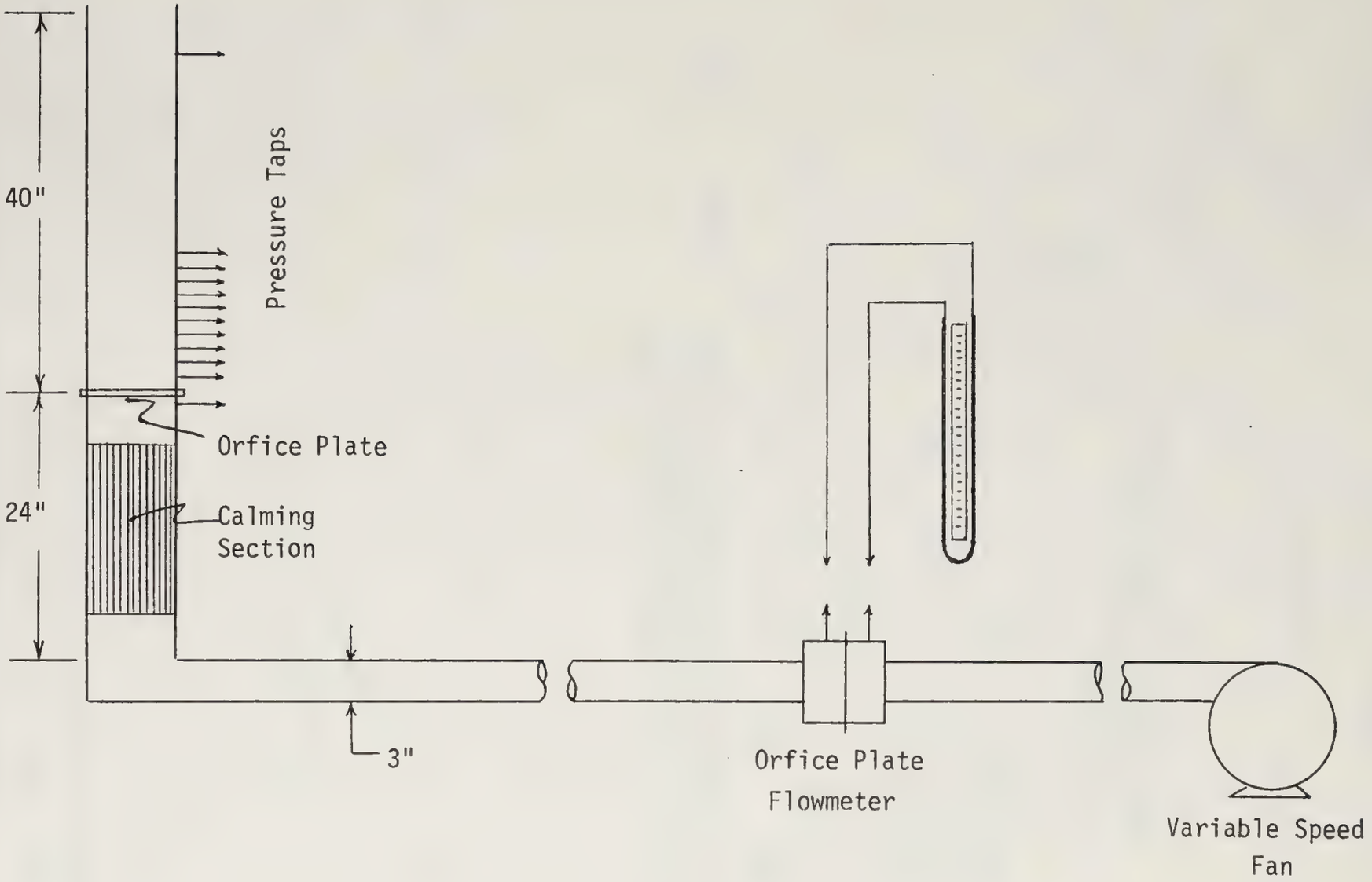

Figure 1. 6-inch batch fluidization column.

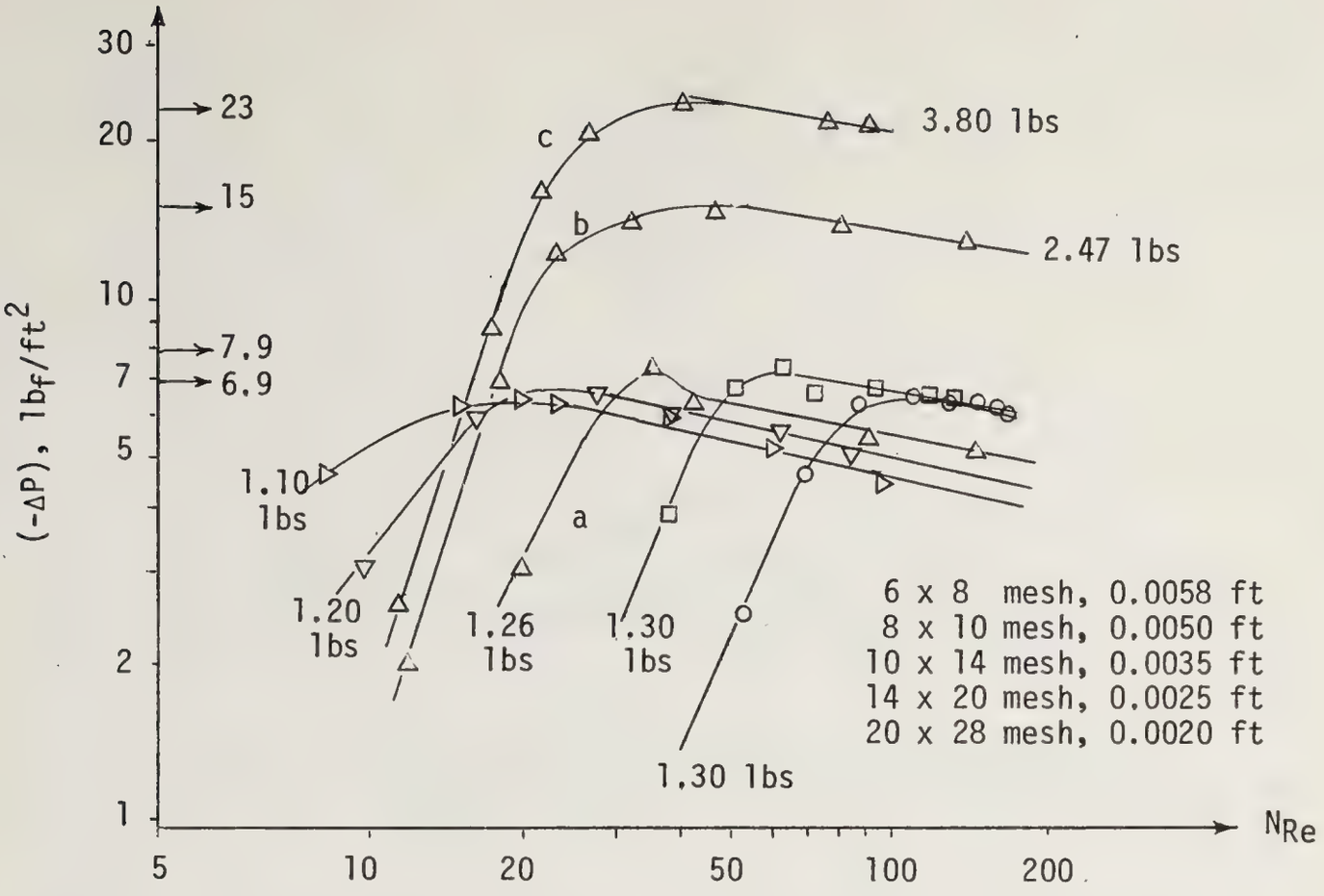

Figure 2. Batch fluidization curves for Rosebud coal in a 6-inch column at room temperature with a 5 percent open area orifice plate.

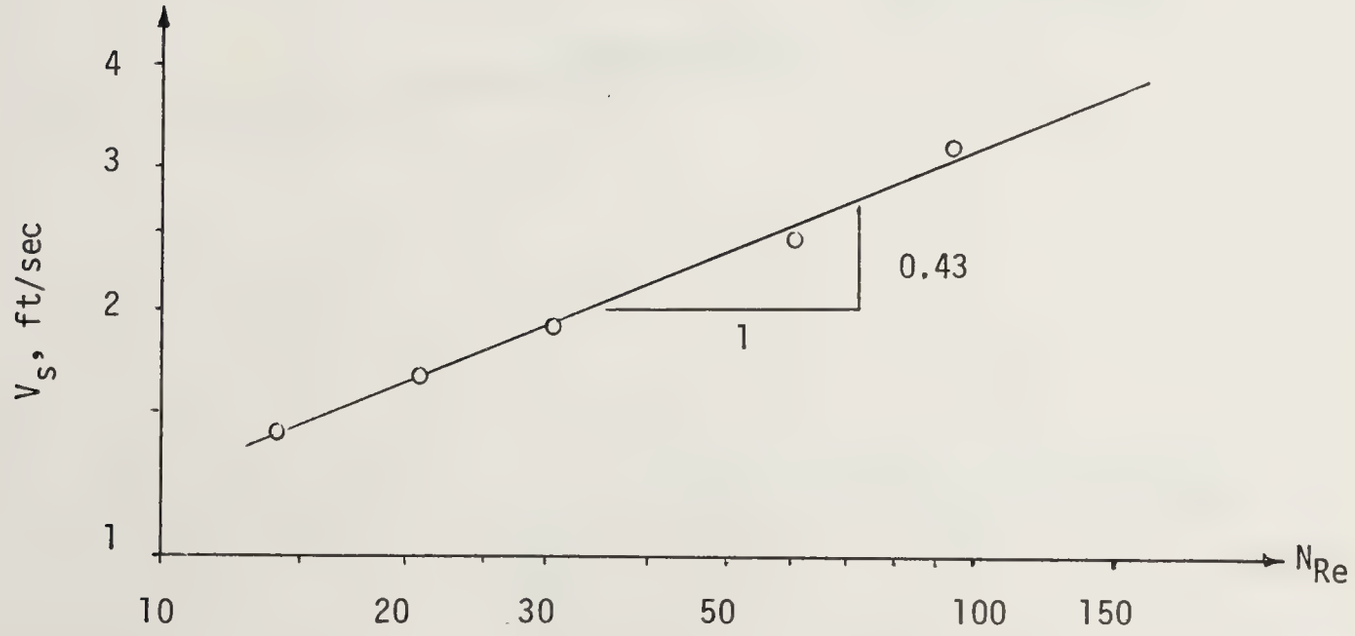

Figure 3. Superficial velocities at incipient fluidization. See Table 2.

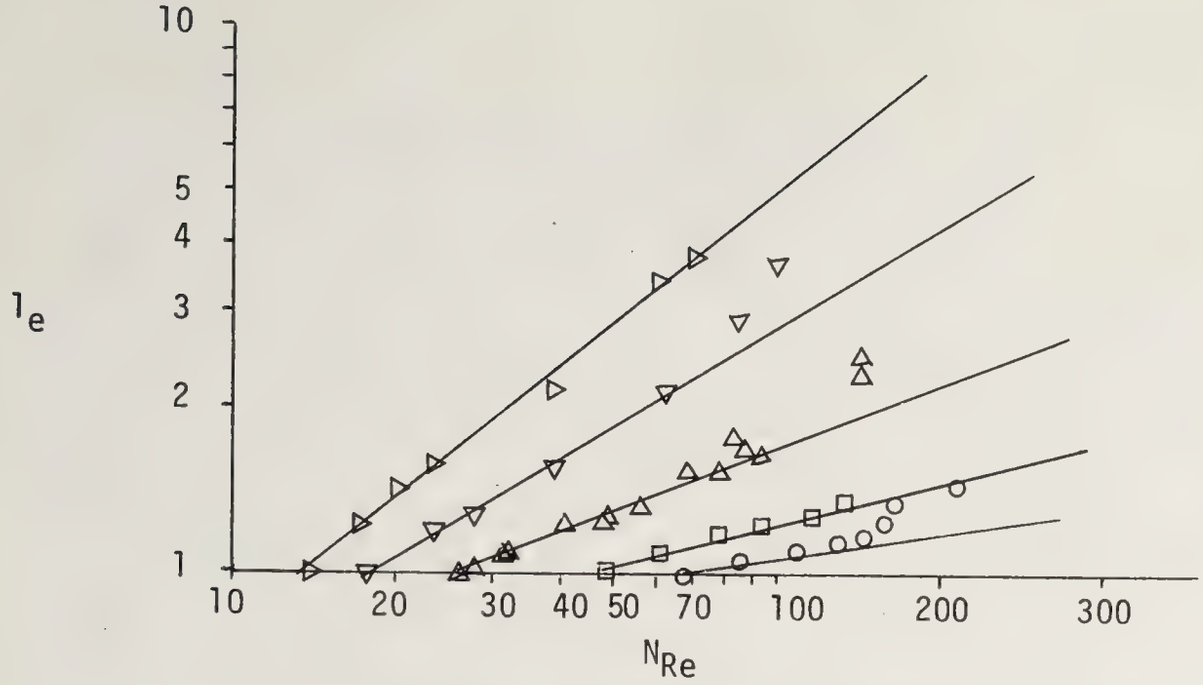

Figure 4. Correlation of bed expansion ratio, l_e, with particle Reynolds Number. See Figure 2 for symbols.

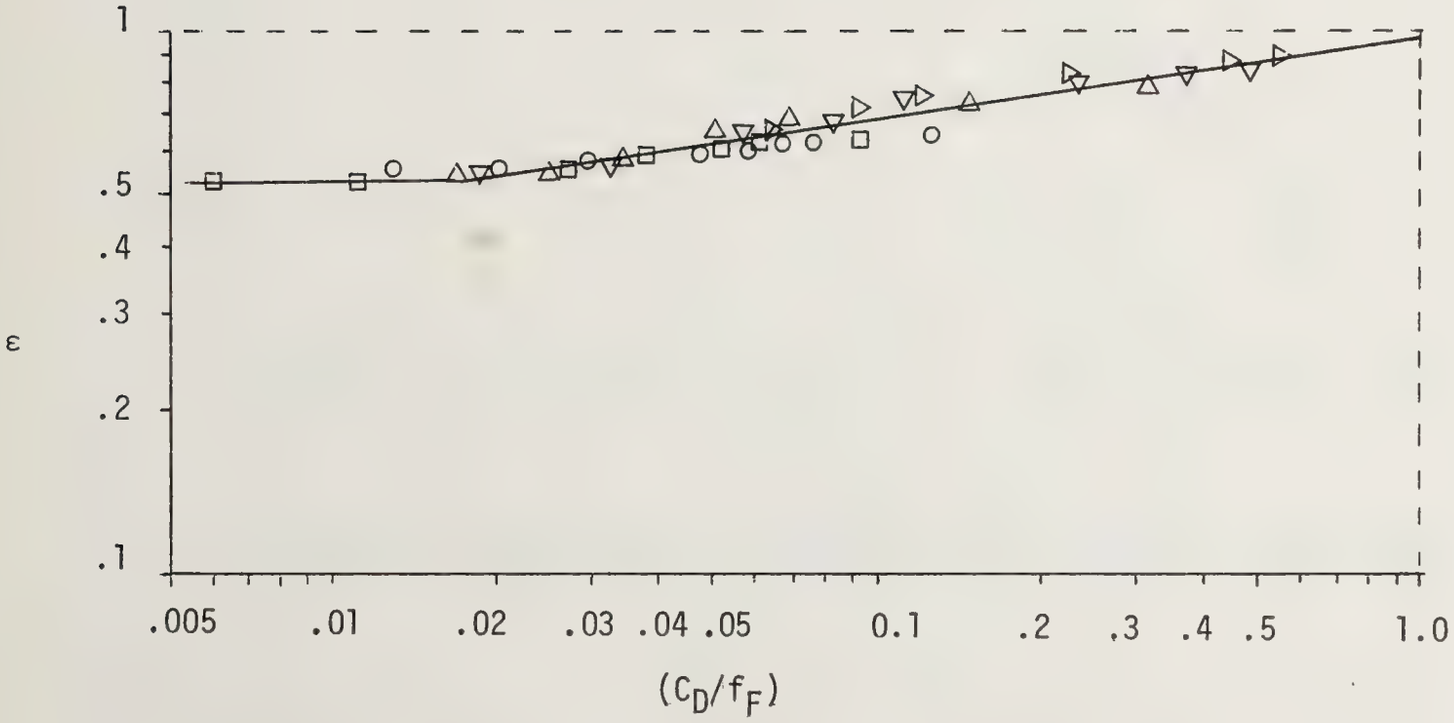

Figure 5. Correlation of bed porosity, ε, with ratio of particle to fluid bed friction factors.

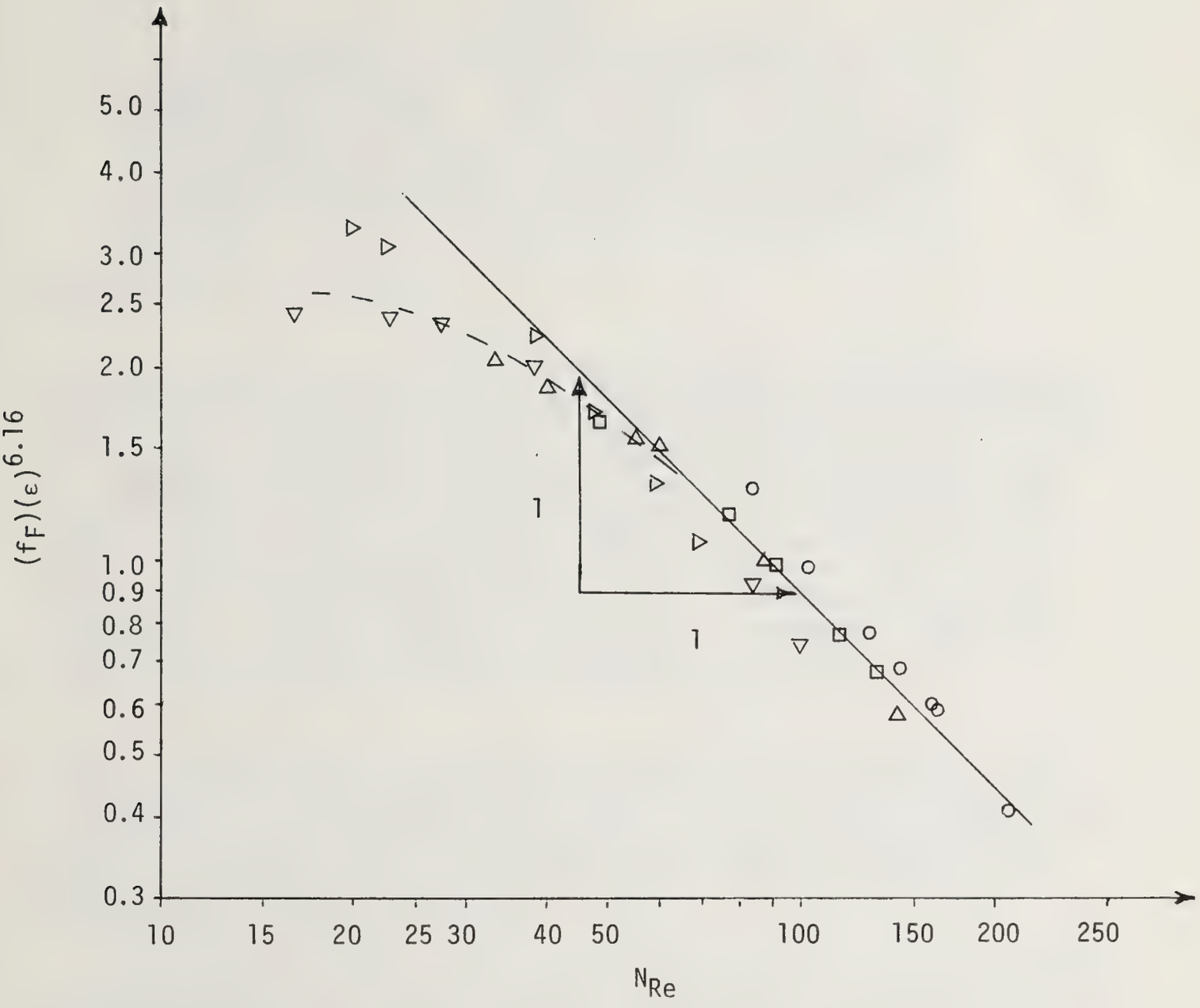

Figure 6. Correlation of fluidization friction factor and particle Reynolds Number for Rosebud seam coal.

Slag Flow and NO_x Kinetics: Moderate Temperature Slag Flow Facility (MTSFF)

H. W. Townes and T. C. Reihman

ABSTRACT

The operation of the moderate temperature slag flow facility (MTSFF) has continued during this quarter at temperatures up to 2000°F. Computer codes for the reduction of the experimental data and the plotting of results have been developed. A comparison of the Nussult vs. Reynolds correlation for the cored ceramic bricks of the MTSFF with several correlations appearing in the literature has been made.

I. OBJECTIVE AND SCOPE OF WORK

The objective of this program is to determine the operational characteristics of a high-temperature packed-bed regenerative heat exchanger for a coal-fired open-cycle MHD system. There is considerable information on the operation of regenerative heat exchangers at temperatures up to 4200°F, but all experience to date has utilized clean fuels such as natural gas. The present work concentrates on the effects that coal slag and MHD seed material have on the performance of regenerative packed-bed heat exchangers. Anticipated effects include the deposition of coal slag and seed materials on the heat exchanger surfaces, the subsequent transport along the surfaces, the obstruction of the passages, the chemical interaction with the heat exchanger material, and changes in the friction and heat transfer coefficients of the heat exchanger flow passages.

An experimental facility, the moderate temperature slag flow facility (MTSFF), is being built and will be operated to study the effects that typical open-cycle MHD channel-exit flows will have on the high-temperature air preheater. The test core of the MTSFF consists of typical MHD air preheater ceramic bricks. A data acquisition and control system is utilized to record gas flow rates and pressures as well as temperatures at approximately two hundred locations.

The effects of the coal slag and MHD seed material on the heat exchanger performance will be determined over a wide range of operational parameters, principally temperature limits of the bed material and flow velocities for the combustion gas and for the air to be heated. The experimental system has been sized so that the above temperatures and velocities can be achieved with a circular flow passage from 0.25 to 1.5 inches in diameter. Initially, natural gas will be used as the fuel. Coal ash will be added to simulate the combustion products of coal firing. The amounts of coal ash added to the combustion gas will simulate the full range that can be expected from the burning of various coals with zero to 95 percent ash removal. The influence of particle size and residence time in the combustor also will be determined. At a later date, it may be desirable to add an actual coal combustion unit to the apparatus.

The overall program consists of analytical as well as experimental work. Analytical studies have been conducted to size the MTSFF, to determine the geometry of the cored ceramic brick, and to determine the ranges of the variables in the experimental program. Current effort is directed toward studies of the transient response of the entire MTSFF during the start-up and cooldown, toward predictions of the slag deposition rates on the heat exchanger surfaces, and toward development of sets of operational test conditions (flow rates and temperature profiles) representing several maximum stress levels in the ceramic bricks.

II. SUMMARY OF PROGRESS TO DATE

The operation of the MTSFF with several different mass flow rates and temperature profiles has continued in order to determine the heat transfer characteristics of the clean cored ceramic brick used in the MTSFF. The analysis of this data has produced a correlation of the Nussult vs. Reynolds numbers for the system which differs slightly from the correlations found in the literature. The reason for the difference in the correlations is most likely due to the roughness of the cored ceramic bricks used in the MTSFF. It is very difficult to properly characterize the roughness of the flow passages in the MTSFF in terms of the roughness elements reported in the literature. A data summary appears in section III.

The slag injection system for the MTSFF has been built and is being installed on the facility. Present plans call for the injection of coal fly ash into the combustion air of the natural gas combustor on the MTSFF.

Work on the simulation of the slag deposition and run off has continued but at a low level.

III. DETAILED DESCRIPTION OF TECHNICAL PROGRESS

A. Work Accomplished

The MTSFF has been operated with the ceramic temperature at the top of the bed varied from approximately 800 to 2000°F and the flow rate through the bed varied from 90 to 180 Kg/hr. The objective of these runs has been the determination of the clean heat transfer and pressure drop characteristics of the MTSFF core. As a result of the data gathered, a correlation of the Nussult vs. Reynolds numbers for the cored ceramic bricks used in the MTSFF has been determined. The correlation (at the 95 percent confidence level) is given by

$$Nu = 0.234 \pm 0.013\ Re^{0.494 \pm 0.007} \qquad (1)$$

Equation (1) is the least-squares curve fit to approximately 8600 data points in the Re range from 330 to 5320 and combines both reheat and blowdown. Slightly different equations result from correlating reheat or blowdown data independently.

The slag injection system has been built and presently is being installed on the MTSFF.

B. Discussion

The determination of the Nussult vs. Reynolds number correlation for the cored ceramic bricks used in the MTSFF is of particular interest because there is a lack of data in the literature for this correlation at the rather low Reynolds numbers at which the MTSFF operates during reheat. In addition, it is difficult, if not impossible, to characterize the roughness of the cored ceramic bricks in terms of the common roughness types reported in the literature. The correlation which has resulted from the experimental data from the MTSFF shows that there is a significant deviation of the heat transfer in the MTSFF from that reported in the literature.

C. Work Forecast

The installation of the slag injection system on the MTSFF is presently being done and should be completed by the end of December. The operation of the MTSFF without slag injection and with ceramic temperatures up to 3000°F should be completed by the end of December also.

The first experimental runs in the MTSFF with slag injection and ceramic temperatures of approximately 2800°F should begin by early January 1978. It had been planned to operate the MTSFF with slag particulates which had been segregated into three size ranges. However, the delivery of the sized slag cannot be made by the supplier until late January 1978, so the decision has been made to proceed with the initial slag injection run with the particulate size distribution as it exists. The initial run is planned to deposit only a small (less than 0.5 mm) layer of slag on the flow passages. This slag layer should plug the small gaps which now exist between the individual bricks and stop the bypass flow which presently occurs. Some additional runs will then be made, and the combustor removed for inspection of the bricks and profiling of the slag layer thickness. Slagging runs with the particulates of given size ranges will be made in the first part of February 1978.

The development of the slag run-off model will be continued. The effects of seed-slag condensation on an existing slag wall layer will be included in the model.

IV. CONCLUSIONS

The correlation of Nussult vs. Reynolds numbers for cored ceramic brick with flow at Reynolds numbers differs from those correlations found in the literature for higher Reynolds numbers flow.

MILESTONE CHART STATUS DATE 12-77

TASK E

PROGRESS

MAJOR MILESTONES

1977

O N D J F M A M J J A S

COMPLETE SLAG-LADEN RUNS FOR FIRST CORE OF MTSFF.

COMPLETE SLAG AND SEED-LADEN RUNS.

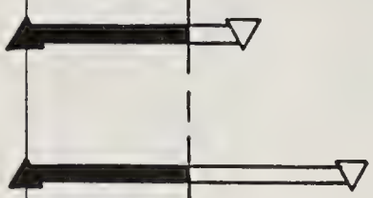

Slag-Seed Equilibria and Separations Related to the MHD System

R. Woodriff, R. Howald, I. Eliezer, J. Amend, and N. Eliezer

ABSTRACT

The determination of vapor pressures is proceeding on schedule. Progress on the thermodynamic analysis of the $KO_{.5}$-$AlO_{1.5}$-SiO_2 system included binary and pseudobinary calculations for the $Al_{1.5}$-SiO_2 and $KAlO_2$-SiO_2 subsystems. Analysis of the $AlO_{1.5}$-SiO_2 binary required a new interpretation of the phase diagram including an unstable, high temperature form of alumina (gamma alumina).

I. OBJECTIVE AND SCOPE OF WORK

The objective of Task F is the measurement and interpretation of vapor pressures over high-temperature oxide systems. The systems for study are primarily synthetic mixtures, actual slags, and seeded slags. The measurements are performed using atomic absorption to measure atom concentration in high-temperature graphite tube furnaces (Woodriff furnaces) produced by diffusion from vapor pressure cells. The interpretation is aimed at providing accurate equations for vapor pressure and activity in multicomponent systems for use in engineering design work where slags are encountered in MHD.

The project includes a continuing effort to obtain and characterize actual MHD slags. In this three month period, the slag work has concentrated on seeded slag samples obtained from Dr. K. Koester of the High Temperature Gas Dynamics Laboratory at Stanford University. The experimental work on synthetic oxide systems has been focused on the $KO_{.5}$-$NaO_{.5}$-SiO_2 system, and the interpretation work has centered on the ternary for which the experiments were completed in the preceding quarter, the $KO_{.5}$-$AlO_{1.5}$-SiO_2 system.

II. SUMMARY OF PROGRESS TO DATE

Measurements on slags have continued. Anomalous vapor pressure readings were discovered, and the causes of these variations was tracked down for certain seeded slag samples from Stanford University. Accurate, reproducible potassium pressure readings were obtained for two of these seeded slag samples.

It was necessary to reinterpret the data on the $AlO_{1.5}$-Si_2 system in view of the probable presence of SiO_2 solutions in gamma alumina in the system. The mathematical difficulty in interpreting the high-temperature liquidus of Aksay and Pask[1] as solutions saturated with corundum was clarified further. The possible solution to this problem in terms of an appreciable solubility of SiO_2 in alpha alumina was examined and rejected. A new interpretation of the data[2] was proposed. This new interpretation was shown to reconcile apparently conflicting phase diagram proposals and

experimental data from three major laboratories: Aksay and Pask,[1] Aramaki and Roy,[2] and Toropov and Galakhov.[3] Thermodynamic parameters have been evaluated for the $AlO_{1.5}$-SiO_2 system and the phase diagram has been calculated. The calculations on the $AlO_{1.5}$-SiO_2 system have been written up for publication. Calculations have been performed on the SiO_2-$KAlO_2$ join in the $KO_{.5}$-$AlO_{1.5}$-SiO_2 ternary system. The stable assemblages of solids at 900 K have been identified by calculations over most of the $KO_{.5}$-$AlO_{1.5}$-SiO_2 ternary system.

Work is proceeding on schedule for the measurement of K and Na pressures over the ternary system $KO_{.5}$-$NaO_{.5}$-SiO_2. A full set of sodium silicate and sodium aluminate samples has been prepared. The first set of three component samples in the $KO_{.5}$-$NaO_{.5}$-SiO_2 system have been prepared. One furnace has been used to make sodium vapor pressure measurements and modified to permit simultaneous K and Na measurements. Plateau measurements have been obtained for sodium pressures on two sodium silicate samples. Literature data on pseudobinary $NaO_{.5}$-$KO_{.5}$ substitution in the β-alumina system has been analyzed mathematically. A system for automated temperature control of the furnaces has been designed and construction of the first control system is underway.

A number of significant developments relating to future work have been achieved in this period. The feasibility of measuring Ca atom concentrations over CaO samples in the Woodriff furnace has been demonstrated. The significant deterioration of molybdenum cells operating with K_2SO_4 in a Woodriff furnace was demonstrated and shown to result in the formation of molybdenum and/or molybdenum sulfide deposits. It was shown that plateau readings can be obtained with K_2SO_4 samples in platinum cells. Thermodynamic properties have been assigned for several gaseous potassium oxides based upon the work of Ehlert et al.[4] A preliminary mathematical fitting of literature data on the SiO_2 activity in the CaO-$AlO_{1.5}$-SiO_2 ternary system was performed. The computer programs were modified to include calculation of mole fractions corresponding to a given enthalpy or heat capacity, and to simplify the calculations of excess free energy for solutions.

III. DETAILED DESCRIPTION OF TECHNICAL PROGRESS

A. Atomic Absorption Furnace Systems

1. Sodium Measurements

A hollow cathode lamp giving both Na and K light has been mounted on one of the furnaces. The graphite tube in this furnace has been replaced because of serious oxidation losses in the preceding tube. The optics have been adjusted to permit simultaneous Na and K measurements with this furnace, and the sodium optical system has been checked out with actual sodium plateau measurements.

2. Automated Temperature Control

Work has continued on the installation of improved electronics on various furnaces used for vapor pressure measurements and on the design of a system for automated temperature control of these furnaces.

B. Vapor Pressure Measurements

Sodium silicate and sodium aluminate samples have been prepared over a range of mole fractions. Vapor pressure measurements have been completed for two of the sodium silicate samples. Difficulties in maintaining plateau measurements due to sodium loss were observed for the sample at the lowest $NaO_{.5}$ mole fraction. Several samples with both $NaO_{.5}$ and $KO_{.5}$ in SiO_2 have been prepared, and are ready for measurements.

Measurements on a K_2SO_4 sample have been attempted in both molybdenum and platinum cells. The molybdenum cell showed enlargement of the diffusion hole and a cone of built-up material around this hole. The material in the cone was identified as molybdenum or molybdenum sulfide. It appears that the O_2 and SO_2 pressures over K_2SO_4 are sufficient to allow appreciable molybdenum volatility at these temperatures, and then molybdenum is redeposited under the reducing conditions outside the cell which are present because of the graphite tube of the furnace. Plateau readings could be obtained with K_2SO_4 in platinum cells, and thus platinum cells are suggested for direct measurements on the $KO_{.5}$-SiO_2-SO_3 ternary system.

Potassium vapor pressure measurements on the $KO_{.5}$-CaO-$AlO_{1.5}$-SiO_2 system are planned. To evaluate the feasibility of measuring the calcium pressures in this system, samples of CaO in open cups were examined with the 228.8 nm calcium line in the Woodriff furnace. Appreciable calcium absorbance was observed at temperatures of 2200° K and above.

On their trip to Stanford, Dr. Howald and Dr. Eliezer obtained from Dr. K. Koester several samples of slag from his experimental slag flow channel. One of these samples, when ground and placed in a sample cell in the vapor pressure furnace, gave initially very high potassium pressures which were not maintained for a long enough period for accurate measurement. This problem was traced to the presence of light colored high-potassium material present in the sample on the surface, apparently from reaction of the slag with the atmosphere. Samples washed briefly with water or dilute acid gave lower initial potassium pressure, and were satisfactory for potassium plateau measurements. These samples are apparently quite reactive glasses. The degree of reactivity is evident in the fact that heating these samples with dilute hydrochloric acid for a period of hours results in almost complete dissolution of the iron, leaving a white alumina-silica gel. The UTSI group has reported the formation of potassium sulfate crystals on the surface of some of their glassy slags on standing exposed to the atmosphere, and it is not unlikely that potassium bicarbonate could be formed as well. The thermodynamically stable potassium alumina silicates such as sanidine and leucite do not show hydration, reaction with the atmosphere at an appreciable rate, or substantial solubility in HCl. It is clear that the rate of cooling of slags (and thus the degree of crystallinity) is one of the important parameters in determining the ease of recovery of potassium seed compounds from the slags.

C. Thermodynamic Analysis

There have been three major achievements in the area of theoretical analysis in this period: 1) a crystallization of ideas on how to teach the

use of Redlich-Kister equations in the analysis of phase equilibria as shown by offering a course in this area to a small selected group of students; 2) the development of a complete and self-consistent notation which is applicable to the full mathematical analysis of systems of eight or more components; and 3) the proposal and development of a new idea concerning the presence of an unstable high-temperature form of alumina in which SiO_2 is appreciably soluble. This was shown to reconcile the contradictory phase diagrams in the literature for the $AlO_{1.5}$-SiO_2 system. Significant work was done on the $KO_{.5}$-$AlO_{1.5}$-SiO_2 ternary system in addition to completion of the $AlO_{1.5}$-SiO_2 binary subsystem, but since this work is still in progress, it will be reported in the next quarterly report.

1. A course, " Chemical Thermodynamics: Computer Calculation of Phase Equilibria," was offered this fall. It did not receive any support from the MHD contract, but several of the MHD personnel were involved in the course, the material covered in the course was directly related to the contract work, and there were very substantial benefits to the contract work from the course.

2. A self-consistent notation for multicomponent systems was developed this quarter. This notation is scheduled for presentation of Calphad VII in April and is described briefly in the following paragraph.

We can define an excess logarithm of activity coefficients, LG^e as

$$LG^e = \sum_i X_i \log \gamma_i$$

by analogy with excess enthalpy

$$H^e = \sum_i X_i \bar{H}_i$$

All the excess quantities, H^e, LG^e, C_p^e, etc., can be represented as power series in mole fractions. The Redlich-Kister coefficients for a binary system are coefficients for power series in X_1-X_2, and thus, the Redlich-Kister coefficient $D_{34}(H)$ corresponds to a term of the form

$$H^e = \ldots + D_{34}(H)X_3X_4(X_3-X_4)^3 + \ldots$$

We have extended this notation by including more subscripts, one for each mole fraction appearing to the first power, and using letter superscripts to identify additional powers of $(1-X_1)$ and (X_j-X_2) as in the term $D^b_{124}(H)$ which corresponds to

$$H^e = \ldots + D^b_{124}\, X_1X_2X_4(1-X_1)^1(X_2-X_4)^1$$

For a six component system there will be terms with two, three, four, five, and even six subscripts; however, the first term with six sub-

scripts must be an E term, E^{aaaa}_{123456}, since the simplest term with six subscripts already corresponds to a sixth power term.

3. A novel analysis of the $AlO_{1.5}$-SiO_2 system which was developed during the last few months, was written up and will be submitted for publication under the title, "The Thermodynamic Properties of Mullite."

Plante's data[5] on vapor pressures in the $KO_{.5}$-$AlO_{1.5}$ system were used together with selections from the literature data for thermodynamic properties of the potassium aluminum silicates, and our values for the potassium silicates $K_2Si_4O_9$ and $KSiO_{2.5}$ to calculate equilibrium activities for various sets of three solids at 900°K. The results are shown in Figure 1. These calculations and further calculations of this type are the first step in getting activity coefficient data from the liquidus curves for the ternary system to compare with our experimental vapor pressure measurements. Recent equilibrium data are available in the National Bureau of Standards work on the $KAlO_2$-SiO_2 join in this system. A preliminary pseudobinary treatment of this join was completed, and this treatment is being refined for improved accuracy and for consistency with the $AlO_{1.5}$-SiO_2 and $KO_{.5}$-$AlO_{1.5}$ binary subsystems. The CaO-$AlO_{1.5}$-SiO_2 ternary was analyzed using only two Redlich-Kister coefficients. The activities at 1600°C calculated from these equations are in error by as much as 30 percent, but this analysis makes it clear that three Redlich-Kister coefficients (i.e. terms through the fourth power in mole fractions) will be adequate for this ternary system. This, together with our work on the $KO_{.5}AlO_{1.5}$-SiO_2 ternary, indicates that inclusion of terms through the fifth power in mole fractions whould be satisfactory for high-temperature oxide systems related to coal slag, and this level of representation was selected for the first major programming efforts for systems of more than three components.

Further miscellaneous achievements in this period include thermodynamic properties for KO(g) and Al_2SiO_3 (c, sillimanite), a pseudobinary treatment of Na and K vaporization from beta aluminas, and several significant additions to the computer programs. The programs now will find mole fractions for particular values of $\bar{H}_1$, H^e, etc., and calculated values for the excess logarithm of activity,

$$LA^e = X_1 \log a_1 + X_2 \log a_2$$

now are included in the computer printout for binary systems. This quantity can be used for the graphical determination of compositions of phases in equilibria with each other.

IV. CONCLUSIONS

Work with the furnaces and on the $KO_{.5}$-$NaO_{.5}$-SiO_2 ternary system is proceeding on schedule. The thermodynamic analysis of the $KO_{.5}$-$AlO_{1.5}$-SiO_2 system is slightly behind schedule because a substantial revision of the $AlO_{1.5}$-SiO_2 phase diagram was necessary to treat that binary system

quantitatively and to reconcile conflicting literature data on the phase diagram. This has been accomplished, and work on the ternary systems is proceeding well.

MILESTONE CHART

STATUS DATE 12-31-77

TASK F

PROGRESS

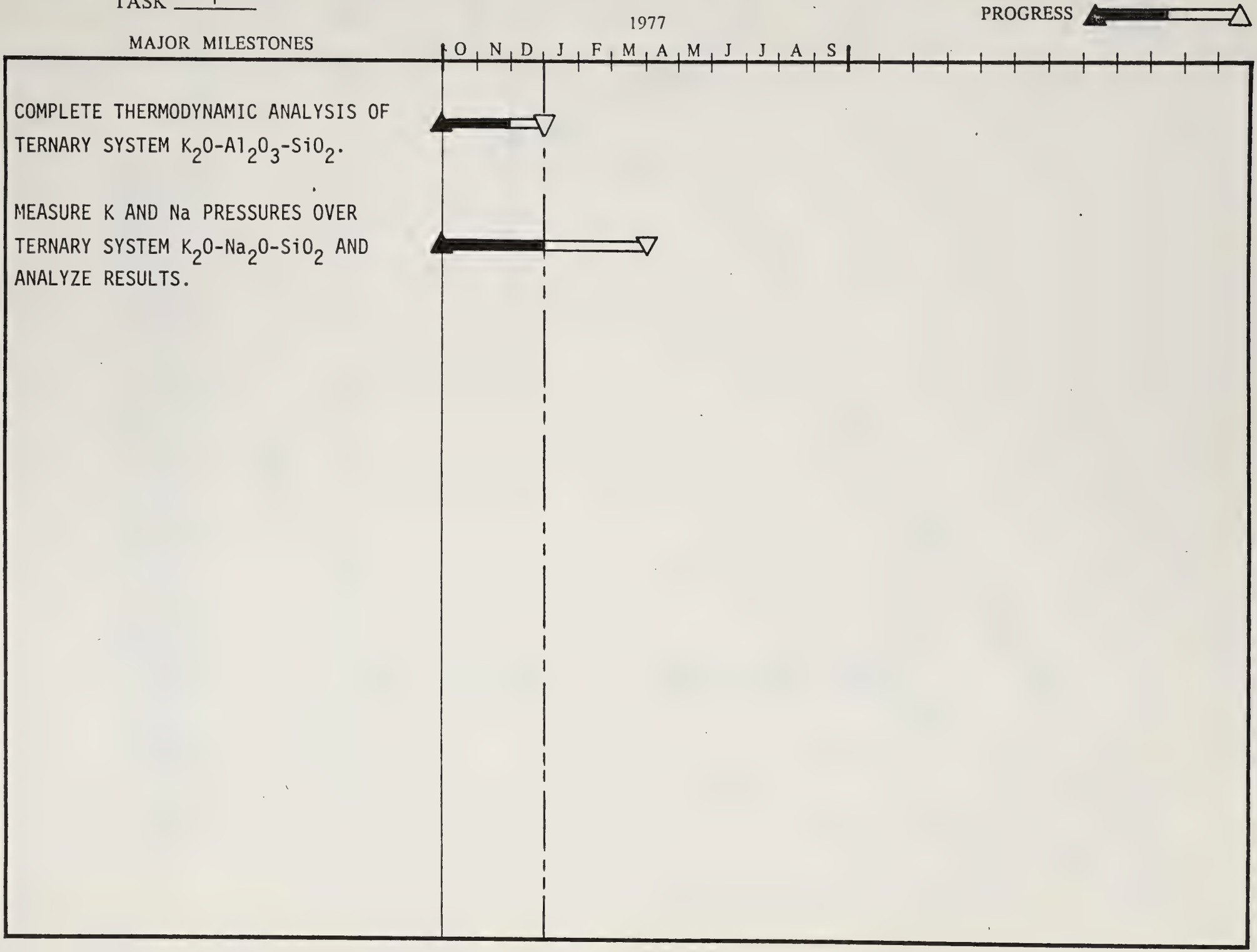

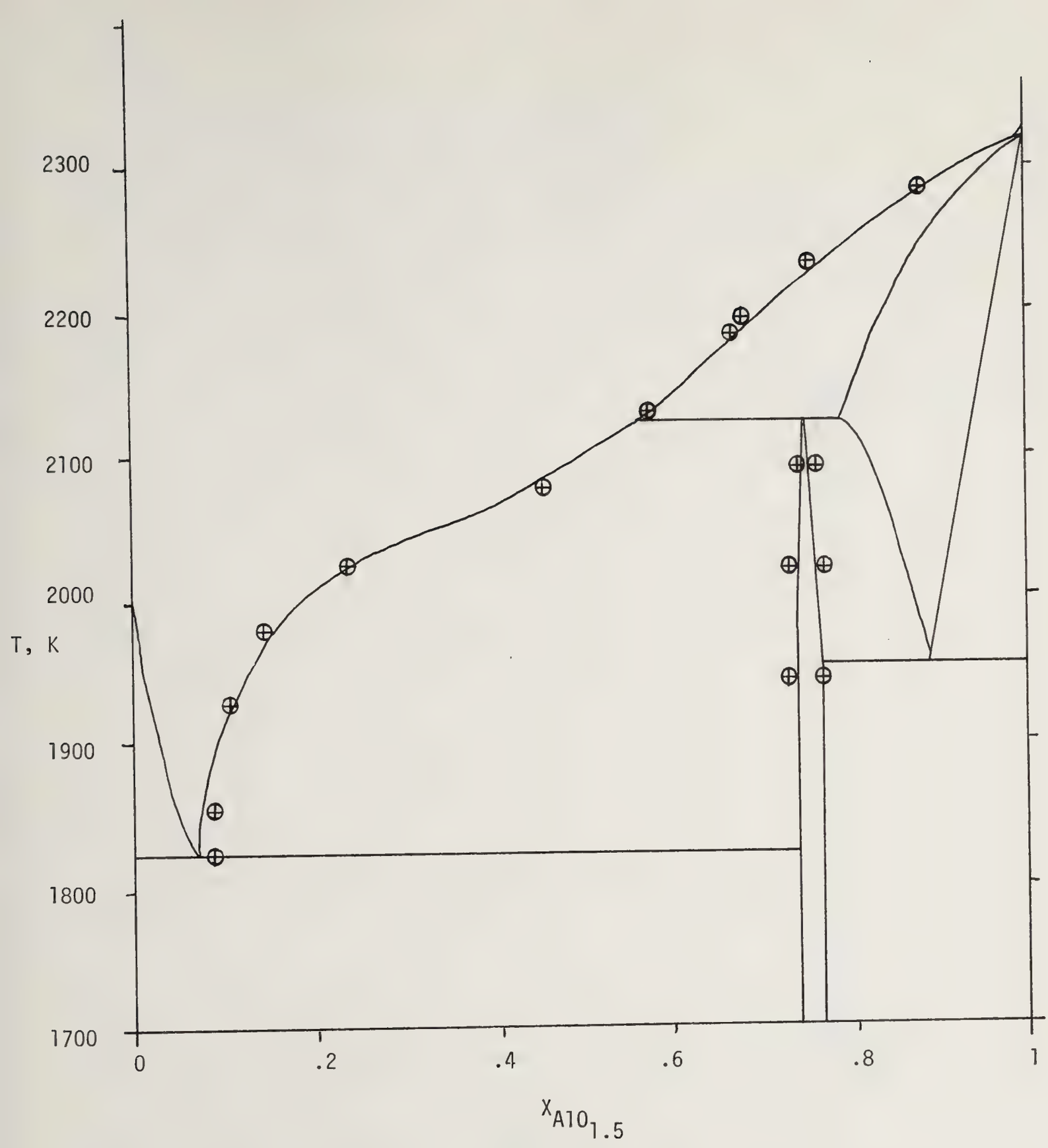

Figure 1.--Calculated $AlO_{1.5}$-SiO_2 phase diagram. This shows a substantial region of stability for solutions of SiO_2 in gamma alumina, and an incongruent melting point for mullite. The circles represent experimental points of Davis and Pask and Aksay and Pask.

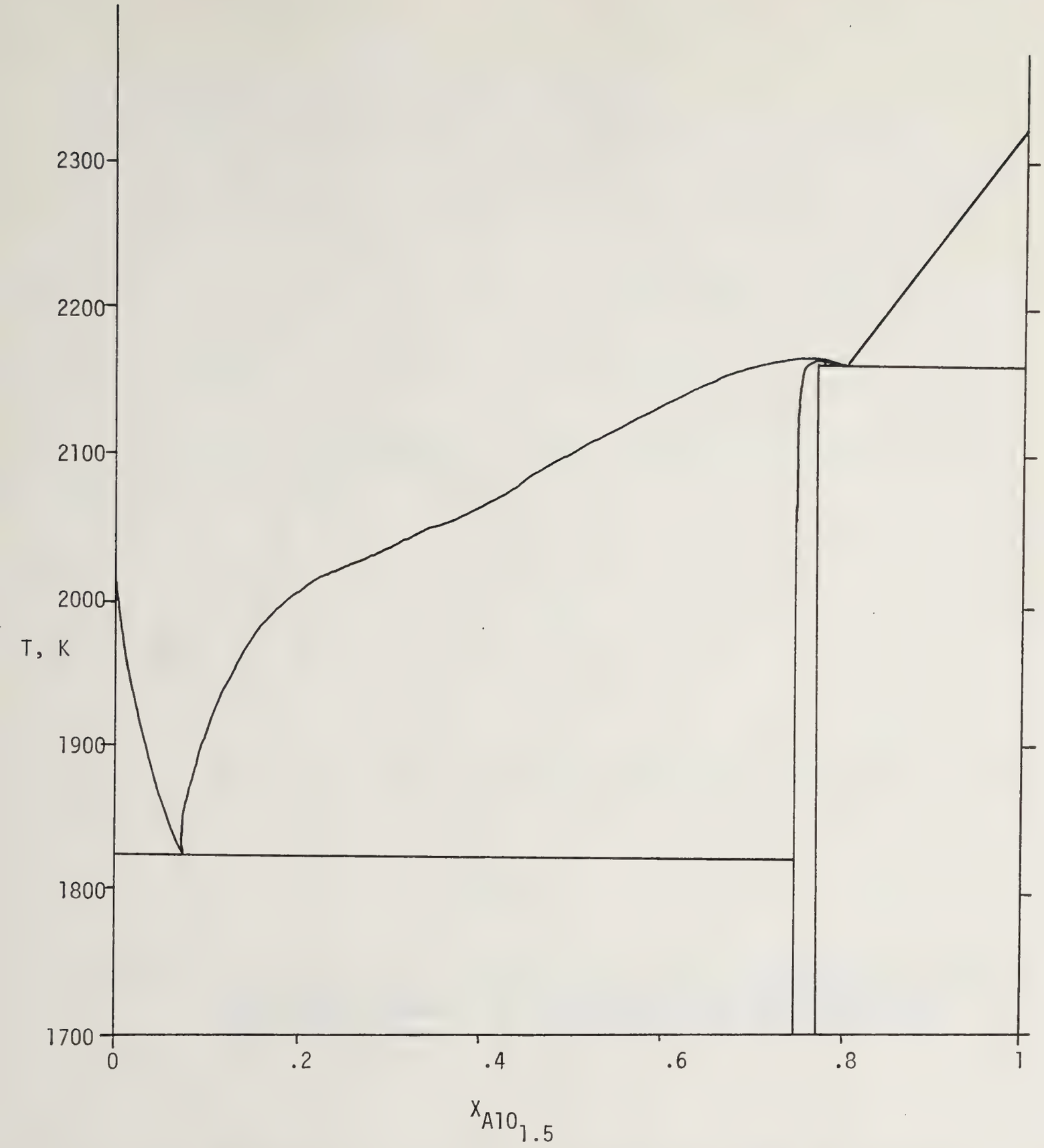

Figure 2.--Metastable $AlO_{1.5}$-SiO_2 phase diagram, calculated omitting the gamma alumina phase. Note that mullite melts congruently just above the mullite-corundum eutectic.

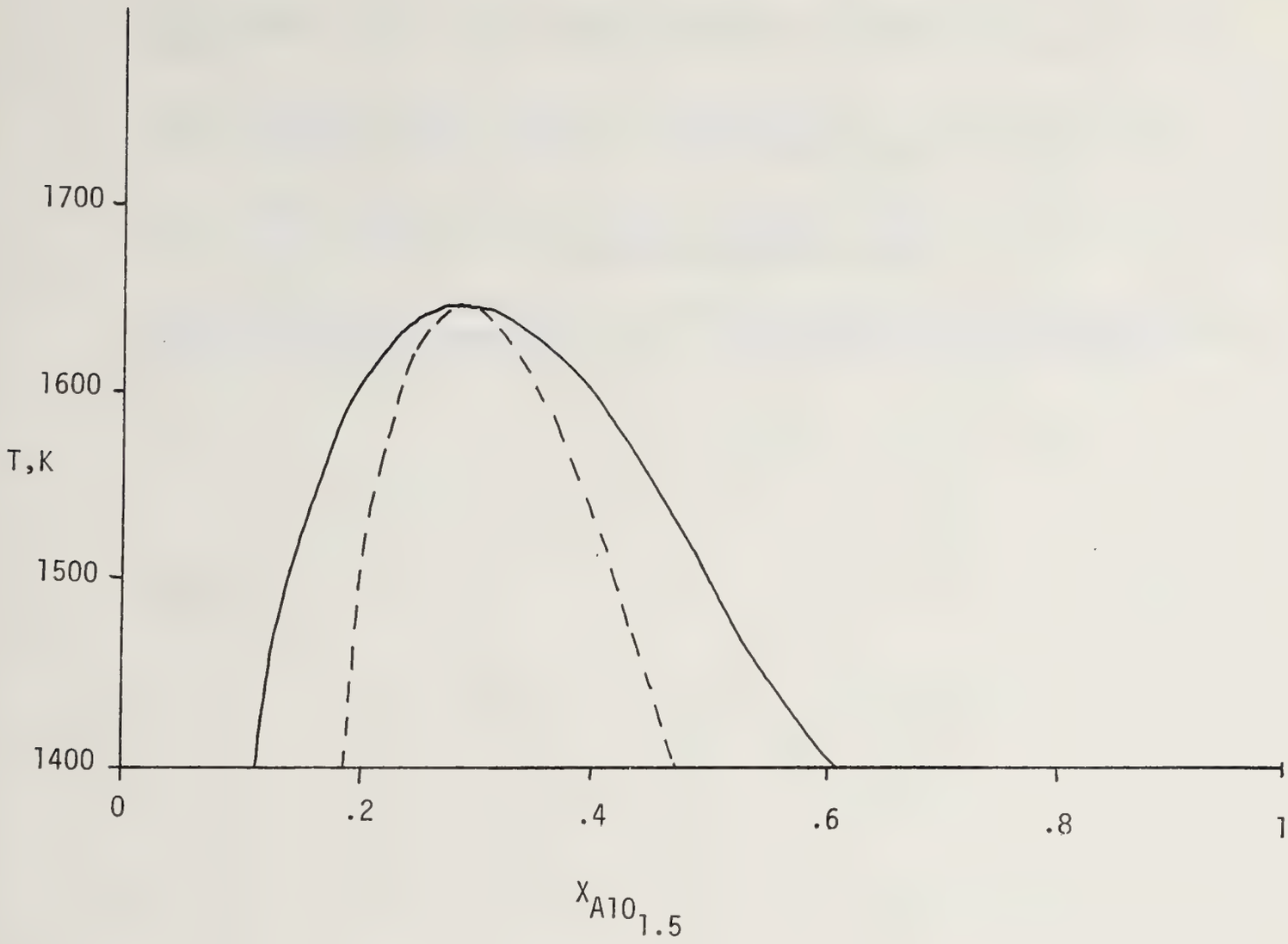

Figure 3.--Calculated curves for liquid-liquid immiscibility in metastable $AlO_{1.5}$-SiO_2 glasses. The dotted line shows the positions of maxima and minima in the activities.

REFERENCES

1. I. A. Aksay and J. A. Pask, Journal of American Ceramic Society, 58, 507, 1975.

2. S. Aramaki and R. Roy, Journal of American Ceramic Society, 45, 229, 1962.

3. N. A. Toropov and F. Y. Galakhov, Doklady Akad. Nauk SSSR 78, 299, 1951: Izv. Akad. Nauk SSSR. Otd. Khim. Nauk, 1958, 8, 1958.

4. T. C. Ehlert, "Mass Spectrometric Investigations of the Oxides of Potassium," submitted to High Temperature Science.

5. E. R. Plante, C. D. Olson, and T. Negas, Sixth International Conference on MHD Electrical Power Generation, Volume 2, p. 211, Washington, D.C., June 1975.

Physical Properties of Coal Slag and Electrode Materials: Thermionic Emission and Effects of Electrical Conduction

G. Lapeyre and J. Anderson

ABSTRACT

During this quarter, work has continued on the investigation of the thermionic emission properties of coal slag. Thermionic emission was studied from a number of synthetic slag samples which contained various amounts of potassium oxide. Although the data are tentative in nature, the emission appeared to be quite sensitive to bulk potassium concentration over a certain range. However, the dependence on potassium was opposite to what might be expected. The emission from a sample containing ten percent potassium oxide was found to be four orders of magnitude lower than another of the same composition containing no potassium and about equal to another sample of a somewhat different composition, but also without potassium. A mass spectrometer was used to identify the previously reported ion emission as being due to potassium.

I. OBJECTIVE AND SCOPE OF WORK

The objective of this project is to determine the thermionic emission properties (e.g., thermionic work function) of coal slag, including slag-seed mixtures. Evaluation of the need for thermionic emission data on electrode materials will be made in the context of clean electrodes in hot-wall, coal-fired channels, and exploratory measurements will be made.

Initial measurements will be performed on synthetic slags of various compositions at temperatures both below and above the temperature at which the slag is liquid.

Since the actual surface composition is of paramount importance in determining the work function and the thermionic emission, in situ surface analysis will be carried out by Auger electron spectroscopy. Materials desorbing and evaporating from the surface will be determined by mass spectrometry.

II. SUMMARY OF PROGRESS TO DATE

Improvements in the design of the thermionic emission apparatus were made. Some difficulty had been experienced in interpreting the thermionic data obtained from synthetic slag K524. To overcome these problems , the collector assembly was redesigned. Data then was obtained from three synthetic slag samples. A large change in emission current was observed with respect to slag composition. Difficulty was encountered with sample K536. Because of its relatively high softening point, the sample could not be melted sufficiently to wet the platinum supporting the slag. The data presented for K536 is, therefore, somewhat in doubt and should be considered tentative.

As reported earlier, large ion currents were observed to be emitted by slag samples when reverse biased. A mass spectrometer was used to determine the mass and hence the identity of the ions emitted from K524 which contained ten percent potassium oxide.

III. DETAILED DESCRIPTION OF TECHNICAL PROGRESS

The anode-guard ring configuration that has been used was found to present certain problems in the measurement of the thermionic emission. In some instances it was not possible to get the measured current to saturate, even though rather large voltages were applied to the anode. The cause appeared to be due to the following process: neutral atoms (probably potassium), evaporating from the slag, would deposit on the anode. The anode would become red-hot because of its proximity to the hot slag and consequently those potassium atoms would re-evaporate from the anode as ions and travel back to the sample. The resulting ion current between the anode and slag then would be indistinguishable from an electron current from the slag to the anode. Because 1) such a current can be much larger than the electron current and 2) the ion mass is much larger than the electron mass, saturation would be more difficult to obtain. To overcome this difficulty, the anode was re-designed so it would stay cool. It was constructed from a massive copper block and positioned farther from the slag sample.

Data were taken for samples K524, K517, and K536 with this collector configuration. The emission saturated for the first two samples. With sample K536 some difficulty was encountered, but it is suspected that this was connected with the inability to melt the sample and form good electrical contact with the platinum underneath. This difficulty is expected to be overcome by substituting indium for the platinum which can be heated to much higher temperatures.

Since the thermionic emission current density, J, can be described generally by the Richard-Dushman equation, the data should lie on a straight line in a Richardson plot, where $\log(J/T^2)$ versus $(1/T)$ is plotted as shown in Figure 1 for two of the three samples mentioned, plus slag K214 which had been measured earlier. When projected to a reasonable channel operating temperature of 1800°K, this data implies that the emitted current density would vary between .3 milliamps/cm^2 and .3 amps/cm^2, depending on slag composition. Although this data is somewhat tentative in nature, it certainly indicates the sensitivity of emission current to slag composition. The observed change in work function with slag potassium content is somewhat surprising. A very common result of work function studies is that an alkali metal such as potassium forms a dipole layer at the surface. This dipole layer is oriented such as to reduce the work function and, therefore, increase the emission current. That this is not necessarily the case here can easily be seen from Figure 1 where the emission current density from K517 (no potassium) is approximately four orders of magnitude larger than that from K524 (10 percent potassium). Both samples were studied with Auger electron spectroscopy. Potassium was detected on the surface of K524, and no potassium was detected in the case of K517.

The mass spectrometer was used to determine the nature of the ions emitted by K524. A plate with a hole was placed over the sample and was biased negative with respect to the emitter. The ions were accelerated, went through the hole, and entered the mass spectrometer head located some distance above. Shown in Figure 2 is a typical mass scan with the filament of the mass spectrometer off. As can be seen, two peaks were obtained which are the two stable isotopes of potassium. When the filament of the mass spectrometer is turned off as for the data just presented,only ions impinging on the mass spectrometer head are detected. It was observed that ions were emitted by the sample at very low temperatures. These temperatures were well below the lower limit of the optical pyrometer and were estimated to be roughly 500°C.

IV. CONCLUSIONS

Initial results from several different slags indicate that the presence of large amounts of potassium does not necessarily lower the work function as expected. Although the data are somewhat tentative, it would appear that the current densities obtained are considerably lower than necessary for arc-free channel operation.

MILESTONE CHART

STATUS DATE 12-31-77

TASK G

PROGRESS

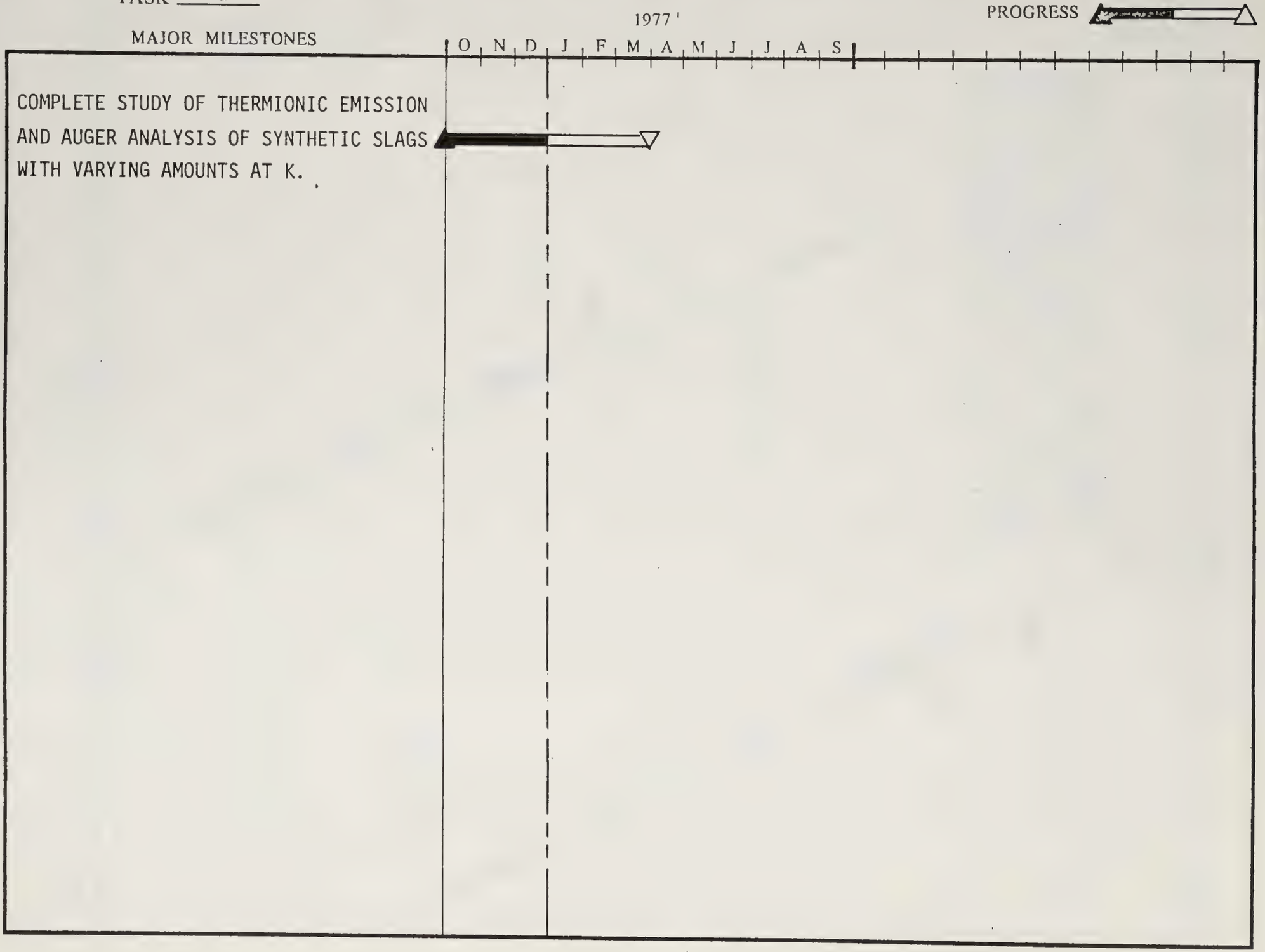

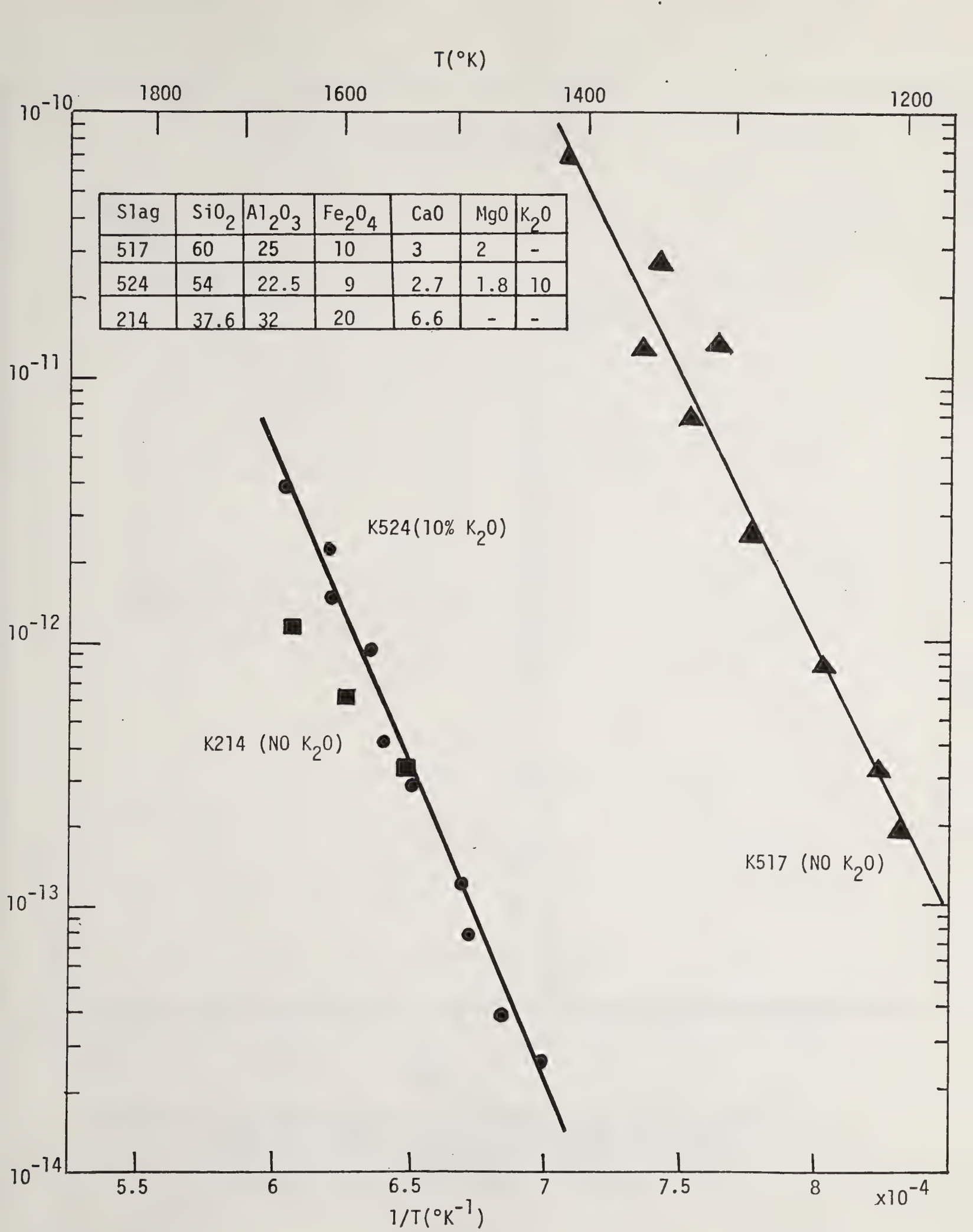

Slag	SiO_2	Al_2O_3	Fe_2O_4	CaO	MgO	K_2O
517	60	25	10	3	2	-
524	54	22.5	9	2.7	1.8	10
214	37.6	32	20	6.6	-	-

Figure 1.--Richardson plots (j/T^2 vs $\frac{1}{T}$) for three samples of synthetic slag

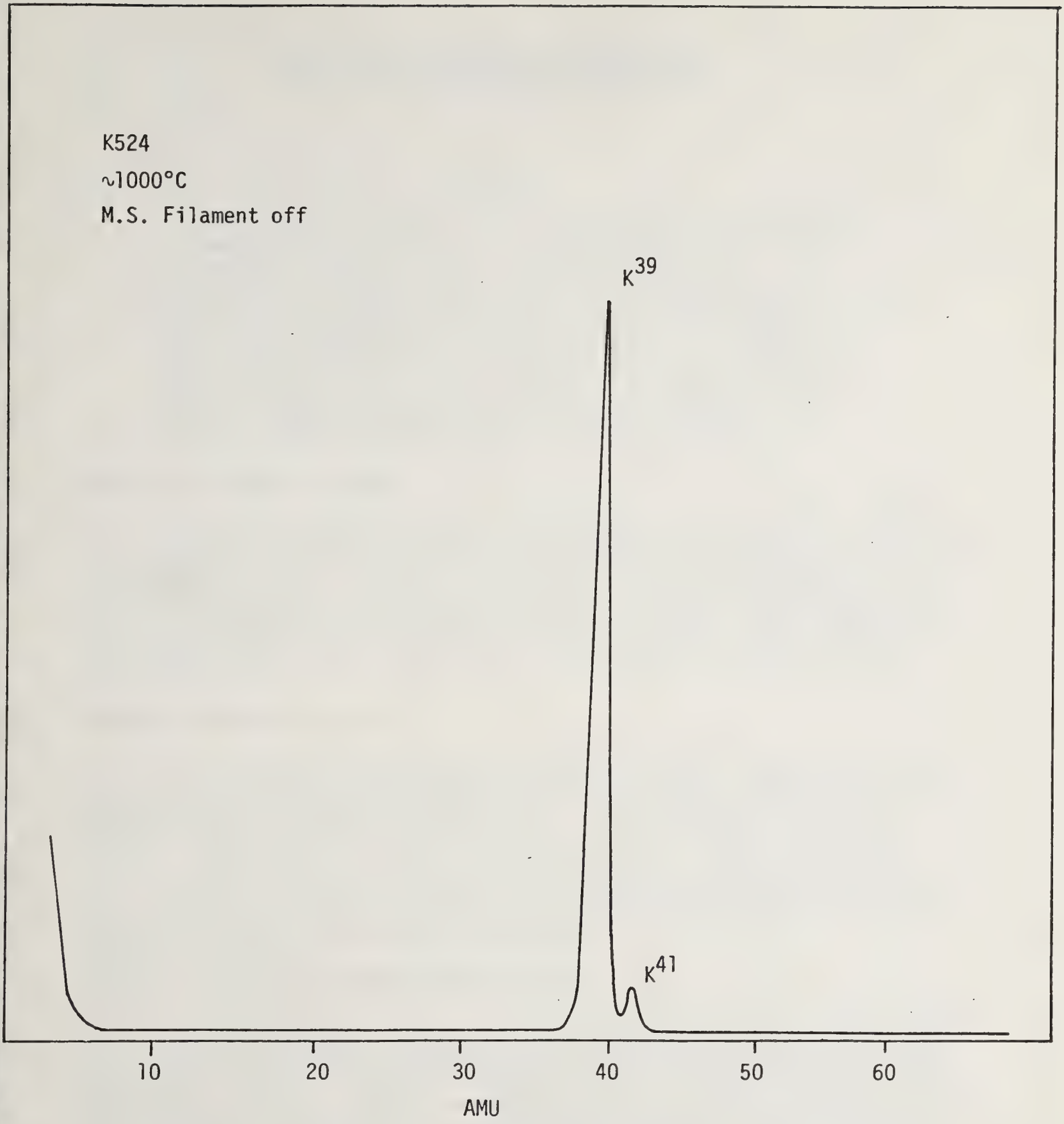

Figure 2.--Mass spectrometer trace measuring the ions emitted from slag K524 (The ionizer filament was turned off so that only ions emitted from the slag and entering the mass spectrometer are detected.)

Slag Physical Properties: Electrical and Thermal Conductivity

R. Pollina

ABSTRACT

This report includes the first preliminary measurement of the thermal conductivity of a Rosebud natural ash sample. The thermal conductivity was 1.5 ± 0.2 watt/m-K up to its softening point. More accurate data will be obtained in future work. A demonstration model a-c resistance bridge on loan from the manufacturer has worked very well in measurements of the a-c electrical conductivity of coal slag to 1750°C. Above 1200°C, in all but low iron simulated ashes, there is negligible difference between d-c electrical conductivity and a-c conductivity from 40 Hz to 10KHz.

I. OBJECTIVE AND SCOPE OF WORK

The objectives of this task are to determine the electrical and thermal conductivity and the thermal expansion of MHD slags and materials under isothermal conditions. The electrical conductivity measurements are controlled atmosphere a-c and d-c measurements to 1750°C. The thermal conductivity is a comparison method useful to 800°C and the thermal expansion upper temperature limit is 1600°C with a controlled atmosphere in both experiments.

II. SUMMARY OF PROGRESS TO DATE

The first preliminary measurements of the thermal conductivity of a Rosebud ash are being reported here. Up to its softening point at approximately 600°C, the thermal conductivity of a porous sample was 1.5 ± 0.2 watt/m-K. This value is expected to show some variation from sample to sample. Excellent results also were obtained in a-c electrical conductivity using a digital a-c bridge borrowed from the manufacturer. On the basis of this successful trial test of the bridge, a similar unit has been ordered with delivery expected in February.

III. DETAILED DESCRIPTION OF TECHNICAL PROGRESS

In an MHD generator channel, the conductivity of the slag layer adhering to the walls of the generator must be in a range appropriate for the slag to act as a good conductor for the generator output current and yet must be low enough to prevent shorting of the axially directed Hall current. The mathematical analysis of the current flow indicates opposing demands upon the slag conductivity.[1] However, the criterion by which the suitability of a given slag with respect to the magnitude and character (ionic or electronic) of its electrical conductivity is judged is yet to be determined. The task's ultimate goal is to satisfy demands of the designers for data necessary in modeling the output of the channel and in predicting

empirically the behavior of slag under any constraints which might occur when larger scale projects such as the CDIF become operational. Interaction and close cooperation with other MHD groups is required and is being sought.

The coal ash used in these experiments is from the Rosebud seam and was obtained from a local power company.[2] The combustor temperature was approximately 1900°K[3] and bottom and fly ash were supplied from the combustor and the base of the stack respectively. The samples were received in the form of powder, and each was homogenized and melted in alumina or platinum crucibles in air at 1700-1750°K for 1 to 36 hours and then air quenched. Corrosion of alumina crucibles generally was not observable until the seed content was increased. Above 10 percent K_2CO_3 a changeover to platinum crucibles was necessary.

In the conductivity tests below 1750°K, samples were contained in alumina boats of 99.8 percent purity[4] (interior dimensions 2 x 4 x 4 mm.). The d-c conductivity was measured using the conventional four-lead technique because of its sensitivity, reproducibility, and ability to separate polarization effects[5,6] from the true conductivity. A-C conductivity was measured using a two-lead technique and an a-c resistance bridge. Pulverized samples were placed in a crucible into which four leads had been suspended. A type-B thermocouple (platinum-6 percent rhodium vs. platinum-30 percent rhodium), which was calibrated at the gold point, monitored the temperature. Above 1750°K, a two-lead technique was used to measure the electrical conductivity. Because of problems in d-c measurement associated with polarization charge buildup in ionically-conducting coal slag when only two leads are used, a-c conductivity was measured above 1750°K and not d-c.

Samples were raised to the maximum temperature, and data was taken starting at the highest temperature and moving downwards. During a run, the ceramic boats developed a web of cracks[7] indicating that the slag had a lower thermal expansion than alumina.

In an effort to determine whether or not there were any time-dependent effects in the d-c conductivity measurements, a sample was held under a d-c current for 25 hours and both the conductance of the sample and the charge buildup at the current electrode were monitored. This charge buildup is measured by the compliance voltage necessary to maintain constant current through the sample. This sample, a Rosebud ash with 20 percent K_2CO_3 equivalent of added potassium seed, was chosen because of its strong ionic effects and strong charge buildup on the electrodes. The compliance voltage between the outer two electrodes varied from 2.5 to 135 volts while the conductance between the inner two drifted slowly and not by an amount sufficient to affect the data. Typically, the conductivity follows the Arrhenius' law and even an error as large as 50 percent is not enough to affect the temperature dependence of the electrical conductivity in coal slag. Because the voltage and current leads were separated, the ionic charge buildup resulting from current flow did not affect the accuracy of the measurements.

Above 1200°C there is negligible difference between d-c electrical conductivity and a-c conductivity from 40 Hz to 10 kHz in all but the low-iron simulated ash. In the natural ash at lower temperatures, the d-c conductivity is consistently lower than the a-c, an effect for which there is no explanation at present. However, the cases which display little if any frequency dependence are those slags likely to be found in an MHD generator, namely, those which contain significantly higher seed or iron than the natural ash. This observation is important experimentally since it will enable utilization of the time-saving features of the digital resistance bridge which has been ordered. It is hoped to incorporate this bridge into a data acquisition system in the future.

In addition, a new sample holder has been tested extensively for a-c measurements. It uses a platinum cup as one electrode and a heavy gauge platinum wire, which penetrates the center of the slag surface, as the other. The agreement between data taken in this configuration in the graphite tube furnace with the data taken using the four-lead technique in the silicon carbide furnace is excellent.

A preliminary thermal conductivity measurement was made on a sample of porous, partially crystalline coal slag from room temperature to approximately 600°C. This preliminary data indicates that the coal slag (Rosebud natural ash) has a thermal conductivity of approximately 1.5 $\pm$ 0.2 watts/m-K and does not vary greatly over the range. More accurate values are anticipated later. If this number is combined with an estimate of the thermal diffusivity taken from Bates's data,[8] 6 x 10^{-3} cm^2/sec, a rough estimate of the heat capacity of Rosebud natural ash is 0.21 cal/gm K (or 0.64 cal/cm^3 K). This value is about the same as for bonded mullite or fused alumina.

IV. CONCLUSIONS

At lower temperatures, below 1200°C, the frequency dependence of coal slag electrical conductivity becomes strong enough that a-c data cannot be used to approximate the d-c conductivity values. In an MHD generator, the conductivity values of interest are d-c since the generator is a steady-state device. So ultimately, designers will need d-c data. However, a-c data is important for characterizing the behavior of the charge carriers. In fact, data to 100 MHz would be especially useful to characterize the electronic and ionic parts of the conductivity since at the high frequencies only the electrons will maintain their response to a rapidly changing electric field. Hence, the contribution to the conductivity remaining at very high frequencies is the electronic part of the low-frequency conductivity.

The thermal conductivity and specific heat values for the coal slag are important, and until now, essentially undetermined parameters. Preliminary values of 1.5 $\pm$ 0.2 watt/m K for the thermal conductivity and, using estimates from Bates' data,[8] 0.21 cal/gm K for the heat capacity of Rosebud natural ash have been reported here. It is especially important now that this task measure the thermal conductivity and that MERDI measure the thermal diffusivity of identical slag samples. Then accurate heat

capacity values to 700°C (our approximate upper temperature limit for thermal conductivity) can be obtained. Since the heat capacity will not change very much for slag above 700°C (a fact which can be checked with DTA), the thermal diffusivity data obtained at high temperatures then can be reduced accurately to thermal conductivity.

MILESTONE CHART

STATUS DATE 12-31-77

TASK J

PROGRESS

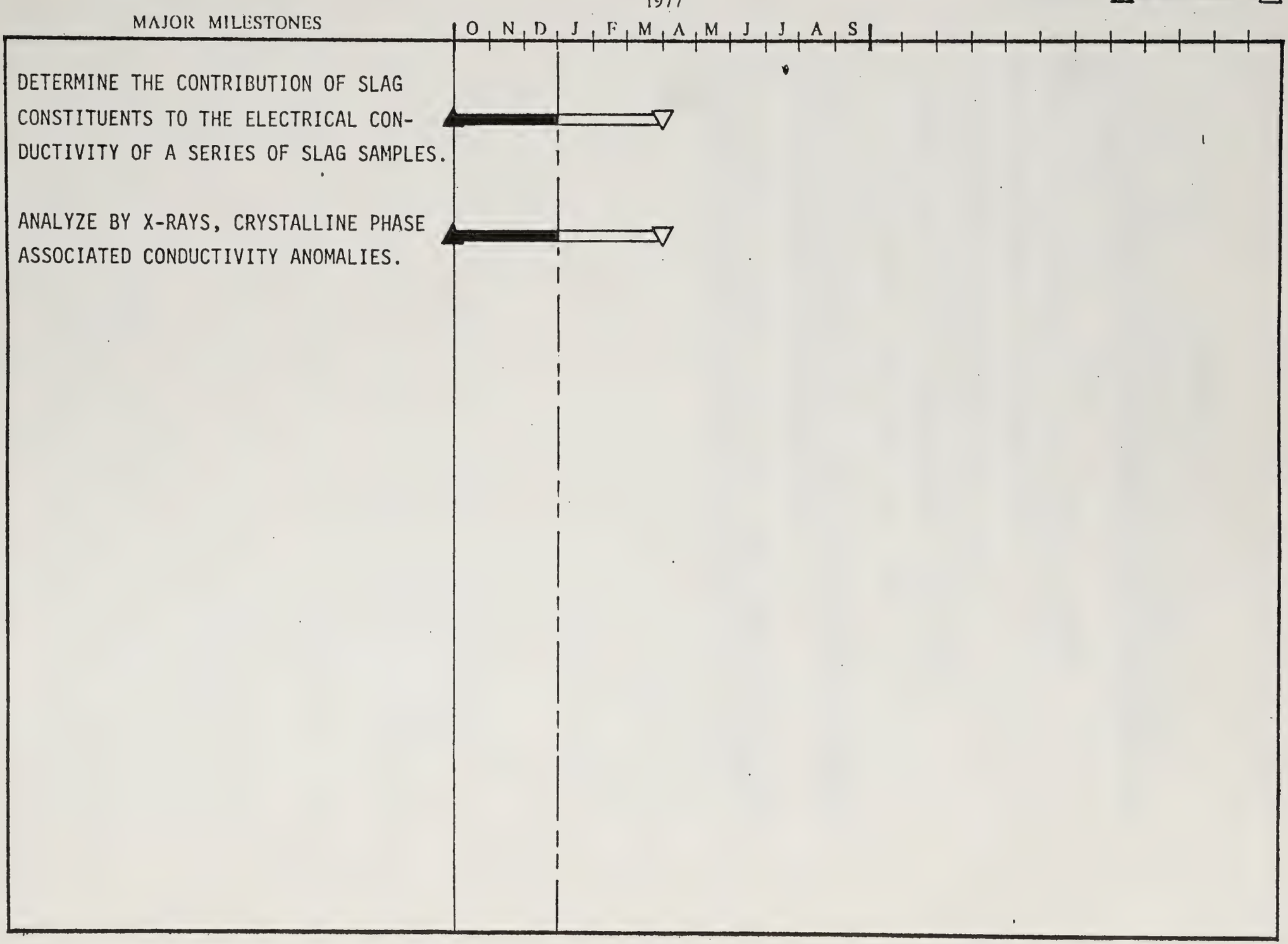

REFERENCES

1. R. J. Rosa, "Design Considerations for Coal-Fired MHD Generator Ducts," Fifth International Conference on MHD Electrical Power Generation, Munich, 1971.

2. Montana Power Company, Corette Plant, Billings, Montana.

3. Montana Power Company, Private Communication.

4. McDanel Refractors, Beaver Falls, Pennsylvania.

5. V. Gottardi and G. Bonetti, Verres Refract., 24, 41, 1970.

6. B. Lotto and S. Lazzari, Vetro Silic., 9, 5, 1965.

7. Montana Energy and MHD Research and Development Institute, MHD Power Generation: Research, Development, and Engineering, Task G1, Quarterly Report Prepared for ERDA, March 1976.

8. Battelle Pacific Northwest Laboratories, Final Progress Report on Properties of Molten Coal Slags Relating to Open Cycle MHD, Richland, Washington, BNWL-B-466, December 1975.

MHD Systems Instrumentation and Data Acquisition

R. Johnson

ABSTRACT

Work has begun on the theory of a dynamic combustor model suitable for coupling to the present nozzle/channel/diffuser dynamic model. The Task H3 plug flow model is being used to provide initial conditions and chemical equilibrium calculations. Component identification and theoretical modeling of a generalized, table-sized consolidation/inversion network simulator also have begun.

I. OBJECTIVE AND SCOPE OF WORK

The work to be performed is in the general area of MHD systems, instrumentation, and control. The work is in two categories:

A. A time-dependent nozzle/channel/diffuser (NCD) model has been completed in sufficient detail to study some configurations of supersonic MHD/steam power plants. Several CDIF and ETF case studies have been started and will continue to be analyzed. In order to properly simulate the strong coupling between the combustor and the channel present in subsonic MHD flow, the theory of a time-dependent (dynamic), one-dimensional, two-stage combustor model is to be developed suitable for coupling to the present NCD model so as to form a dynamic CNCD model when programming is completed. The Task H3 plug-flow combustor model will be used to provide the initial state conditions for the model.

B. The design of a table-sized generalized consolidation/inversion simulator is to be undertaken to provide the basis for study and evaluation of several proposed d-c to a-c power conversion schemes. The system should be modular to permit the maximum flexibility possible in the interchangeability of components; studies of hybrid schemes involving the best features of competing designs then will be possible.

Component selection will emphasize existing devices and technology so as to minimize subsequent development efforts for commercial-scale systems.

II. SUMMARY OF PROGRESS TO DATE

During the period, which is the first quarter of a six-month extension of the previous contract, work was carried out on the following items:

A. Several very long dynamic response runs were conducted to ascertain the effects on generator performance of inverter ignition angle changes. Analysis of the results of these computer simulations are still in progress. Modifications of the present NCD dynamic model computer programs to hopefully increase its speed are proceeding in parallel with this analysis.

B. Work has begun on deriving a theoretical model for a dynamic, one-dimensional, two-stage combustor simulation.

C. Design work on a table-sized consolidation/inversion simulator for the study of various alternative power conversion configurations has begun. Dr. K. Marcotte, who has extensive experience in the design of power interface equipment, has replaced Dr. Robles, who has taken another job. First priority is being given to the design layout of generator-inverter simulator and the inverter-power grid interfaces.

D. Preparation for and delivery of results were completed for a MHD/DOE formal review (November 14-16).

E. A technical paper abstract, entitled "Transient Response of MHD/Steam Bottoming Plants with Phase Air Preheaters and Heat Capacitor," was submitted to the 17th Symposium on Engineering Aspects of MHD.

III. DETAILED DESCRIPTION OF TECHNICAL PROGRESS

A. Time-Dependent and Steady-State Computer Models

The time-dependent NCD ETF computer simulations program completed during the previous quarter was used to perform several transient response simulations for various ignition angle changes. These computer runs required periods of up to 21 hours of computer time to simulate 6.5 seconds of real-time generator performance. The results obtained are still being analyzed; however, several modifications of the program already have been initiated to improve the performance. Modifications presently underway include the following: 1) introduction of plotting routines into the program for better presentation of results, 2) the reformatting of printer output to allow intermediate storage on either magnetic tape or disc, and 3) study of modifications to increase the speed of computation. In addition, it has been noted that because of different assumptions in the steady-state program MHDAV and the dynamic program MHDTD, the steady-state solution predicted that MHDAV does not give exactly the same results as that obtained by MHDTD. Although the differences are small, methods are being sought to eliminate the discrepancy so as to produce consistent results from both programs.

B. Dynamic, Two-Stage Combustor Model

To permit the study of general subsonic MHD combustor-generator interaction, a dynamic two-stage combustor model is being formulated to interface with the present NCD dynamic program MHDTD. A plug flow combustor model developed by Task H3 is being used to supply initial and boundary conditions for the dynamic combustor model. The assumptions which are being made include the following:

1. The model is one-dimensional,

2. Dynamic changes are slow compared to chemical kinetic rates so that chemical equilibrium may be assumed, and

3. There are nearest neighbor char burn interactions only.

General eigerfunction expansions of the linearized Navier-Stokes Green's function problem are used to predict the response to a change in boundary conditions at the combustor-nozzle interface.

C. Design of a Generalized Consolidation/Inversion Simulator

Methods for the study of alternative designs for MHD d-c power to three-phase a-c power conversion equipment are highly desirable as detailed design of an ETF plant is contemplated. There are three approaches which appear feasible:

1. Construction of full-scale power conversion networks for use on existing facilities,

2. Computer simulation of full-scale power conversion networks, and

3. Construction of a generalized low power level conversion network simulator with backup computer simulation.

The first approach is not feasible for more than a single network design because of expense. The second approach is the cheapest to implement but is only cost effective when performed on a hybrid computer. The validity of the results also is questionable unless a hardware model is available for comparison of selected results.

The third approach is that taken here; the advantages are as follows:

1. Using low power components ($\sim$ 1 KW), the cost of components is small, and specialized components can be fabricated quickly and at minimum cost.

2. Simulations can be performed in real-time so that hundreds of different operational and fault conditions can be studied in a realistic time frame.

3. Many different power conversion schemes may be studied by interchanging components.

4. The interaction of the network with a power grid may be simulated safely without concern for destruction of expensive components.

5. Certain selected configurations can be computer modeled and checked against the simulator results for validity of model theory and optimization of design.

6. Programmable generators which will closely simulate realistic MHD generator voltage-current characteristics are available commercially in this power range.

During the present period, work has concentrated on defining the power level (set by commercially available, programmable power supplies), study of the available literature, study of the present work at Avco, GE, and EPRI relative to MHD inverters, and selection of several components.

IV. CONCLUSIONS

Work is progressing according to schedule on modified work statements as approved by the November 14-16 DOE review committee.

MILESTONE CHART

STATUS DATE 12-31-77

TASK H1

PROGRESS

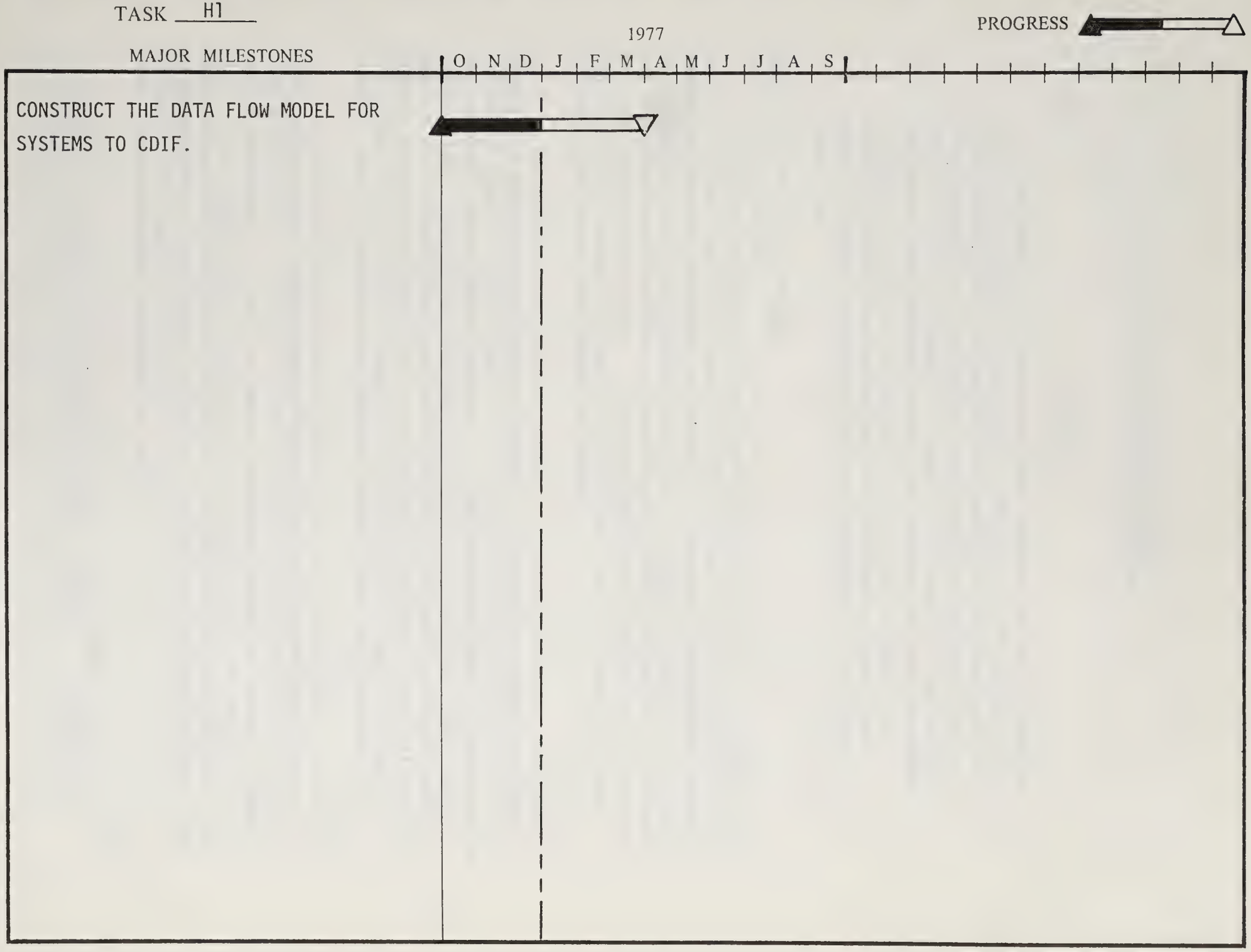

Cycle Analysis and Control

D. A. Pierre and D. A. Rudberg

ABSTRACT

Combined-cycle MHD-steam power systems are being modeled by digital computer simulations. Methods of providing efficient control of such systems are being investigated by use of the simulations to ensure stable modes of response and to obtain coordinated control of many interdependent subsystems. Two papers were prepared during the quarter and are described. Efforts are directed at improving the component models, especially that of the combustor, and first-principle dynamic models of plant components are being embedded in the latest simulation.

I. OBJECTIVE AND SCOPE OF WORK

Task H3 is developing system component models which are suitable for control system simulations studies. The purpose of these studies is to determine control structure and controller parameter values which result in safe, stable, fast, and smooth transitions in operating points. The results of the studies are to be generally applicable to the ETF and commercial MHD-steam power plants. By performing these studies now, it may be possible to influence the design of MHD-steam plants to make them more reliable, efficient, and easier to control.

The time-dependent combustor model is important from the view point of combustion stability and channel response. Combustion stability is an extremely important topic because it affects plant integrity and safety and smoothly controllable response. A time-dependent model, incorporating compressible fluid flow, chemical equilibrium and enthalpy, char particle heating and burnout kinetics, devolatilization (rate and general endothermic nature), and heat loss from radiation and convection, will be an effective tool in studying combustion stability and associated topics of acoustic wave propagation and standing waves within the combustor.

The time-dependent combustor model also will constitute an essential part of the overall time-dependent model that will permit analysis of channel electrical and fluid dynamic response to perturbations originating in the combustor. It will be one of the parent model set used in generating input-output models, which are described below. The model will be a combination of fluid dynamic equations and solution techniques from time-dependent channel work done by Task H1, and of chemical equilibrium, char burnout kinetics, heat loss, etc., from a steady-state, plug-flow, two-stage combustor model developed by Task H3.

From the detailed time-dependent models, input-output models will be produced for specific ETF and base-load MHD components. Input-output models contain no internal detail and consist only of a set of curve fits of desired outputs to input values. Parameters of the system are

implicit in the curve-fit coefficients. In this manner, models of large systems can be run in orders of magnitude less time and with greatly reduced computer requirements than if detailed parent models were used. A change of system parameters requires only that another set of input-output models be made from the detailed parent models, thus embodying those new parameters.

Several input-output modeling runs already have been made using existing parent models of the plug-flow, steady-state combustor for combustor input-output models and detailed chemical equilibrium, electrical conductivity, and enthalpy programs for channel gas modeling. An automatic parameter sweeping routine is used, and the results are stored in a file for reduction to input-output models by an existent multi-variable curve-fitting routine.

The computer-controlled, combined-cycle plant model is an important step in the progression from conceptual system studies to a functional piece of hardware. There is a tendency to confuse control system information flow and selection of information processing algorithms with the completion of the control problem. But the selection of system topology, information flow, and control algorithms are only initial steps (albeit essential ones) in the process of ultimately exerting effective control. The mechanization of specified information flow, of algorithmic computation, and of assertion of control variables at proper points in the controlled plant are the finale in real-time control.

It has been the investigators' experience in providing real-time computer control for an aluminum processing plant and other smaller projects, that actual coding of algorithms and supervisory programs immensely sharpens understanding of preceding conceptual studies. It crystallizes the notion that a physical plant (in this case the MHD-steam plant) having a set of measurable variables, a set of controllable variables, and a system of dynamics by which it operates is being dealt with.

The investigators will use their set of system models to act as the plant. The computer controller will be a set of algorithms and a simple supervisory routine to properly sequence data inputs, algorithm computation, and control signal assertion at proper points. The value of beginning this essential step as early as possible lies in its intrinsic feedback to the conceptual process as well as its being a necessary bridge between conceptual studies and hardware.

II. SUMMARY OF PROGRESS TO DATE

The cycle analysis and control task expanded both its detailed two-stage combustor model and its combined-cycle control system models. Two papers were prepared for consideration of presentation at the 17th Symposium on Engineering Aspects of MHD. One of the papers is entitled "Reducing Combustion Air Temperature Variations in MHD-Steam Power Plants" and is attached as an appendix to this report. Also attached is a detailed abstract of the second paper, "Sensitivities of Outputs to Variations of Inputs in MHD Combustors."

During the quarter, a full-scale review of this program was conducted by the Department of Energy. In summary, the work of Task H3 was viewed as being very critical to the success of the national MHD program, and significant progress was recognized. A proposal was prepared to continue and expand the work during the thirty-month period which follows the current six-month contract period.

III. DETAILED DESCRIPTION OF TECHNICAL PROGRESS

In the attached paper on MHD-steam power plants, the combined-cycle simulation of System Model III is used to evaluate the effectiveness of a heat capacitor in smoothing short-term temperature ripple caused by regenerative air preheater switching. Temperature transients are important because they affect the electrical conductivity of the MHD generator working fluid and, in turn, net plant output power. The heat capacitor is shown to be a desirable MHD system component from the standpoint of the ceramic mass required to reduce combustion air temperature ripple.

A computer code was written to incorporate a first-principle dynamic model of the radiant boiler in the combined-cycle system simulation. The new simulation is called System Model IV and will contain dynamic control characteristics of the air compressor, the boiler feed pumps, radiant boiler, economizers, superheater, and reheater. The dynamics of each component of the bottoming plant are governed by conservation equations for mass, momentum, and energy, as are described in the 1977 annual report.

During the quarter, several modifications were made to the combustor program to improve performance with respect to heat loss associated with slag rejection, and to treat more accurately the water that is tightly bound to the coal and which appears as oxygen in the ultimate analysis. The combustor program was embedded in an automatic parameter sweeping routine, and initial data were calculated for development of input-output combustor models. An existent optimization routine will be used to convert datum points into curve fits for the input-output models. The models then will be incorporated into the combustor-nozzle-channel-diffuser model (CNCD) to be used in combined-cycle-control System Model IV.

As part of the same activity, sensitivities of selected output variables with respect to variations of combustor geometry and operating conditions were calculated. An abstract for a paper based on these results was submitted to the 17th Symposium and is attached.

Discussions about the time-dependent combustor model were held with personnel of Task H1. The manner in which compressible fluid flow equations will be merged with thermochemical behavior, heat loss, char burnout, and enthalpy relations was discussed.

IV. CONCLUSIONS

The combustor model is now producing results. It is being used at MSU in making input-output models and in making sensitivity studies. Its thermochemical, char burnout, heat loss, and energy balance features will

be combined with fluid dynamic equations in formulation of a time-dependent combustor model. It also is being used at MERDI by groups interested in combustor behavior per se and in the effects of combustor performance on plant effluent.

It is planned to continue development of input-output models suited to use in the overall steady-state CNCD model and to continue sensitivity studies on combustor outputs as a function of combustor parameters and inputs. Discussion and plans will continue for the formulation of a time-dependent combustor model, based on merging appropriate features of the current steady-state model with fluid dynamic equations and solution techniques.

During the next quarter, a framework will be developed for a computer controlled combined-cycle power plant model in which separate routines are used to simulate 1) a combined-cycle power plant in the 250 MWt range and 2) a central control computer. Both centralized and distributed control will be considered. Simulated real-time outputs from the MHD-steam plant model will be used by the computer-control model to test and evaluate real-time, on-line control policies.

MILESTONE CHART

STATUS DATE 12-31-77

TASK H3

PROGRESS

MAJOR MILESTONES

1977

O N D J F M A M J J A S

DEVELOP DYNAMIC COMBUSTION MODEL AND INTRODUCE IN TIME DEPENDENT MHD STEAM SIMULATION MODEL.

EXPAND THE PRESENT SET OF COMBINED SYSTEM MODELS TO INCLUDE STEAM FLOW RATES, PRESSURES, AND TEMPERATURES.

APPENDIX

REDUCING COMBUSTION AIR TEMPERATURE VARIATIONS IN MAGNETOHYDRODYNAMIC/STEAM POWER PLANTS

J. D. Aspnes
University of New Hampshire
Durham, New Hampshire

D. A. Pierre
Montana State University
Bozeman, Montana

T. C. Robles
Tennessee Technological University
Cookville, Tennessee

Abstract

A dynamic computer model of a magnetohydrodynamic (MHD)/steam power plant is used to evaluate methods for reducing temperature variations in preheated combustion air. The effectiveness of a heat capacitor in smoothing short-term temperature ripple caused by regenerative air preheater switching is discussed. In addition, the results of utilizing a control loop specifically to reduce long-term fluctuations in preheated air temperature are given. Representative computer simulations showing the effects of specific overall plant control configurations are included.

I. INTRODUCTION

In this paper, computer simulation of a commercial scale magnetohydrodynamic (MHD)/steam combined-cycle power plant is used to model dynamic characteristics of the overall system. The effect of a heat capacitor on net MHD electrical output power, net steam turbine output power, and net plant output power is given. The results of using a control loop specifically to reduce long-term variations in preheated combustion air temperature is described. Simulation results are shown for a 4000 MW (fuel thermal input), coal-fired plant with an MHD topping cycle and a steam turbine bottoming cycle.

The purpose of this paper is: (1) to describe the dynamic model of an overall MHD/steam combined cycle; (2) to define the regenerative air preheater

and heat capacitor in a physical sense, and to describe their associated models; (3) to determine the effect of the heat capacitor on key system variables; and (4) to show the result of including a preheated combustion air temperature controller. Previous papers have not investigated these means of controlling preheated air temperature variations with an overall system dynamic simulation model.

II. THE OVERALL SYSTEM MODEL

The plant configuration is assumed to be a coal-fired, direct open-cycle MHD/steam combined cycle with regenerative air preheaters utilizing MHD exhaust gases to preheat combustion air. The overall system model block diagram is shown in Figure 1. Detailed block diagrams defining major divisions of the overall system have been published [1]. The combustor/nozzle/channel/diffuser model has been described in [2]. Briefly, the control scheme is derived from boiler-following or conventional power plant control with the addition of feedforward controllers for the steam turbine valves and the firing system. This configuration results in 12 independently adjustable controller design parameters. Throttle pressure error primarily controls the firing system and generation error governs turbine valve area and ultimately steam turbine output power. The combustor/nozzle/channel/diffuser (CNCD) model is of input/output form because the CNCD has much smaller time constants than other system components such as the steam bottoming plant and the regenerative air preheaters. This model is developed from the quasi one-dimensional conservation equations for mass, energy, and momentum in the MHD channel, and an energy balance equation for combustion equilibrium.

The steam boiler and turbine valve description is patterned after the Laubli-Fenton model [3] and has thermal power from the air preheaters and

water heating, and fractional change in turbine valve area as inputs. Outputs are stack and boiler losses, fractional change in throttle pressure, and power to the steam turbines.

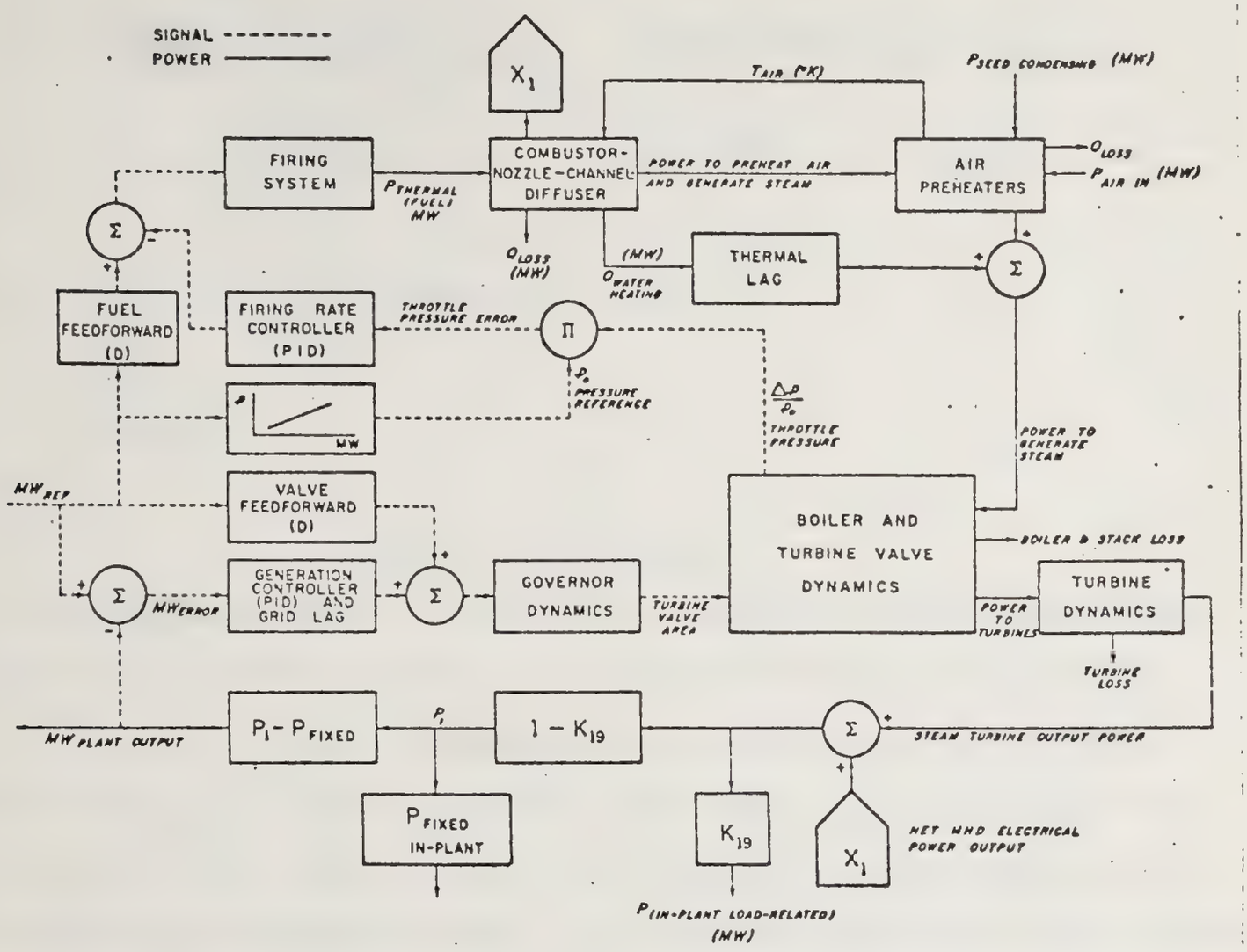

Figure 1. System model block diagram

The overall system model contains 85 variables and 50 constants.

III. AIR PREHEATER MODEL

The air preheaters are modeled as shown in Figure 2. Inputs to the preheaters are combustion gases from the diffuser outlet, thermal power recovered from condensing seed, and power of incoming air due to the air compressor. Outputs are preheated air temperature, thermal power loss to ambient, and thermal power available to the steam (bottoming) plant.

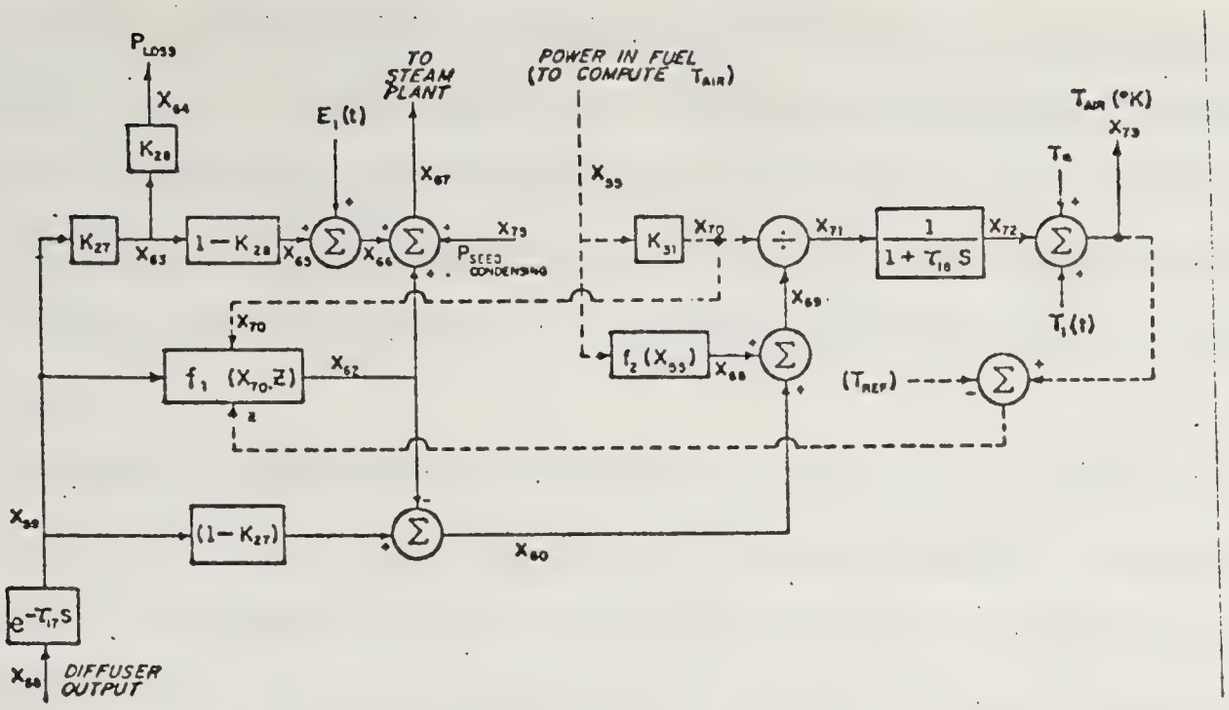

Figure 2. Air preheaters

Of particular interest in Figure 2 is a controller which is suitable for reducing or eliminating long-term variations in preheated air temperature. The difference, z, between preheated air temperature, x_{73}, and a reference temperature, T_{REF}, is used to specify a power level, X_{62}, which changes the fraction of diffuser output thermal power available to preheat combustion air or drive the steam bottoming plant. By specifying air/fuel mass ratio, calorific value of fuel, fuel thermal input power, and specific heat of air at constant pressure, the power required to raise combustion air temperature a desired amount may be determined. Multiplier K_{31} performs this required conversion and for the system under consideration:

$$X_{70} = K_{31}\, X_{55} \tag{1}$$

$$= (3.64 \times 10^{-4}\ \frac{MW}{MW_T\,°K})(X_{55}\ MW_T)$$

or

$$X_{70} = (3.64 \times 10^{-4})(X_{55}) \quad MW/°K \tag{2}$$

also,

$$X_{62} = (A)(X_{70})(z) \quad MW \tag{3}$$

where A is a constant which is altered in following computer simulations to vary loop gain. Since the time constant associated with the regenerative air preheaters, T_{18}, is of the order of 500 seconds, the above means of reducing preheated air temperature variations is not suitable for rapid transients such as caused by cycling heat exchanger units. It will be seen that a heat capacitor is an effective method for reducing fast temperature fluctuations in preheated combustion air.

Ten separate regenerative heat exchangers are assumed, all cycling between reheat and blowdown according to the schedule shown in Figure 3. Reheat is the part of the exchanger cycle in which the ceramic core of the heat exchanger is heated by combustion gas passing through the core from the diffuser to the steam plant. Blowdown occurs when air is heated by being moved through the heat exchanger from the compressor to the combustor.

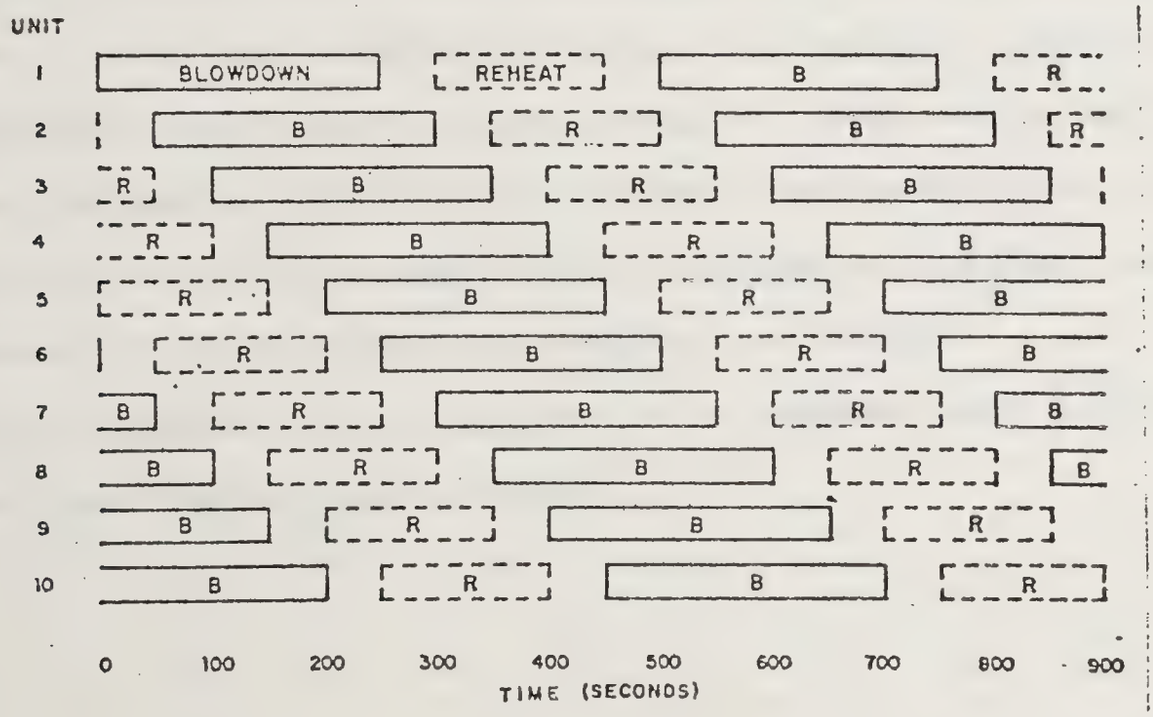

Figure 3. Regenerative heat exchanger schedule

Figure 3 illustrates important details about the heat exchanger format assumed in this paper: (1) three units are on reheat, five units are on blowdown, and two units are switching at any instant of time; and (2) a particular unit has a 500 second period consisting of 250 seconds on blowdown, 150 seconds on reheat, and two 50 second settling intervals between reheat and blowdown. Heat exchanger cycling results in preheated air temperature variations at the heat exchanger exit during blowdown, $(T_1(t))$, and also thermal power variations at the heat exchanger exit during reheat $(E_1(t))$. This thermal power variation is a disturbance input to the steam bottoming cycle. Graphs of $T_1(t)$, both with and without a heat capacitor placed in series with the heat exchanger array, are presented in Figure 4. The nominal value of preheated air temperature is 1800°K. A plot of $E_1(t)$ is given in Figure 5. All graphs have a 50 second period which follows from the heat exchanger schedule of Figure 3. These temperature and power functions as well as the heat exchanger and heat capacitor designs were developed using a lumped-mass model for the analysis of cored-brick regenerative heat exchangers described in [4] and [5]. The peak value of temperature ripple without a heat capacitor is 7.7°K. With a heat capacitor, $T_1(t)$ has extremes of -0.58°K and + 0.44°K about the average value of 1800°K. By comparison, doubling the number of heat exchangers on blowdown reduces the preheated air temperature ripple to a peak value of 3.85°K.

Design parameters for the regenerative air preheater units and the heat capacitor simulated are given in Table 1.

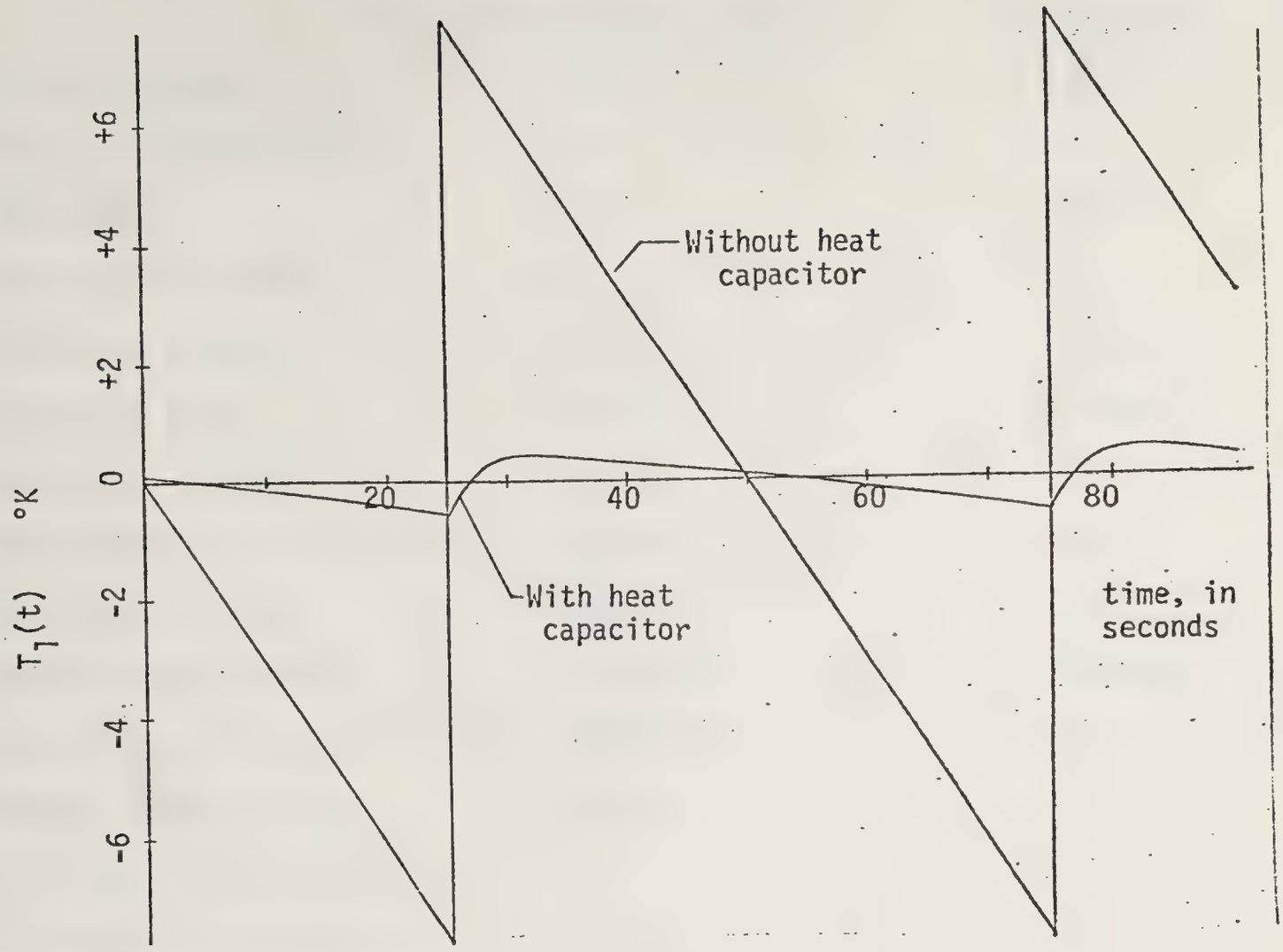

Figure 4. Variations in preheated air temperature

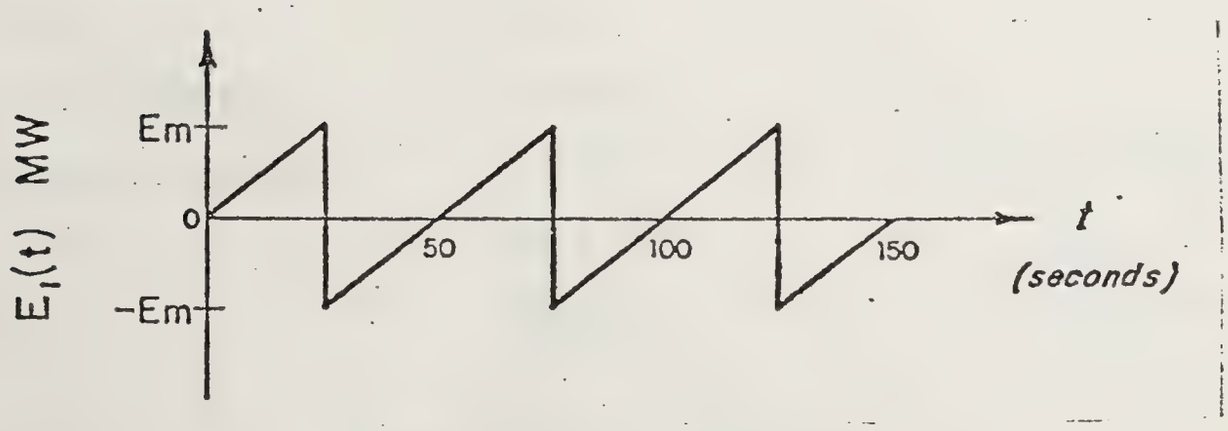

Figure 5. Thermal power variations at heat exchanger exit during reheat

Table 1. Air preheater and heat capacitor design parameters

	Air preheater(single unit)	Heat capacitor
Flow hole diameter	0.019 m	0.0127 m
Spacing to diameter ratio	1.4	1.4
Bed length	4.2 m	1.835 m
Total number of units	10	1
Ceramic bed diameter	8.72 m	10.8 m
Ceramic bed area	59.64 m^2	91.58 m^2
Reheat inlet velocity	75 m/sec	----
Reheat Reynolds no. inlet/exit	4801/5605	----
Reheat pressure drop	4080 Pa	----
Blowdown inlet velocity	3.54 m/sec	20 m/sec
Blowdown Reynolds no. inlet/exit	3588/2599	----
Blowdown pressure drop	263 Pa	----
No. blowdown heat exchangers	5	----
No. reheat heat exchangers	3	----
No. switching heat exchangers	2	----
Reheat time	150 sec	----
Blowdown time	250 sec	----
Switching time	50 sec	----
Reheat ripple temperature	$\pm$ 23.25°K	----
Blowdown ripple temperature	$\pm$ 7.7°K	approx. $\pm$ 0.51°K
Ceramic volume	134.6 m^3	87.7 m^3
Ceramic mass	444,080 kg	296,788 Kg

IV. COMPUTER SIMULATION RESULTS

Representative computer simulation results are given in Figures 6 through 13. Controller design parameters for the cases shown appear in Table 2. Case 1 is used as a comparison for Case 2 and exhibits underdamped system response.

Case 2 controller parameters were fixed by an optimization routine [6] that minimizes integral-square generation error of net plant output power X_2 compared with MW_{REF}. Other cases have been reported in [2]. In Figures 6 through 13, the disturbance input to the system is a -50MW step change in MW_{REF} at t=0.

Table 2
Controller Design Parameters for Simulation Cases

Case	Controller Design Parameters											
	K_2	K_3	K_4	K_5	K_{20}	K_{21}	K_{22}	K_{23}	τ_2	τ_3	τ_{13}	τ_{14}
1	10^{-4}	10^{-3}	0.0	0.0	0.0	10^{-4}	10^{-4}	0.0	0.0	0.0	0.0	0.0
2	1.13×10^{-3}	5.15×10^{-4}	1.59×10^{-4}	10^{-2}	10^{-2}	4.84×10^{-4}	0.0	1.90×10^{-3}	0.5	0.2	0.2	0.1

K_2, K_3, K_4, K_5, τ_2, and τ_3 are design parameters of the generation and valve feedforward controllers. K_{20}, K_{21}, K_{22}, K_{23}, τ_{13} and τ_{14} are design parameters of the firing rate and fuel feedforward controllers. K_{20} corresponds to K_5, K_{21} corresponds to K_2, K_{22} corresponds to K_3, K_{23} corresponds to K_4, τ_{13} corresponds to τ_3, and τ_{14} corresponds to τ_2. The generation controller and the firing rate controller are both of the same form as are the valve and fuel feedforward blocks.

Figures 6 and 7 show $X_2(t)$ with and without a heat capacitor included in the air preheater system. The magnitude jump due to air preheater cycling is 5.6 MW for case 1 and 4.74 MW for Case 2. This rapid fluctuation is not evident in Figure 7 where the heat capacitor is used.

Figures 8 and 9 illustrate net steam turbine output power, $X_{41}(t)$, with and without the heat capacitor included. Increased disturbances may be noted when the heat capacitor is not used, even though $E_1(t)$, the variation in thermal power to the steam plant, is unchanged with the addition of the heat capacitor.

Figures 10 and 11 show net MHD electrical output power as a function of time, $X_{42}(t)$, with and without the heat capacitor included. The source of magnitude jumps in plant output power due to preheater cycling is evident, as is the improvement resulting from the addition of the heat capacitor.

Figures 12 and 13 represent results of a study to determine the effectiveness of long-term combustion air temperature control. Figure 12 illustrates

long-term variations in preheated air temperature, X_{73}, for cases in which A of Equation 3 is given values ranging from 0 (no feedback) to 10^3. A heat capacitor was not included in these simulations and T_{REF} = 1800°K in all cases. The resulting shift in diffuser thermal power, X_{62}, from the steam plant to the air preheaters is given for these cases in Figure 13.

V. CONCLUSIONS

The conclusions are based on results presented in this paper and by Robles and Johnson [5].

The heat capacitor has been shown to be an effective method of reducing rapid transients in preheated combustion air temperature caused by cycling heat exchanger units. Rapid temperature transients caused by any other means will, of course, be similarly reduced. Temperature transients are important because they affect key system variables such as MHD generator electrical output and, in turn, net plant output power. This situation occurs because electrical conductivity of the MHD generator working fluid is an exponential function of temperature.

From the point of view of ceramic mass requirements above (Table 1), a heat capacitor is an economically attractive alternative to additional air preheater units as a means of reducing combustion air temperature ripple. Additional valves are also required as the number of air preheater units is increased [5], which further improves heat capacitor economics.

The steam plant is essentially unaffected by thermal power fluctuations induced by heat exchanger cycling as shown in Figures 8 and 9. Comparing these figures in regions of heat exchanger switching, it appears possible for controls to be implemented which would force the steam turbines to partially counteract the fluctuations in MHD generator output. This might be achieved through feed-forward control synchronized to heat exchanger switching. In view of the

magnitude of steam turbine time constants and allowable rates of change, however, it seems evident that the best means of reducing heat exchanger-induced transients is to reduce preheated air temperature variations.

Figures 12 and 13 show that long-term variations in combustion air temperature may be reduced or eliminated by appropriate controls. Throttling high temperature gas will probably create excessively strigent operating conditions on valves in implementing this scheme. A potential solution may be to have several small on/off valves to adjust thermal power to the air preheaters in discrete steps.

Finally, the magnitude of plant generation controller and firing rate controller design parameters used in these simulations does not significantly affect heat capacitor results or long-term variations in combustion air temperature.

ACKNOWLEDGEMENTS

The authors wish to acknowledge the financial support of the Research Office of the University of New Hampshire, the Electrical Engineering Department of Montana State University, and the Montana Energy and MHD Research and Development Institute under contract no. EF-77-C-01-2524 with the Department of Energy. Credit is due Professors Roy Johnson and Donald Rudberg for contributions on several aspects of system modeling.

REFERENCES

[1] J. Aspnes and D.A. Pierre, "Dynamic Modeling and Control of Magneto-hydrodynamic/Steam Systems," IEEE Special Publication Energy Development III, 77CH1215-3-PWR, January, 1977, pp. 7-15.

[2] J.D. Aspnes and D.A. Pierre, "Dynamic Modeling and Control of Magneto-hydrodynamic/Steam Electrical Power Generating Plants," Proceedings of the 16th Symposium on Engineering Aspects of Magnetohydrodynamics, May, 1977, pp. X.1.1-X.1.7.

[3] F. Laubli and F.H. Fenton, Jr., "The Flexibility of the Supercritical Boiler as a Partner in Power System Design and Operation; Part I: Theoretical Relationships; Part II: Application and Field Test Results," IEEE Transactions on Power Apparatus and Systems, Vol. PAS-90, No. 4, July-August, 1971, pp. 1719-1733.

[4] T.C. Reihman, H.W. Townes, and C.J. Moser, "Thermal Analysis Techniques for Regenerative Heat Exchanger Simulation," ASME Paper 76-WA/HT-7, July 26, 1976.

[5] T.C. Robles, and R.M. Johnson, "Heat Capacitor for MHD Electric Power Generation System, "Proceedings of the 16 Symposium on Engineering Aspects of Magnetohydrodynamics, May, 1977, pp. IX.7.41-IX.7.46.

[6] D.A. Pierre and M.J. Lowe, Mathematical Programming Via Augmented Lagrangians, Addison-Wesley, Reading, MA, 1975.

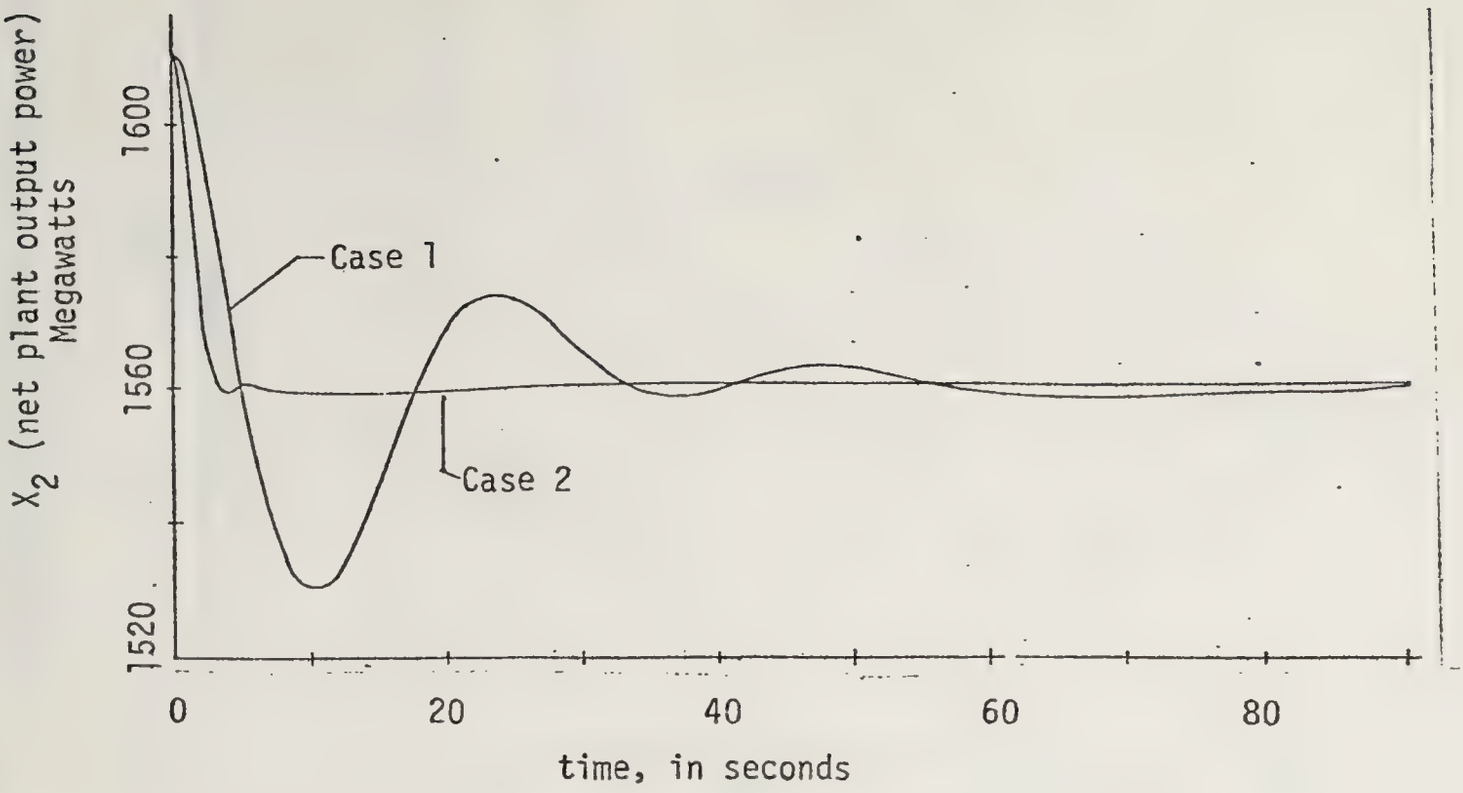

Figure 6. Net plant output power with heat capacitor

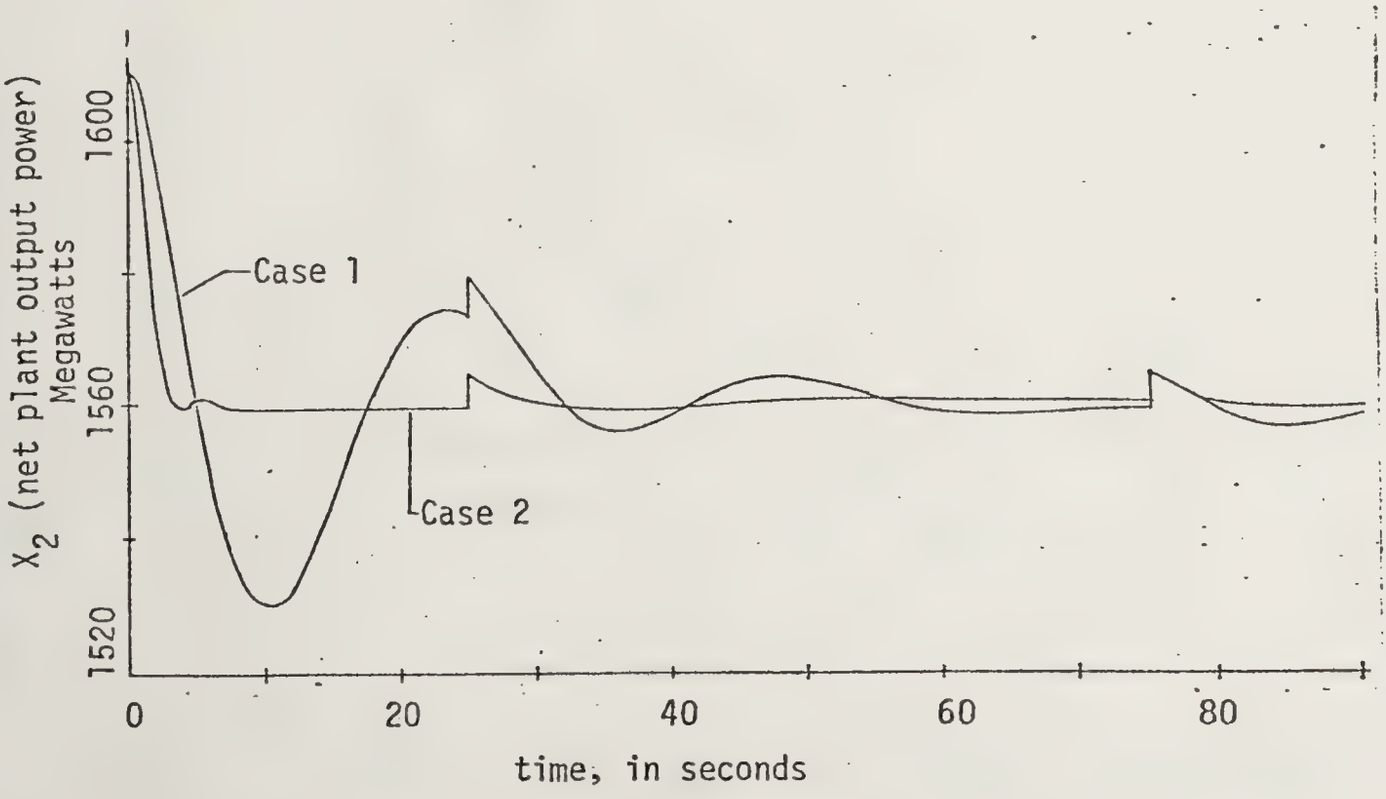

Figure 7. Net plant output power without heat capacitor

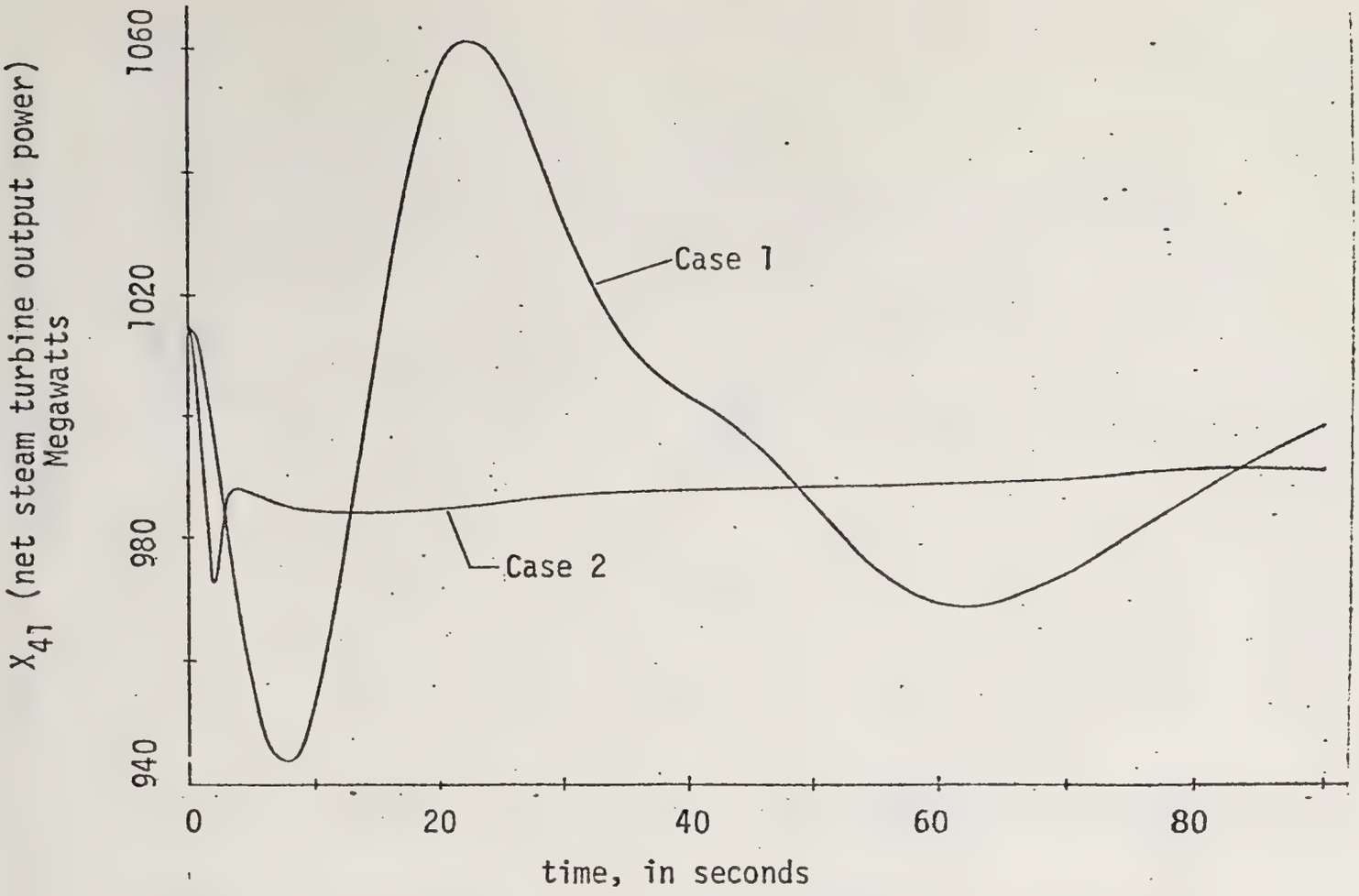

Figure 8. Net steam turbine output power with heat capacitor

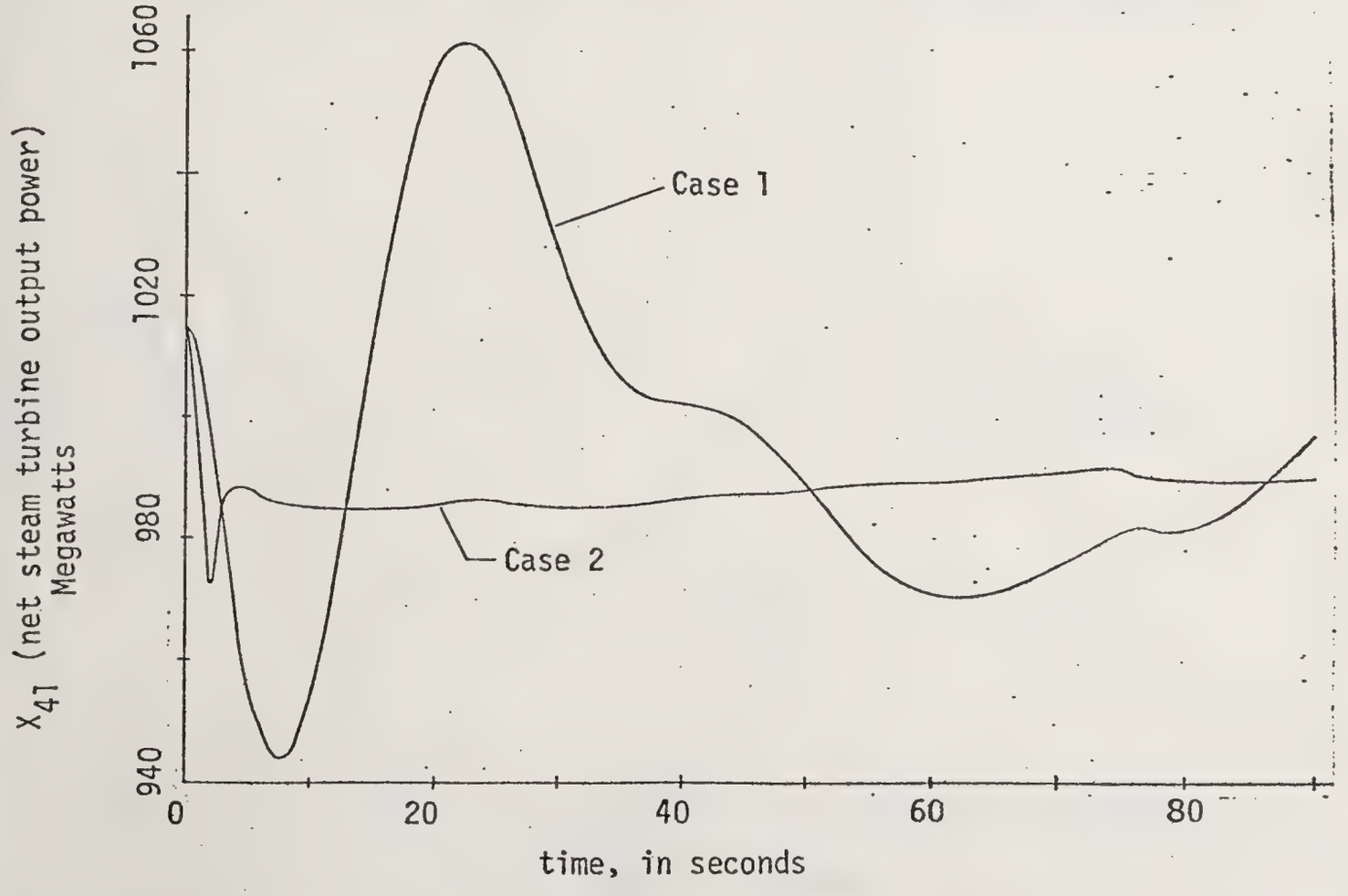

Figure 9. Net steam turbine output power without heat capacitor

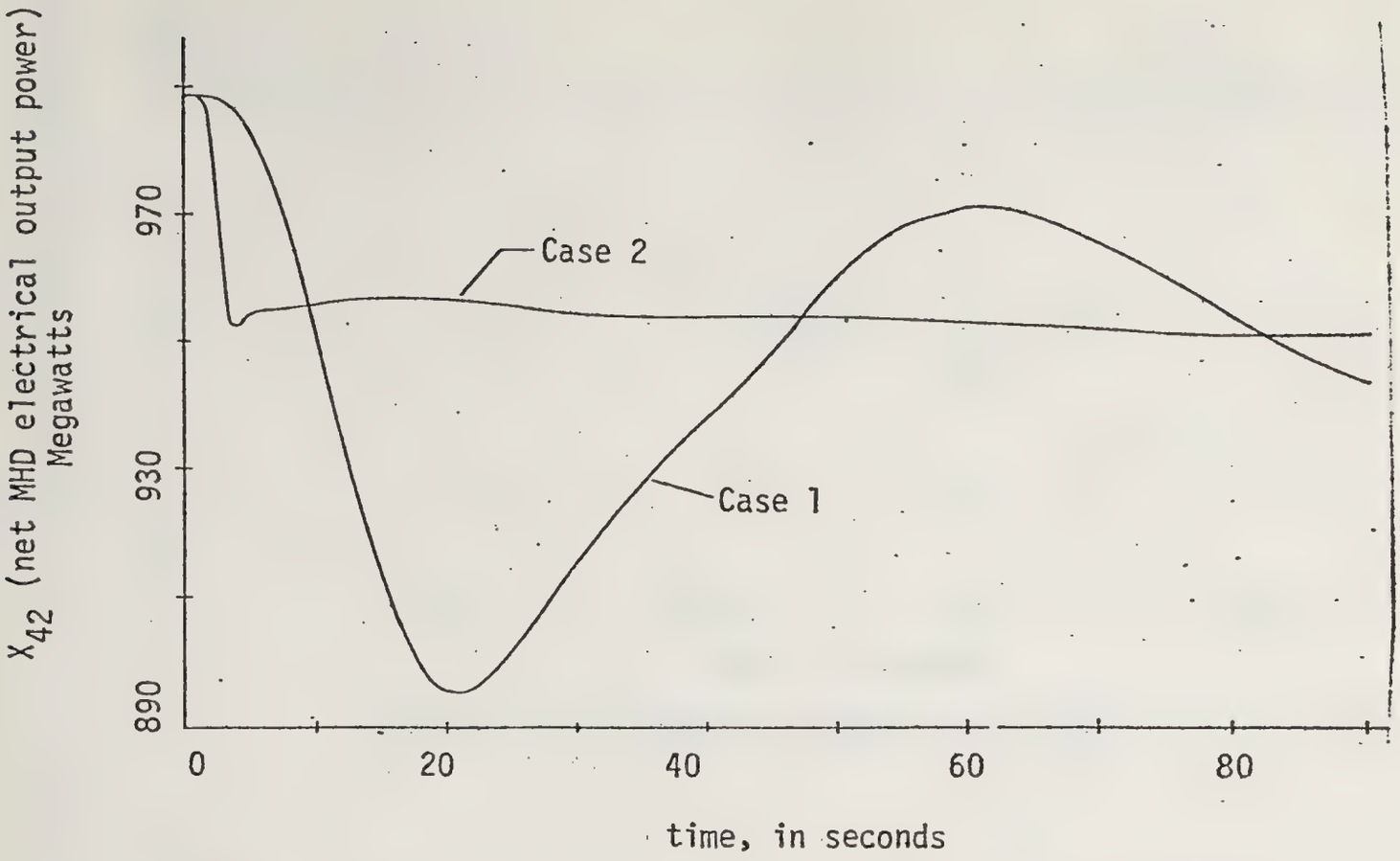

Figure 10. Net MHD electrical output with heat capacitor

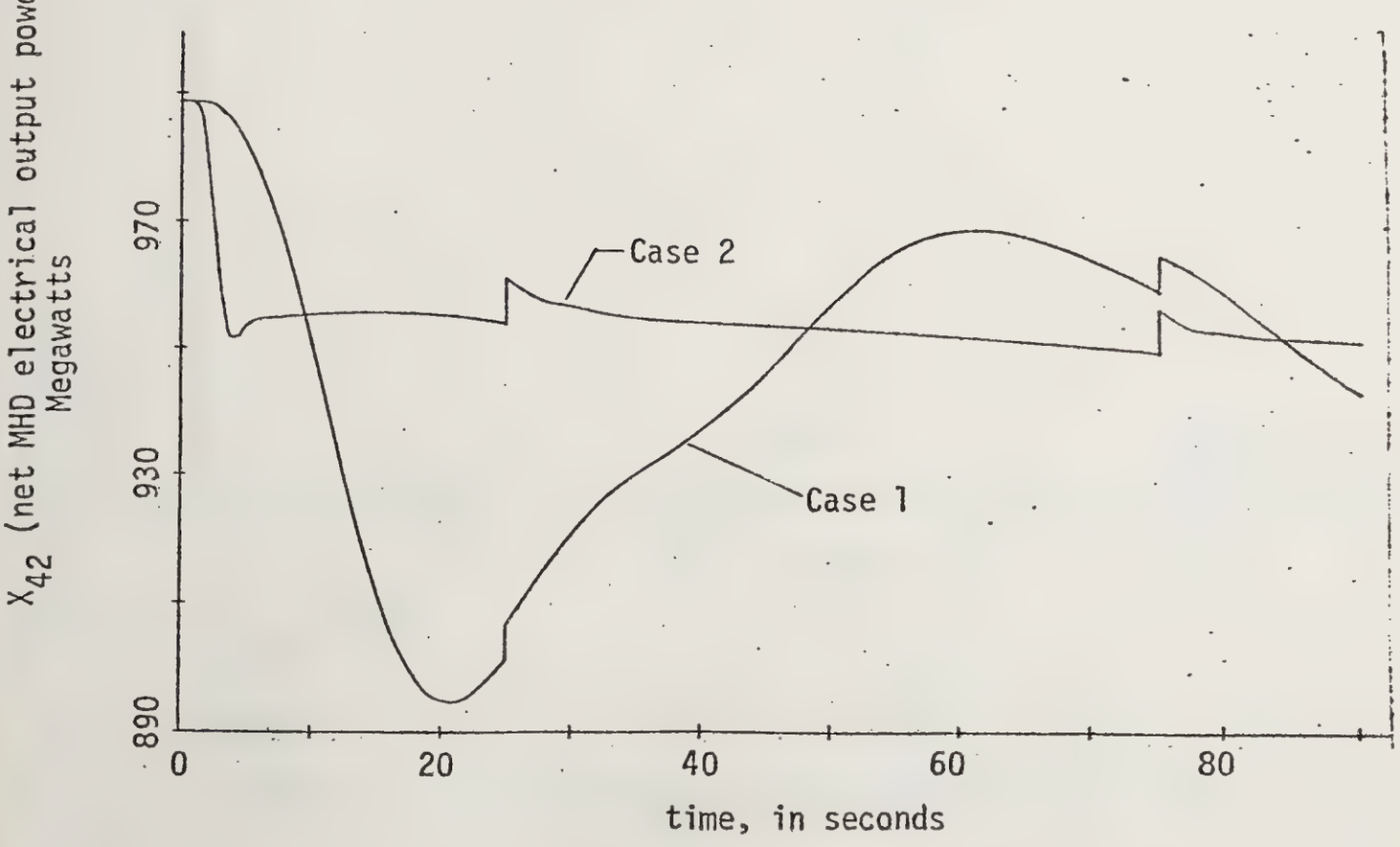

Figure 11. Net MHD electrical output without heat capacitor

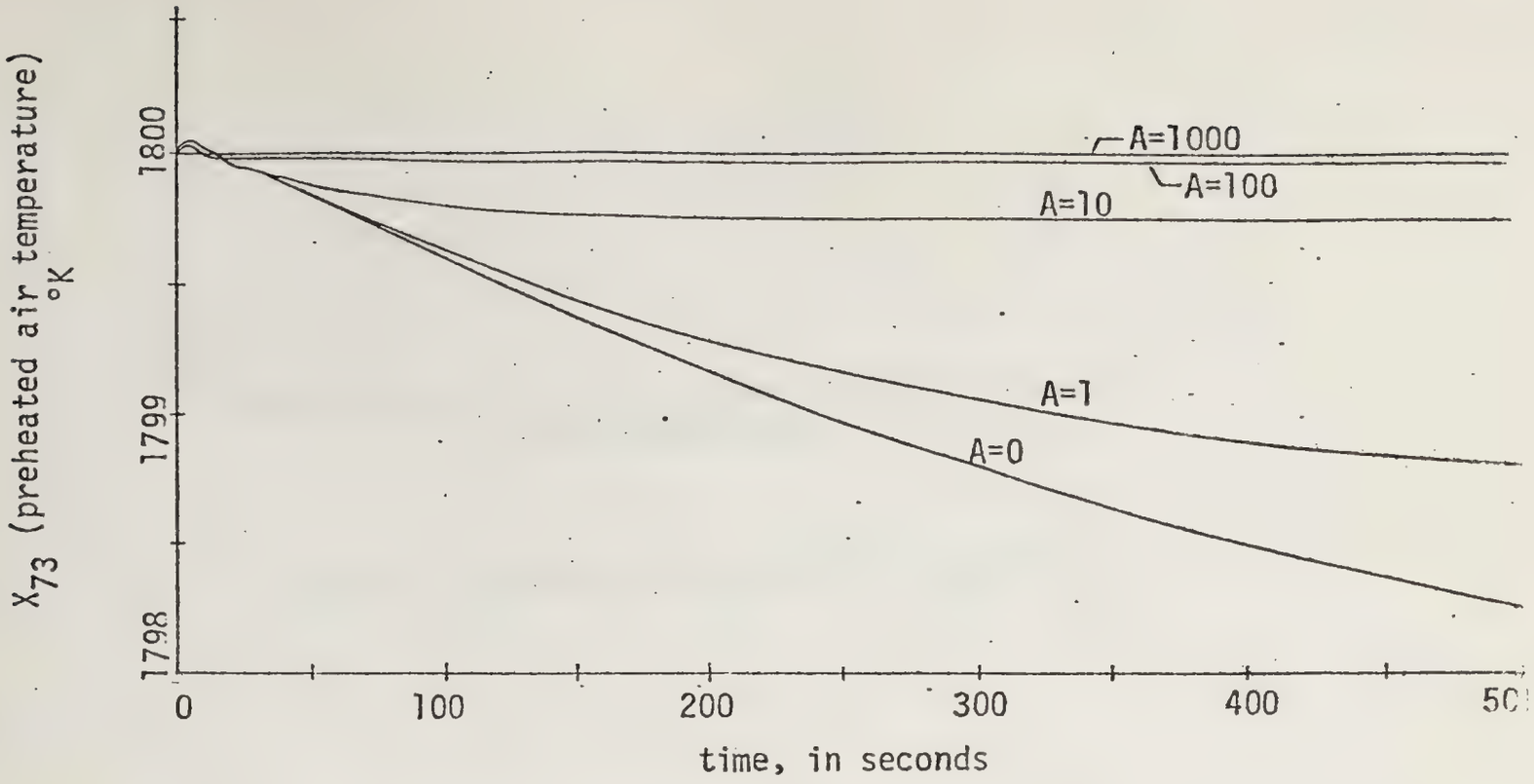

Figure 12. Preheated air temperature ($E_1(t) = 0_1 T_1(t)=0$)

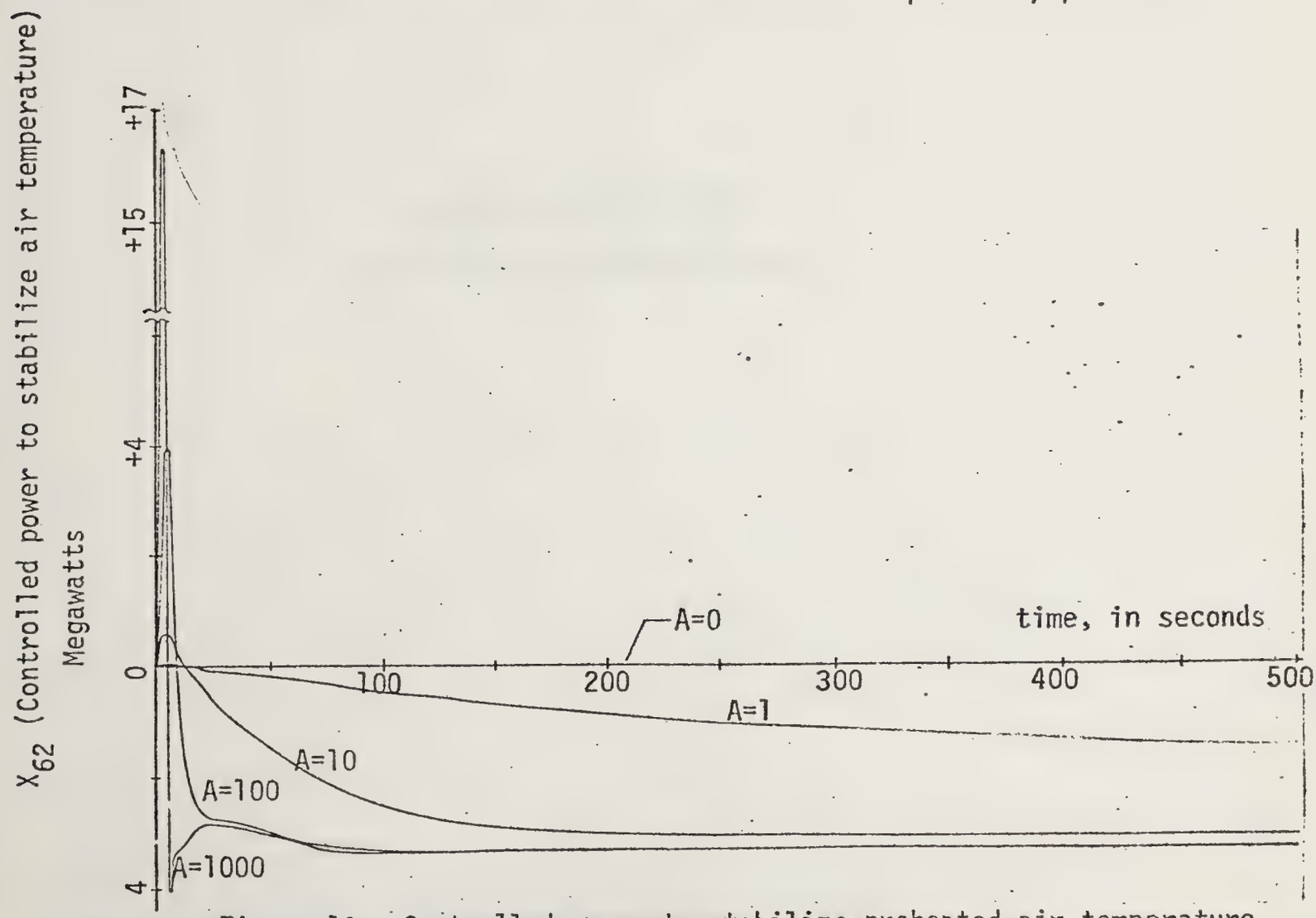

Figure 13. Controlled power to stabilize preheated air temperature

SENSITIVITIES OF OUTPUTS TO VARIATIONS OF INPUTS IN MHD COMBUSTORS

by

Donald A. Rudberg* and Charles H. Dudding

Electrical Engineering Department

Montana State University

MHD and Energy Research Program

Work performed under MERDI Subcontract Number 77-002 and ERDA Contract Number EF-77-C-01-2524.

*To present paper.

ABSTRACT

As part of a DOE contract to analyze combined cycle behavior of coupled MHD/steam-turbine power plants and to synthesize control policies for such plants, the Electrical Engineering Department of Montana State University has constructed models of various components proposed for use in the combined cycle system. This paper reports on results obtained from one of those component models, a steady-state, plug-flow combustor model [1] designed to predict operating states of single-stage or two-stage pulverized-coal-fired combustors operating in the 1800 K to 3000 K range, which is appropriate for MHD generators.

The model basically is intended as an aid in system analysis and control policy synthesis. It is a tool for predicting behavior of already designed combustors rather than for analysis of detailed internal behavior as a part of the combustor design process. A rigorous treatment would call for information on fluid flow and swirl patterns on slag particle size distribution and trajectories in the first stage [2], and on kinetics of ash vaporization [3]. None of these are embodied in the model but it is conceivable that they could be added, particularly the topic of ash vaporization.

The program can be used either in a stand-alone mode to make fairly detailed studies of combustor behavior under variations of inputs and operating conditions, or as a parent model from which can be derived a family of models having the same relations between input variables and are given the name "input-output models". Their calculational speed will be greatly in excess of the parent model making them much more suited to overall system analysis.

The basic combustor model assumptions are:

(1) Plug flow exists with perfect mixing in the radial direction and with no significant mixing in the axial direction.

(2) Devolatilization of coal particles follows an exponential rate law.

(3) Char particles are carbon spheres, perfectly entrained in the combustion gas, and at the same temperature as the combustion gas.

(4) Chemical equilibrium exists at every point in the combustor.

(5) Sidewall temperatures are uniform throughout each combustor stage.

(6) Gases conform to the perfect gas law.

(7) Velocities are low so that the difference between actual pressure and stagnation pressure is insignificant.

(8) A gas temperature gradient exists in the axial direction only.

(9) Specified slag rejection can be attained with no change in plug flow properties by assuming that swirl flow combustion causes uniform plug rotation with no change in axial or radial properties of the plug (except slinging of larger slag droplets to the combustor walls). Non-rejected slag consists of a vapor-droplet mixture and is perfectly entrained in the combustion gas.

(10) Heat loss is due to both radiative and convective effects.

The first set of results included in this paper are axial profiles of temperature, chemical concentration for selected compounds, electrical conductivity of the combustion gas, char particle burnout, heat loss, and residence time. Input variables and combustor parameters varied are air preheat temperature, oxidant composition (vitiated air, ambient air, oxygen enriched), coal composition and particle size distribution, seed concentration, stoichiometric ratio, combustion pressure, and sidewall temperature.

A second set of results shows the sensitivities of selected output variables to variations in inputs and combustor parameters. A nomial center operating point is assumed and variations of output temperature, chemical concentration of selected compounds, conductivity, heat loss,

residence time, and char particle burnout as functions of fractional variations of inputs are plotted. Inputs varied are coal moisture fraction, ambient relative humidity, oxygen enrichment, coal feed rate, stoichiometric ratio, seeding level, air preheat temperature, combustion pressure and combustor geometry. Results are given for combustors in the 32 MWT coal input range (CDIF sized), the 250 MWT coal input range (possibly ETF sized), and the 1200 MWT coal input range (a base load plant). When preheated air is accounted for, total thermal inputs become 45 MWT, 350 MWT, and 1700 MWT, respectively. Economics of size, shifts of operating characteristics and sensitivities of output to variations of inputs are immediately apparent from the plots. Input-output models that are multivariable curve fits have been made from these results. They will be used in further control system analysis.

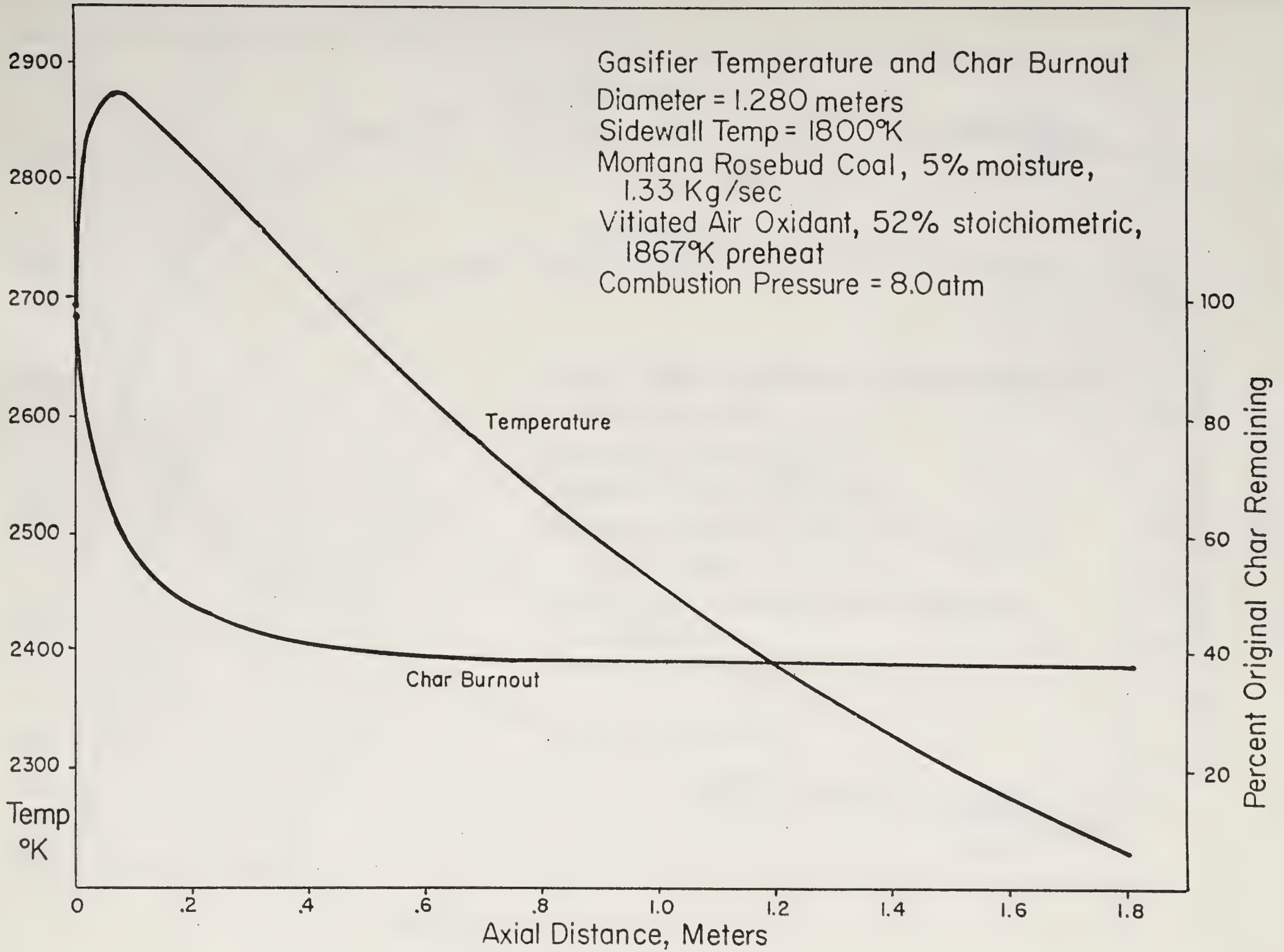
Gasifier Temperature and Char Burnout
Diameter = 1.280 meters
Sidewall Temp = 1800°K
Montana Rosebud Coal, 5% moisture, 1.33 Kg/sec
Vitiated Air Oxidant, 52% stoichiometric, 1867°K preheat
Combustion Pressure = 8.0 atm
Temperature
Char Burnout
2900
2800
2700
2600
2500
2400
2300
Temp °K
100
80
60
40
20
Percent Original Char Remaining
0
.2
.4
.6
.8
1.0
1.2
1.4
1.6
1.8
Axial Distance, Meters

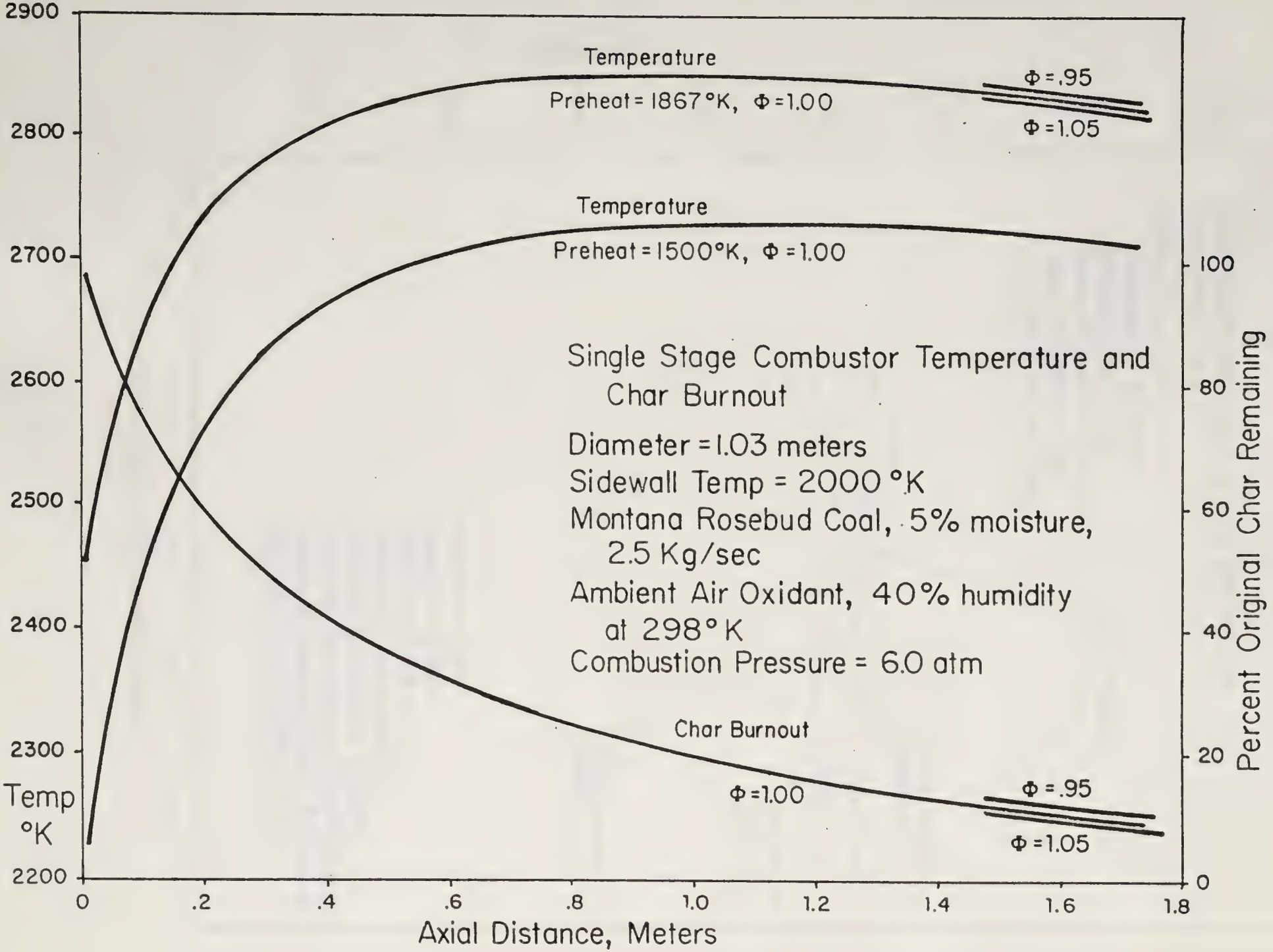
Temperature
Preheat = 1867°K, Φ = 1.00
Φ = .95
Φ = 1.05
Temperature
Preheat = 1500°K, Φ = 1.00
Single Stage Combustor Temperature and Char Burnout
Diameter = 1.03 meters
Sidewall Temp = 2000 °K
Montana Rosebud Coal, 5% moisture, 2.5 Kg/sec
Ambient Air Oxidant, 40% humidity at 298° K
Combustion Pressure = 6.0 atm
Char Burnout
Φ = 1.00
Φ = .95
Φ = 1.05
Temp °K
2900
2800
2700
2600
2500
2400
2300
2200
Percent Original Char Remaining
100
80
60
40
20
0
0
.2
.4
.6
.8
1.0
1.2
1.4
1.6
1.8
Axial Distance, Meters

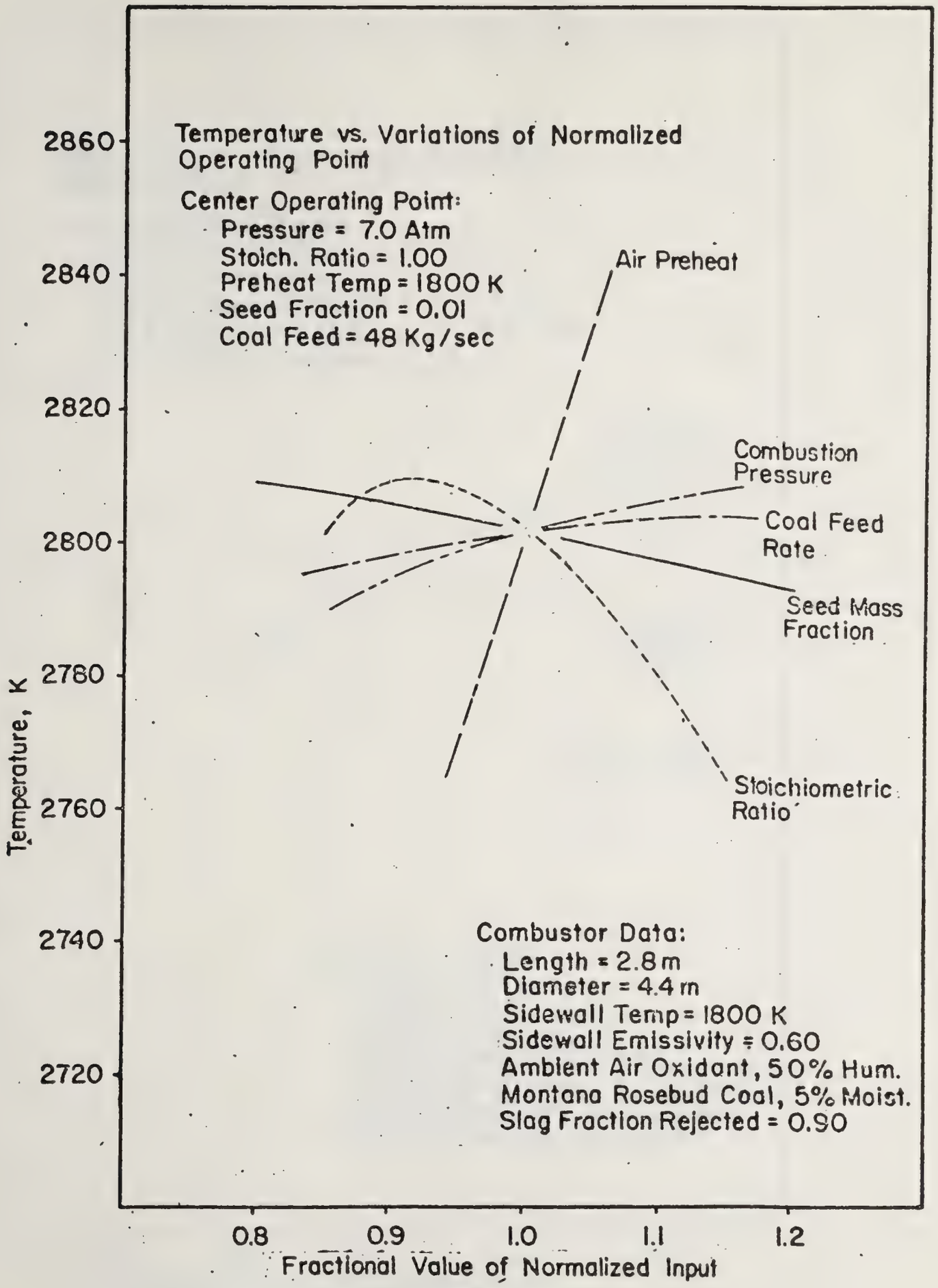
Temperature vs. Variations of Normalized Operating Point
Center Operating Point:
Pressure = 7.0 Atm
Stoich. Ratio = 1.00
Preheat Temp = 1800 K
Seed Fraction = 0.01
Coal Feed = 48 Kg/sec
Air Preheat
Combustion Pressure
Coal Feed Rate
Seed Mass Fraction
Stoichiometric Ratio
Combustor Data:
Length = 2.8 m
Diameter = 4.4 m
Sidewall Temp = 1800 K
Sidewall Emissivity = 0.60
Ambient Air Oxidant, 50% Hum.
Montana Rosebud Coal, 5% Moist.
Slag Fraction Rejected = 0.90
Temperature, K
2860
2840
2820
2800
2780
2760
2740
2720
0.8
0.9
1.0
1.1
1.2
Fractional Value of Normalized Input

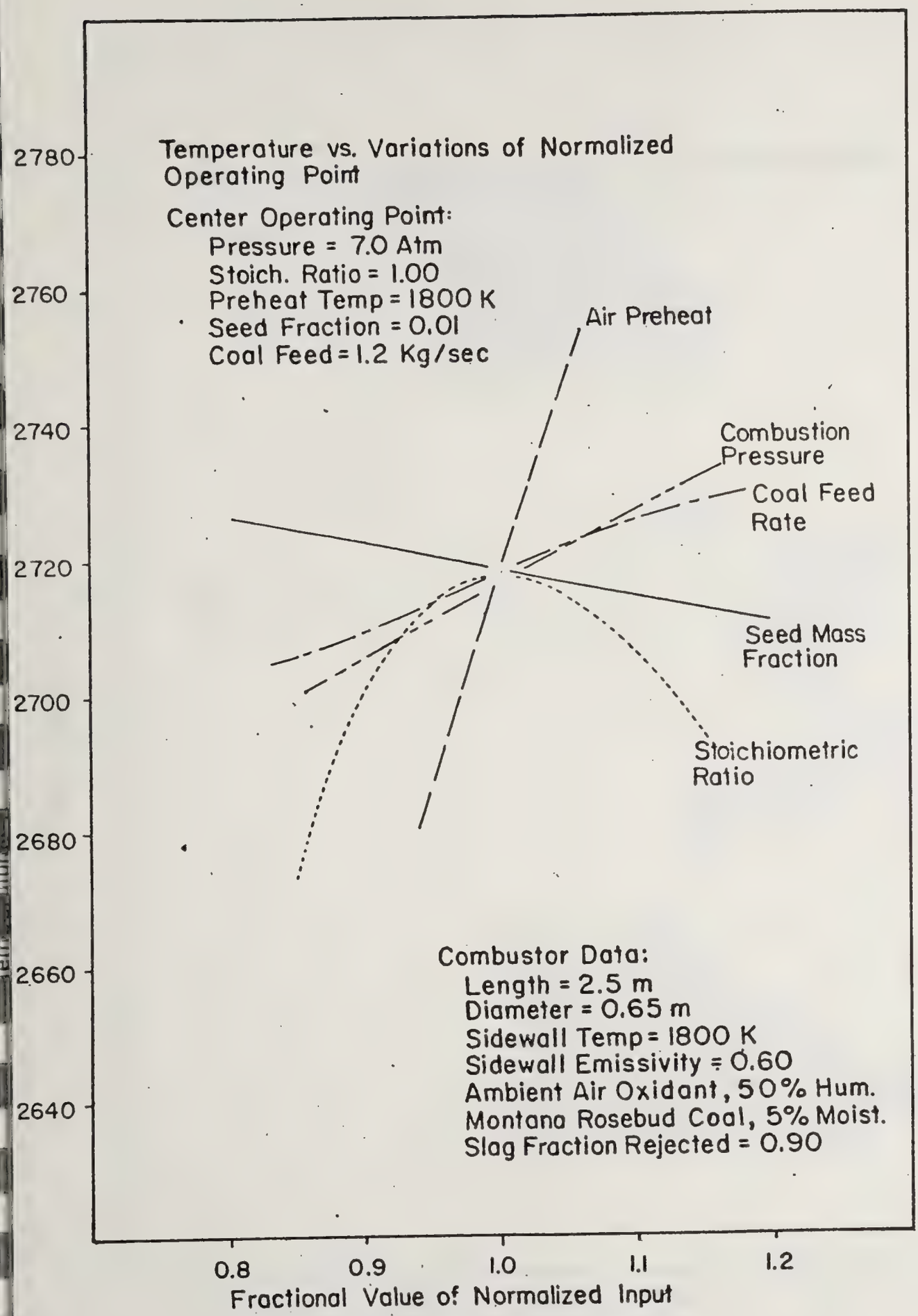
Temperature vs. Variations of Normalized Operating Point
Center Operating Point:
Pressure = 7.0 Atm
Stoich. Ratio = 1.00
Preheat Temp = 1800 K
Seed Fraction = 0.01
Coal Feed = 1.2 Kg/sec
Air Preheat
Combustion Pressure
Coal Feed Rate
Seed Mass Fraction
Stoichiometric Ratio
Combustor Data:
Length = 2.5 m
Diameter = 0.65 m
Sidewall Temp = 1800 K
Sidewall Emissivity = 0.60
Ambient Air Oxidant, 50% Hum.
Montana Rosebud Coal, 5% Moist.
Slag Fraction Rejected = 0.90
2780
2760
2740
2720
2700
2680
2660
2640
0.8
0.9
1.0
1.1
1.2
Fractional Value of Normalized Input

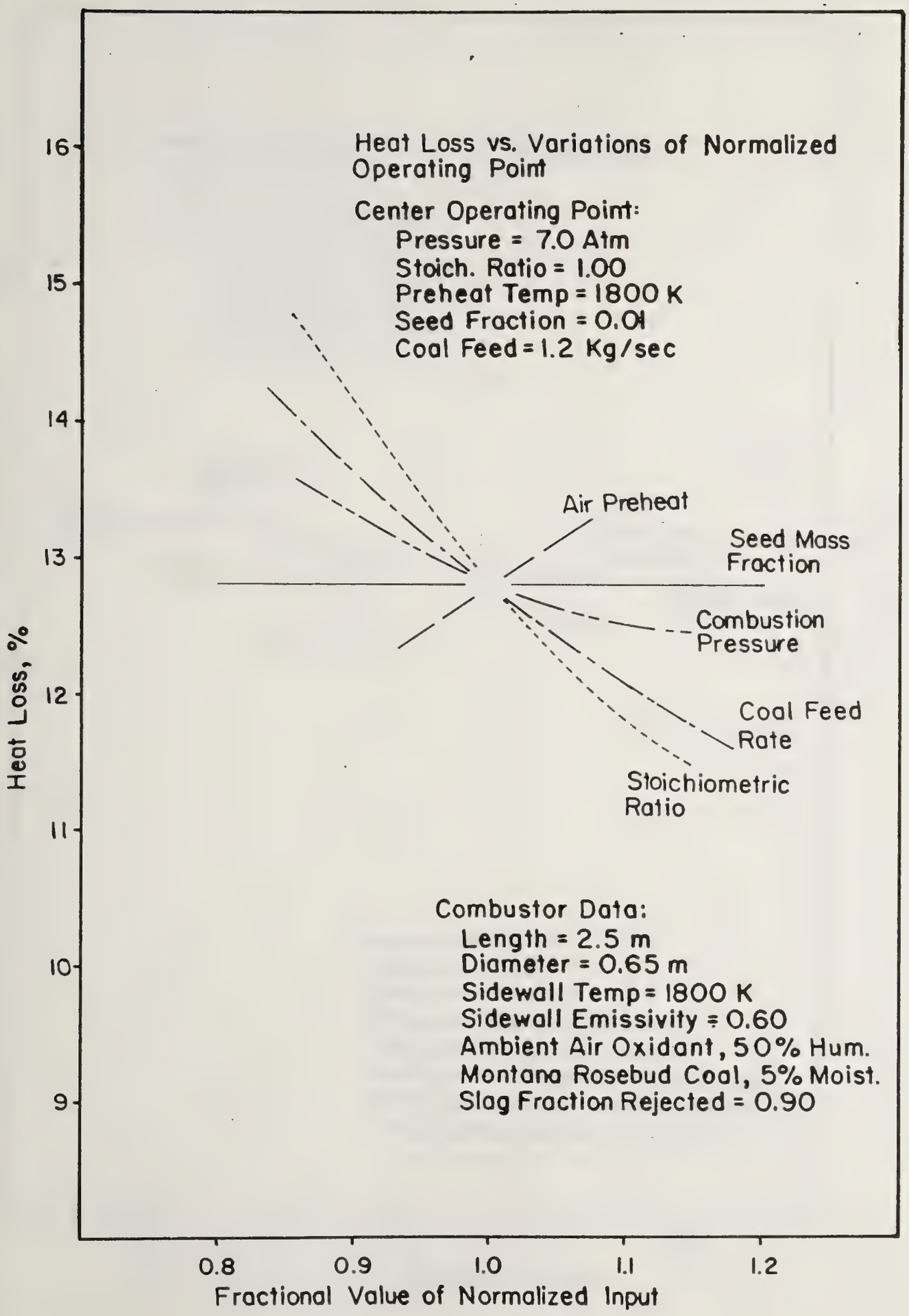
Heat Loss vs. Variations of Normalized Operating Point
Center Operating Point:
Pressure = 7.0 Atm
Stoich. Ratio = 1.00
Preheat Temp = 1800 K
Seed Fraction = 0.01
Coal Feed = 1.2 Kg/sec
Air Preheat
Seed Mass Fraction
Combustion Pressure
Coal Feed Rate
Stoichiometric Ratio
Combustor Data:
Length = 2.5 m
Diameter = 0.65 m
Sidewall Temp = 1800 K
Sidewall Emissivity = 0.60
Ambient Air Oxidant, 50% Hum.
Montana Rosebud Coal, 5% Moist.
Slag Fraction Rejected = 0.90
Heat Loss, %
16
15
14
13
12
11
10
9
0.8
0.9
1.0
1.1
1.2
Fractional Value of Normalized Input

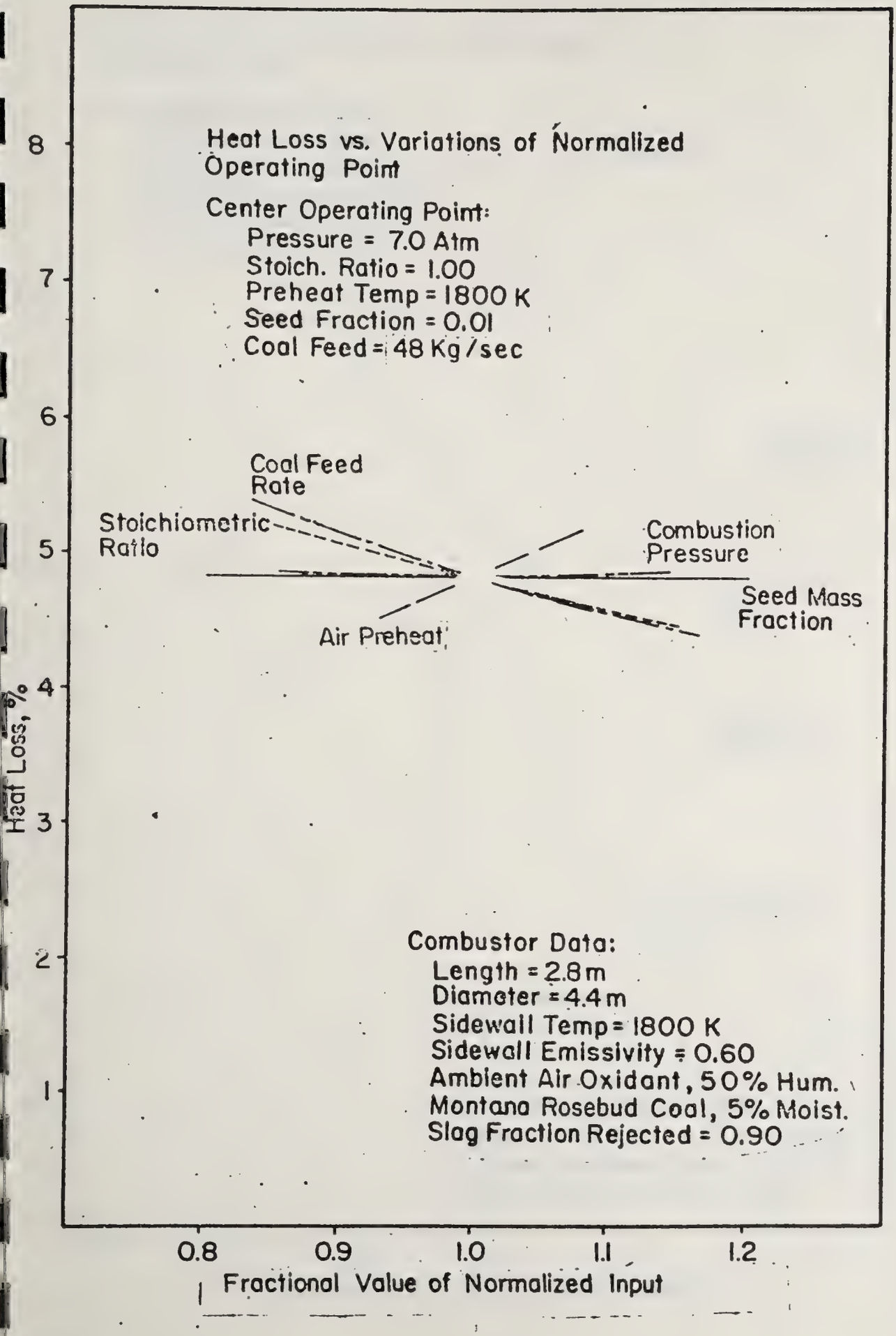
Heat Loss vs. Variations of Normalized Operating Point
Center Operating Point:
Pressure = 7.0 Atm
Stoich. Ratio = 1.00
Preheat Temp = 1800 K
Seed Fraction = 0.01
Coal Feed = 48 Kg/sec
Coal Feed Rate
Stoichiometric Ratio
Combustion Pressure
Seed Mass Fraction
Air Preheat
Heat Loss, %
8
7
6
5
4
3
2
1
Combustor Data:
Length = 2.8 m
Diameter = 4.4 m
Sidewall Temp = 1800 K
Sidewall Emissivity = 0.60
Ambient Air Oxidant, 50% Hum.
Montana Rosebud Coal, 5% Moist.
Slag Fraction Rejected = 0.90
0.8
0.9
1.0
1.1
1.2
Fractional Value of Normalized Input

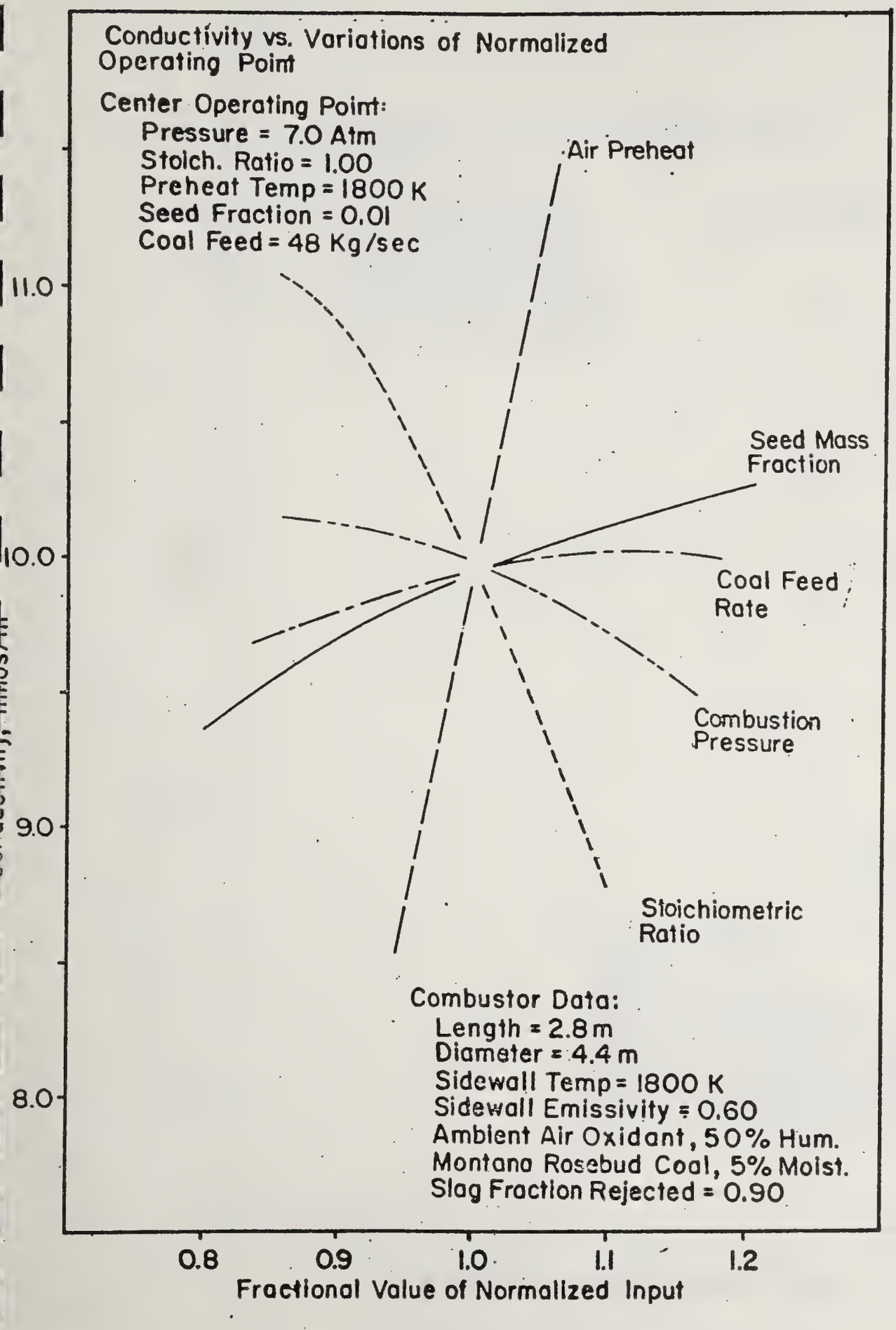
Conductivity vs. Variations of Normalized Operating Point
Center Operating Point:
Pressure = 7.0 Atm
Stoich. Ratio = 1.00
Preheat Temp = 1800 K
Seed Fraction = 0.01
Coal Feed = 48 Kg/sec
Air Preheat
Seed Mass Fraction
Coal Feed Rate
Combustion Pressure
Stoichiometric Ratio
11.0
10.0
9.0
8.0
Conductivity, mhos/m
Combustor Data:
Length = 2.8 m
Diameter = 4.4 m
Sidewall Temp = 1800 K
Sidewall Emissivity = 0.60
Ambient Air Oxidant, 50% Hum.
Montana Rosebud Coal, 5% Moist.
Slag Fraction Rejected = 0.90
0.8
0.9
1.0
1.1
1.2
Fractional Value of Normalized Input

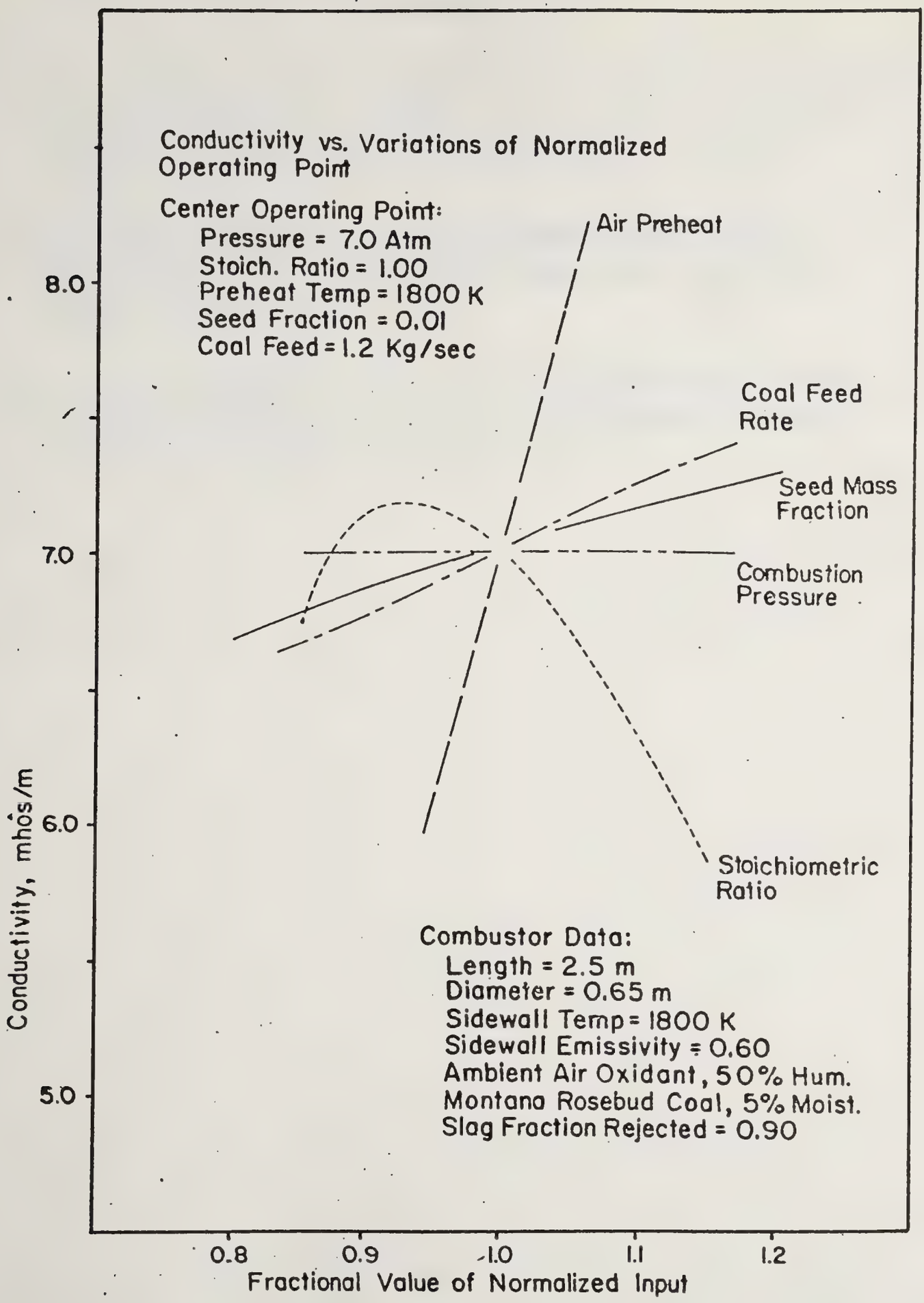
Conductivity vs. Variations of Normalized Operating Point
Center Operating Point:
Pressure = 7.0 Atm
Stoich. Ratio = 1.00
Preheat Temp = 1800 K
Seed Fraction = 0.01
Coal Feed = 1.2 Kg/sec
Air Preheat
Coal Feed Rate
Seed Mass Fraction
Combustion Pressure
Stoichiometric Ratio
Combustor Data:
Length = 2.5 m
Diameter = 0.65 m
Sidewall Temp = 1800 K
Sidewall Emissivity = 0.60
Ambient Air Oxidant, 50% Hum.
Montana Rosebud Coal, 5% Moist.
Slag Fraction Rejected = 0.90
Conductivity, mhos/m
8.0
7.0
6.0
5.0
0.8
0.9
1.0
1.1
1.2
Fractional Value of Normalized Input

REFERENCES

[1] D. A. Rudberg, "A Digital Computer Model and Simulator for Pulverized Coal-Fired Combustors," ERL Report No. 677, Electronics Research Laboratory, Montana State University, 46 pp., August 1977.

[2] TRW 25 MWT Staged MHD Coal Combustor Conceptual Design Study, TRW Defense and Space Systems Group, Redondo Beach, California, Document TID-26145, June 4, 1976.

[3] A. Padia, "The Behavior of Ash in Pulverized Coal Under Simulated Combustion Conditions," Sc.D. Thesis, MIT, Department of Chemical Engineering, Cambridge, Massachusetts, 1976.

ETF Siting and Environmental Screening

Jeff Chaffee and Doug Rognlie

ABSTRACT

Selection of an environmentally and socially acceptable MHD Engineering Test Facility (ETF) site in Montana requires that a scientific and justifiable methodology be developed for screening the state. Extensive research is being carried out to identify sound methodologies and to combine them into a useable siting plan.

In addition, state and local facility siting regulations are being identified and reviewed in preparation for setting up a compliance plan. These laws and regulations, along with a methodology for siting the ETF, will be presented in an ETF environmental siting plan.

I. OBJECTIVE AND SCOPE OF WORK

The objective of MERDI's Environmental Division is to develop a plan to assure compliance with Public Law 93-404, Section 107, which requires that an MHD Engineering Test Facility (ETF) be constructed in the state of Montana. Currently under development, this plan will address the following categories:

- Development of a site selection methodology based on a review of the literature and current practices;
- Identification and review of state and local facility siting laws and regulations that may apply to the ETF; and
- Application of the siting methodology (following approval by the DOE) in siting the ETF in Montana.

In the later stages of the site selection process, an environmental impact assessment/statement will be necessary under state and federal laws. Use of this plan should result in a socially, economically, and environmentally acceptable site for the ETF in Montana.

II. SUMMARY OF PROGRESS TO DATE

Early in the first quarter of FY 78, a draft topical report was completed on environmental baseline conditions in five Montana areas. Subsequently, the ETF siting process was re-examined, and a revised plan was adopted.

A review of power plant siting documents and papers concerning projected impacts from construction and operation is being conducted as the first stage of the revised plan. Because this stage was deemed so important, a variance was requested to extend the deadline for the completed ETF environmental siting plan to April 1, 1978.

Information gathered to date has concerned alternative screening techniques such as map overlays, population indicators, cost-benefit analysis, decision analysis, ranking and weighting, and computer mapping. Various constraints which must be evaluated during site screening also have been identified.

Since the ETF site selection process will be affected by state and local facility siting regulations, identification and review of applicable laws is necessary. A literature search, which is continuing, has identified the following Montana regulations:

- Montana Major Facility Siting Act;
- Montana Clean Air Act;
- Prevention of Significant Deterioration (PSD);
- New Source Performance Standards (NSPS);
- Montana Pollutant Discharge Elimination System (MPDES); and
- Montana Water Use Act.

This list does not cover all state and local siting regulations; however, it does identify some of the major laws requiring compliance. Since the Major Facility Siting Act was designed as a "one-stop" approach to the permit gathering process, it is one of the most important statutes that must be addressed.

As indicated on the milestone chart, revision of the siting methodology and identification of siting laws and regulations will be continued during the second quarter of FY 78. An ETF environmental siting plan will be drafted to present the results of the designated studies.

III. DETAILED DESCRIPTION OF TECHNICAL PROGRESS

In the first month of FY 78, a draft topical report entitled Preliminary ETF Environmental Analysis and Site Suitability Study was completed; it described environmental baseline conditions (i.e., air quality, transportation network, groundwater hydrology, etc.) in five Montana areas. Subsequently, a re-evaluation of the ETF siting process indicated the need for revising the chosen siting methodology. Therefore, research is being conducted to provide a scientific and thoroughly justifiable siting plan.

A. Siting Methodology

1. Literature Search

The first step in the revision of the siting process involves an extensive literature search into power plant siting methodologies and anticipated impacts from construction and operation. Originally, this phase of the ETF siting study was to be completed and a suitable methodology was to be selected by February 1, 1978. Because of the difficulties in obtaining this data and becuase of the need for an extremely

scientific and non-biased study, a variance was requested to extend the deadline to April 1, 1978.

2. General Method

Although there seems to be no methodology which is satisfactory for universal application, most siting studies are conducted in a similar manner (Figure 1). A large tract of land (nation, several states, one state, several counties) initially is identified as a study area. Using screening techniques, large areas of totally unsuitable land are eliminated from further consideration and the remaining ground is broken into candidate regions.

These regions then are analyzed by using secondary screening methods. Large sections of land again are eliminated, and candidate areas are designated from the remaining ground.

Candidate sites then can be chosen within these candidate areas after the worst sites are identified and deleted. Then, intensive field studies are conducted on the remaining potential sites so that preferred sites can be designated.

3. Alternatives

Within the general methodology noted above, there is room for a myriad of alternate screening techniques.

The decision regarding which alternatives to use in a particular facility siting study is very dependent upon the potential impact of the plant on its environment, which in turn is determined by the physical characteristics of the facility.

This decision also is based on the type of constraints to be analyzed. Because the site selection process can only be as good as the data and constraints used, care must be exercised in these areas.

Some of the many constraints which must be considered during site selection are air quality/meteorology, socioeconomics, water availability/quality, transportation access, transmission line proximity, ecology, land use, aesthetics, program continuity, and noise.

Of the many alternative screening techniques, the predominant methods are listed below.

a. Map overlay

This technique, which normally is used for primary screening, involves mapping the study area on numerous transparent films. Each map is shaded to represent the effect of a particular siting constraint in all areas, with the darker shading representing the most unsuitable areas in terms of that constraint. Once the films are overlaid, the lightest areas on the resulting map represent the most suitable regions for siting the plant.

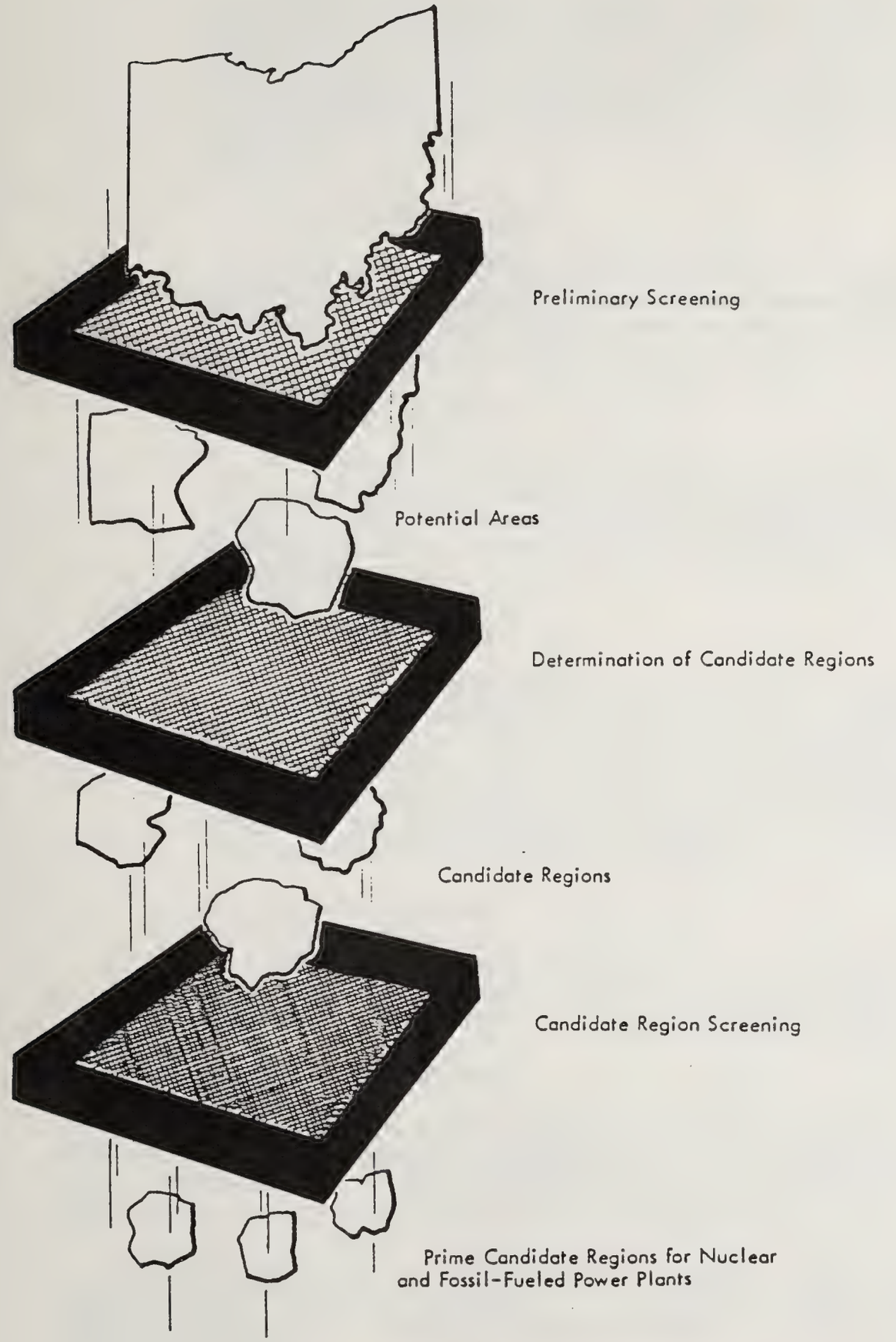

Figure 1.--General study methodology

b. Population indicator

Because the influx of a large number of "outsiders" can be socially disruptive and economically disasterous to a sparsely populated agricultural area, socioeconomic impact can be justifiably used as a major decision criteria for siting power plants. Since population is a good measure of a community's ability to withstand this impact, it may be used in primary or subordinate screening.

c. Cost-benefit analysis

This method involves quantification of perceived costs and benefits for the purpose of comparison. When used to compare potential sites, both monetary and non-monetary considerations must be expressed in a common measure (dollars).

d. Decision analysis

Specific sites can be compared through decision analysis by again quantifying the perceived costs and benefits of each constraint. The likelihood of possible consequences along with the preferences of the decision makers and affected parties must be considered.

e. Ranking and weighting

As a secondary screening technique and as a method used in cost-benefit and decision analysis, this is a widely used system with various names. Essentially, a set of constraints is weighted according to importance. These same constraints then are ranked according to their projected impact in several candidate areas or sites, and the summation of the products of ranking and weighting factors determines the most suitable site.

f. Computer mapping

Computers may be utilized as a tool in applying the various techniques listed above. Maps can be drawn, and weightings on rankings can be assigned to the various constraints.

B. Siting Laws and Regulations

Laws and regulations pertaining to facility siting are an important consideration in developing and implementing a site selection plan. Therefore, identification of state (Montana) and local facility siting laws and regulations was initiated during the first quarter of FY 78.

Emphasis was placed on an extensive literature search for any regulations that could affect siting of an ETF in Montana. At present, this ongoing search has identified the following regulations (this list is not totally inclusive):

1. Montana Major Facility Siting Act--This law, which requires a certificate of environmental compatibility and public need from the Board of Natural Resources and Conservation before construc-

tion is allowed, covers siting of a "major facilities" in the state of Montana. Although the ETF may be exempt from the act (it will be a federally owned facility), compliance may be desirable since the law was designed as a "one-stop" approach to the permit process.

2. Montana Clean Air Act--Under this act, both a preconstruction (120 days before construction) and an operating permit are required from the Department of Health and Environmental Sciences (DHES).

3. Prevention of Significant Deterioration (PSD)--A preconstruction review process conducted by the DHES is required under these rules to assure that air quality increments (Class I, II, or III) are met.

4. New Source Performance Standards (NSPS)--These regulations, which are administered by the DHES, require a preconstruction review of the proposed facility to substantiate compliance with applicable air emission standards.

5. Montana Pollutant Discharge Elimination System (MPDES)--These regulations, which are modeled after the National Pollutant Discharge Elimination System (NPDES) rules, require a MPDES permit issued by the DHES (subject to EPA approval) for any wastewater discharge.

6. Montana Water Use Act--This law establishes a water allocation process administered by the Department of Natural Resources and Conservation (DNRC)--Water Rights Bureau. A permit to allocate water, following a review process, can be issued by the department.

Other state laws regulate the crossing of streams, disposal of solid wastes, and release of toxic substances, If a decision is made to comply with the Major Facility Siting Act, strict local regulations (i.e., zoning) should not cause problems since the act states that "no local regulations that are unduly restrictive need be complied with." Air pollution laws and regulations appear to be one of the biggest restrictions to siting a facility in Montana.

In addition to identification of siting regulations, time was spent attending a hearing on proposed changes to rules implementing the Major Facility Siting Act. This hearing, sponsored by DNRC, identified problems in the amendments through the testimony of both utility companies and environmental groups. As a result of attendance, MERDI reviewed the rule changes and submitted comments on the amendments. Because the MHD plants (CDIF and ETF) are designed primarily as test facilities, MERDI's comments emphasized that certain portions of the rules applying to public utilities are not relevant. Therefore, it was recommended that the development of new technologies, such as MHD, be given special consideration in implementing the laws. It also was suggested that applicants supplying information relevant to the environmental and public need review process be given consideration when submitting the filing fee.

C. Work Forecast

Continuation of a literature search into siting methodologies and siting

laws and regulations will proceed into the second quarter of FY 78. As a result of this search, an environmental siting plan will be developed for the ETF. Included in this plan will be an outline of the siting process as it advances toward site selection, a methodology for screening Montana for potential ETF sites, and a discussion of laws and regulations that may affect ETF siting. Major criteria that can be applied in the siting process (i.e., water availability, existence of railroad and transmission lines, etc.) also will be investigated in preparation for insertion into a siting methodology.

IV. CONCLUSIONS

Research into siting methodologies has indicated the need for expanding the literature search to assure that a scientifically justifiable siting methodology can be developed. Furthermore, information gathered on siting laws has emphasized the importance of the Montana Major Facility Siting Act, especially its "one-stop" approach in the permitting process; a decision on compliance will be necessary well in advance of site selection.

The best possible site for any major facility is extremely dependent upon the potential impact of that plant on its environment. Therefore, more detailed information on characteristics of the ETF (i.e., conceptual design, time schedules/construction dates, work force, etc.) will be needed as the siting study proceeds.

DIVISION OF MAGNETOHYDRODYNAMICS

MONTHLY PROJECT MANAGEMENT STATUS REPORT

REPORT DATE 1/13/78

FOSSIL ENERGY

CONTRACT/PROJECT	
ETF SITING AND ENVIRONMENTAL SCREENING	
CONTRACT NO.	VENDOR MERDI

SCHEDULE

MAJOR MILESTONES AND DECISION POINTS	YEAR / MONTH: 1977 (O N D) 1978 (J F M A M J J A S)	VARIANCE
1. Preliminary ETF Environmental Analysis and Site Suitability Study		
2. Re-evaluation and Revision of the Site Methodology		
3. Identification of Siting Laws and Regulation		
4. Drafting of an ETF Environmental Siting Plan		
5. Application of the Siting Methodology in Siting the ETF in Montana		

STATUS DATE

SCHEDULE PLAN

PROGRESS

STATUS DATE

VARIANCE OR PROBLEM FLAG IN RIGHT COLUMN

Materials Evaluation--MERDI Applied Research Division and University Management

J. J. Rasmussen

ABSTRACT

The thermal diffusivities for two magnesia-aluminate spinel refractories, two synthetic coal slags, a candidate MHD-electrode material ($La_{.84}Sr_{.16}CrO_3$), and an insulating material ($MgAl_2O_4$) were measured. Analysis of the thermal transport properties of these materials after exposure to simulated MHD-operating conditions is in progress.

High density ceramic rods are being fabricated and characterized at MERDI before use in Task B slag-corrosion studies.

Measurements of the surface tension of synthetic coal slags and characterization of the interaction boundary between the slags and ceramic substrates are continuing. A basic synthetic slag was found to wet magnesia-rich spinel ($65^m/o$ $MgO.35^m/oAl_2O_3$) much more readily than stoichiometric spinel.

I. OBJECTIVE

The objective of Task N is to provide technical and administrative management of the research being conducted by the units of the Montana University System and to perform and coordinate the materials research and evaluation work in Montana in support of the national plan for MHD electrical power development formulated by the DOE-FE-MHD Division. The research emphasis is placed on elements of open-cycle MHD utilizing coal as the primary fuel.

The objectives will be met by including the following subtasks at MERDI:

- Maintain a survey on MHD materials development to remain aware of advances and problems in this area;
- Select, evaluate, and characterize materials, including testing to simulate performance under actual MHD conditions;
- Perform pre- and post-test analysis of materials and materials from components tested under simulated or actual MHD conditions; and
- Provide materials and specimen fabrication facilities and services required to assist other experimental investigators to obtain data needed to supply well-characterized materials for MHD test applications.

Specific activities which are being conducted to meet these objectives include the following:

- Studies of the thermal conductivity and diffusivity of MHD materials;
- Development and fabrication of controlled structure MHD materials; and
- Studies of wettability of MHD materials by slag-seed mixtures.

II. SUMMARY OF PROGRESS TO DATE

A. Thermal Conductivity and Diffusivity of MHD Materials

In cooperation with researchers at Montana State University and FluiDyne Engineering Corporation, the MERDI program to characterize the thermal transport properties of candidate MHD-preheater refractories continues. The thermal diffusivities of a rebonded magnesia-aluminate spinel and a fused-cast spinel were determined and compared to previously measured results for a chrome-magnesite refractory. Thermal cycling experiments on virgin materials indicated that the rebonded spinel performed better than the fused-cast spinel or the chrome-magnesite material.

From estimated values of heat capacity and measured values of density and thermal diffusivity, the thermal conductivities for synthetic slags (composition $60SiO_2.15Al_2O_3.25CaO$ and $60SiO_2.15Al_2O_3.25MgO$) were calculated to be 1.3 ± 0.2 and 1.4 ± 0.2 watts/m^oK, respectively.

Thermal diffusivity measurements were made for $La_{.84}Sr_{.16}CrO_3$ and $MgAl_2O_4$ from 200^{o}C to 1500^{o}C.

To make dependable radiation heat loss corrections to thermal diffusivity measurements in the range of 1500^{o}C, a digital data acquisition system is necessary. Below 1000^{o}C, present methods are adequate to determine the thermal diffusivity to $\pm$ 5%.

B. MHD Materials Fabrication and Characterization

A total of 20 rods (1/2" diameter x 5" long) of dense polycrystalline spinel ($MgAl_2O_4$) have been fabricated for slag-corrosion studies. Automatic powder compaction and green-machining have improved the quality of the final product. Initial tests on spray-drying ceramic powders have been carried out. A newly designed heating element for the high-temperature sintering furnace has been received.

C. Wettability of MHD Materials by Slag-Seed Mixtures

In wettability studies in air by the sesile-drop method, a basic synthetic slag (composition $60SiO_2.15Al_2O_3.25CaO$) was found to wet magnesia-rich spinel ($65MgO.35Al_2O_3$) much more readily than stoichiometric spinel ($50MgO.50Al_2O_3$). Post-test analysis of the microstructural features and elemental

diffusion at the interaction boundary between the slags and substrates are being pursued. Slag surface tension results have been delayed because of computer programming problems.

III. DETAILED DESCRIPTION OF TECHNICAL PROGRESS

A. Thermal Conductivity and Diffusivity of MHD Materials

1. Efforts during the past year were directed primarily toward designing and checking out a test system for the rapid evaluation of thermal transport properties of real MHD materials--particularly those subjected to the hostile MHD environment of high and cyclic temperatures and of slag/seed exposures for various lengths of time. It is anticipated that these data will provide input for the various mathematical models which simulate MHD operations as well as additional criteria for evaluating a material's long-term suitability for use in a particular component. The operating efficiency and long-term durability of an MHD system depend directly on a component's thermal transport properties. This is particularly true since many physical properties such as electrical conductivity, viscosity, diffusion, reaction rates, creep rates, stress magnitudes, etc. are so sensitive to temperature or temperature gradients.

The laser-flash diffusivity technique was selected as the primary method for determining the thermal diffusivity (α), mainly because of its simplicity and high-temperature adaptability. The thermal conductivity (λ) can be calculated from α, the density (ρ), and the specific heat capacity (C_p) by the equation

$$\lambda(T) = \alpha(T) \cdot \rho(T) \cdot C_p(T) \qquad (1)$$

where all of the terms are functions of temperature (T). When possible, values of $\lambda(T)$ and $\alpha(T)$ are expressed in analytical form for ready application in engineering design or systems thermal analysis.

The technique, equipment check-out, and numerous experiments designed to provide a data base necessary to characterize MHD materials are described in detail in the Task N section of Reference 2.

Emphasis this quarter was placed on the following projects:

- Continuing the evaluation of the thermal transport properties of potential preheater refractories, both in the virgin state and as a function of slag/seed/atmosphere exposure time in cyclic temperature ranges typical of a regenerative type heat exchanger with ceramic heat storage;
- Starting the evaluation of real and synthetic coal slags; and
- Improving the method for making heat loss corrections for high-temperature (>1000^{o}C) thermal diffusivity measurements.

In addition, preliminary thermal diffusivity measurements were made on a perovskite, $La_{.84}Sr_{.16}CrO_3$, a member of a class of potential electrode materials; and on a stoichiometric magnesium aluminate spinel, $MgAl_2O_4$, a potential channel insulator material.

The materials for these studies were provided by the following cooperating MHD contractors:

- FluiDyne Engineering Corporation and Montana State University--refractory brick:
- Montana College of Mineral Science and Technology (MCMST) and Montana State University (MSU)--real and synthetic coal slags.
- A.T. Research--electrode materials; and
- MERDI in-house--channel insulator materials.

In turn, the collected thermal transport data and analysis have been provided directly to the contractors.

2. Preheater Refractories

Figure 1 shows thermal diffusivity results for two different magnesia-aluminate spinel refractories, one rebonded and the other fused-cast, designated SX487A and X317, respectively. The rebonded material SX487A has a composition 50 $MgO.50Al_2O_3$(m/o), 2.91gm/cm^3 density, and 12.5v/o open porosity; the fused-cast material X317 has a composition of 82.5 $MgO.17.5\ Al_2O_3$(m/o)-periclase and spinel mixture, 3.43 gm/cm^3 density, and 2.3v/o open porosity. The fused-cast material has been found to be corrosion resistant in preheater tests at FluiDyne.[1] Open (closed) symbols indicate measurements taken on heating (cooling).

The thermal diffusivity magnitude and temperature dependence of the rebonded spinel SX487A is similar to the values reported previously for RFG,[2] a fused grain and rebonded chrome magnesite brick of about 13v/o open porosity. The thermal diffusivity of the virgin fused-cast spinel X317 is about twice that of the rebonded spinel. Since the thermal conductivity is related to the thermal diffusivity through Equation 1 and the density of X317 is greater than that of SX487A, the thermal conductivity of the more dense material also should be a factor of two greater. Only small differences in heat capacity are expected.

Values of thermal diffusivity were reproducible on heating to 1473°K and cooling for the SX487A material, indicating good thermal cycling stability for this material. In contrast, the thermal diffusivity of the virgin RFG was not stable on temperature cycling to 1773°K. Although there were differences in the upper test temperatures, it is felt that the virgin SX487A material performs better than the virgin RFG during temperature cycling. However, no hysteresis was observed in the data for RFG after 200 hours of exposure to

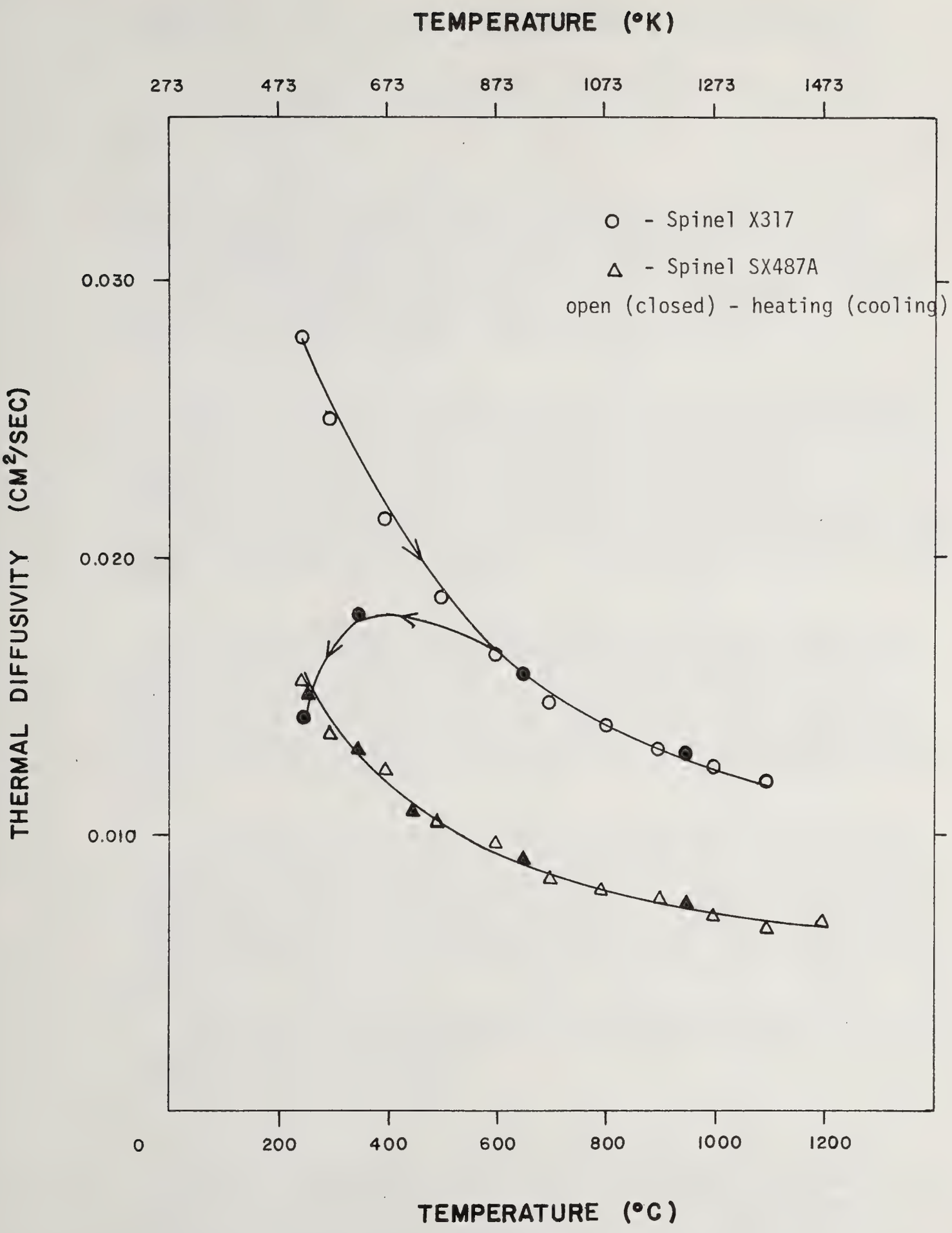

Figure 1. Thermal diffusivities of two as-fabricated magnesia aluminate refractories

temperature cycling and gas/seed/slag in the FluiDyne preheater test facility.[1]

Previous work[2,3] on porous materials indicated that the semi-emperical equation

$$\lambda/\lambda_o = (1 - P) / (1 + \beta P) \qquad (2)$$

(where λ and λ_o are the thermal conductivities of porous and non-porous materials, respectively, P is the fractional porosity, and β is a parameter which depends upon pore shape, P, and T) describes the thermal conductivity dependence on porosity many times. Neglecting composition effects, a value of $\beta \gtrsim 5$ best fit the data for the more porous rebonded spinels. This is a reasonable value for the flat, crack-like pores expected in a rebonded material.

Figure 2 shows the effects of temperature cycling on the thermal stability of the virgin fused-cast spinel. On cooling, the thermal diffusivity is reproducible to below 600°C but then dramatically decreases by a factor of two on further cooling to 200°C. On the second heating cycle to 500°C, the thermal diffusivity decreases; then it begins to increase again until it reaches the initially measured values above 800°C. On the second cooling cycle, the thermal diffusivity was reproducible to 500°C; then again, it dropped dramatically by a factor of two on further cooling to 200°C.

Complex hysteresis effects have been observed in single-phase polycrystalline materials due to microcracking caused by anisotropic thermal expansion between grains.[2] Similar effects have been observed in alumina-zirconia composite materials.[4] Recently, a study[5] reported that hysteresis in physical properties such as thermal expansion and elastic moduli caused by irreversible microcrack formation and healing during temperature cycling is affected by atmosphere as well.

Although the hysteresis effects displayed here in Figure 2 for the virgin fused-cast spinel and earlier for the virgin RFG resemble hysteresis effects caused by microcracking, there is no other direct evidence for the presence of microcracks. Microstructural examinations and thermal expansion measurements are in progress to provide further information. It should be noted, however, that the fracture toughness of a material can be enhanced by the presence of microcracks.[4]

Future work will concentrate on the effects of slag/seed/atmosphere exposure in MHD preheater tests on the thermal transport properties of candidate refractory brick.

3. Synthetic Coal Slags

The thermal diffusivities were determined for two solid synthetic coal slags obtained from Montana Tech researchers; the results are depicted in Figure 3. Details on the slag preparation were presented in the Task B section of Reference 2. Table 1 lists the compositions and measured densities for these component slags. These

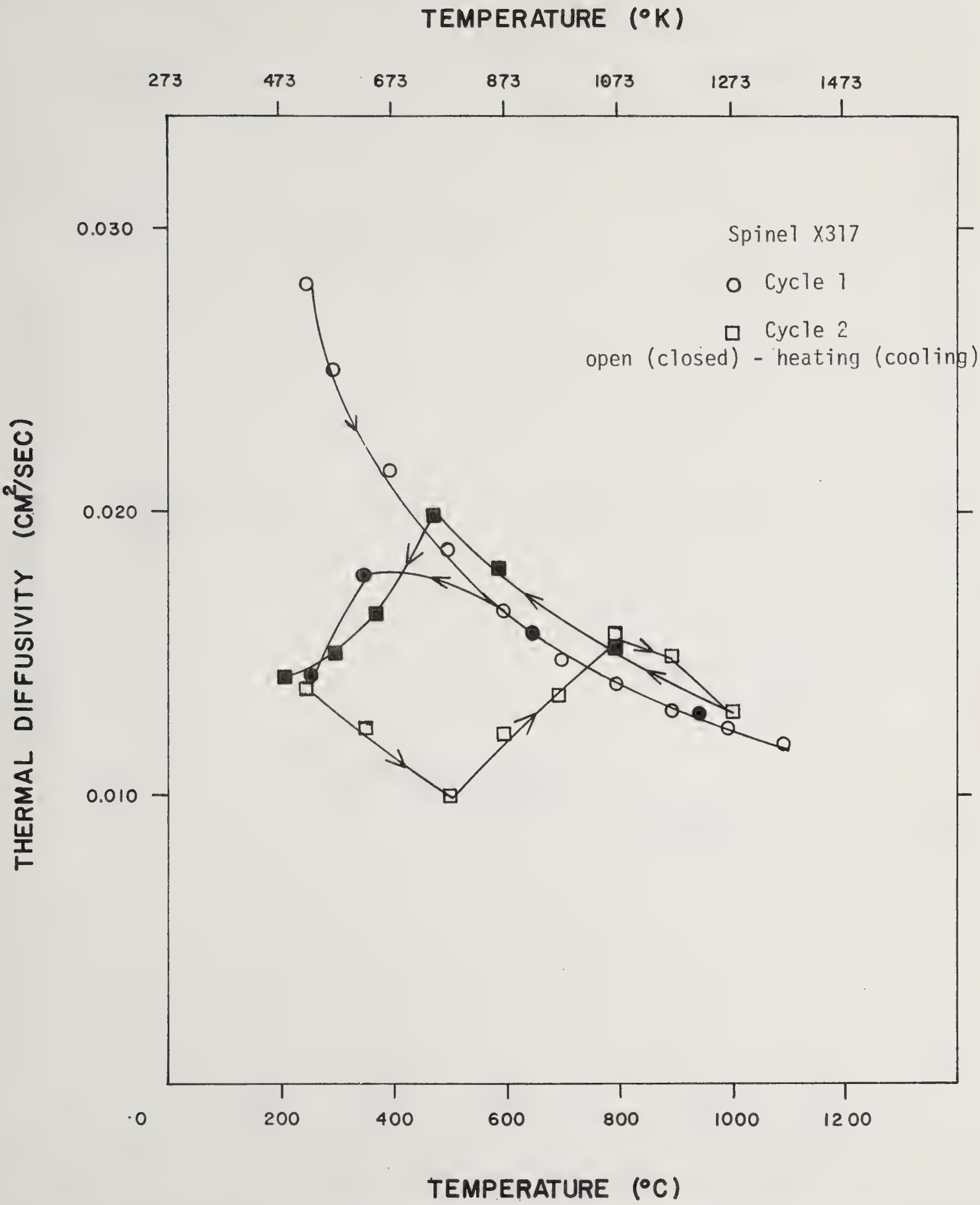

Figure 2. Effects of thermal cycling on the thermal diffusivity of as-fabricated fuel cast spinel refractory

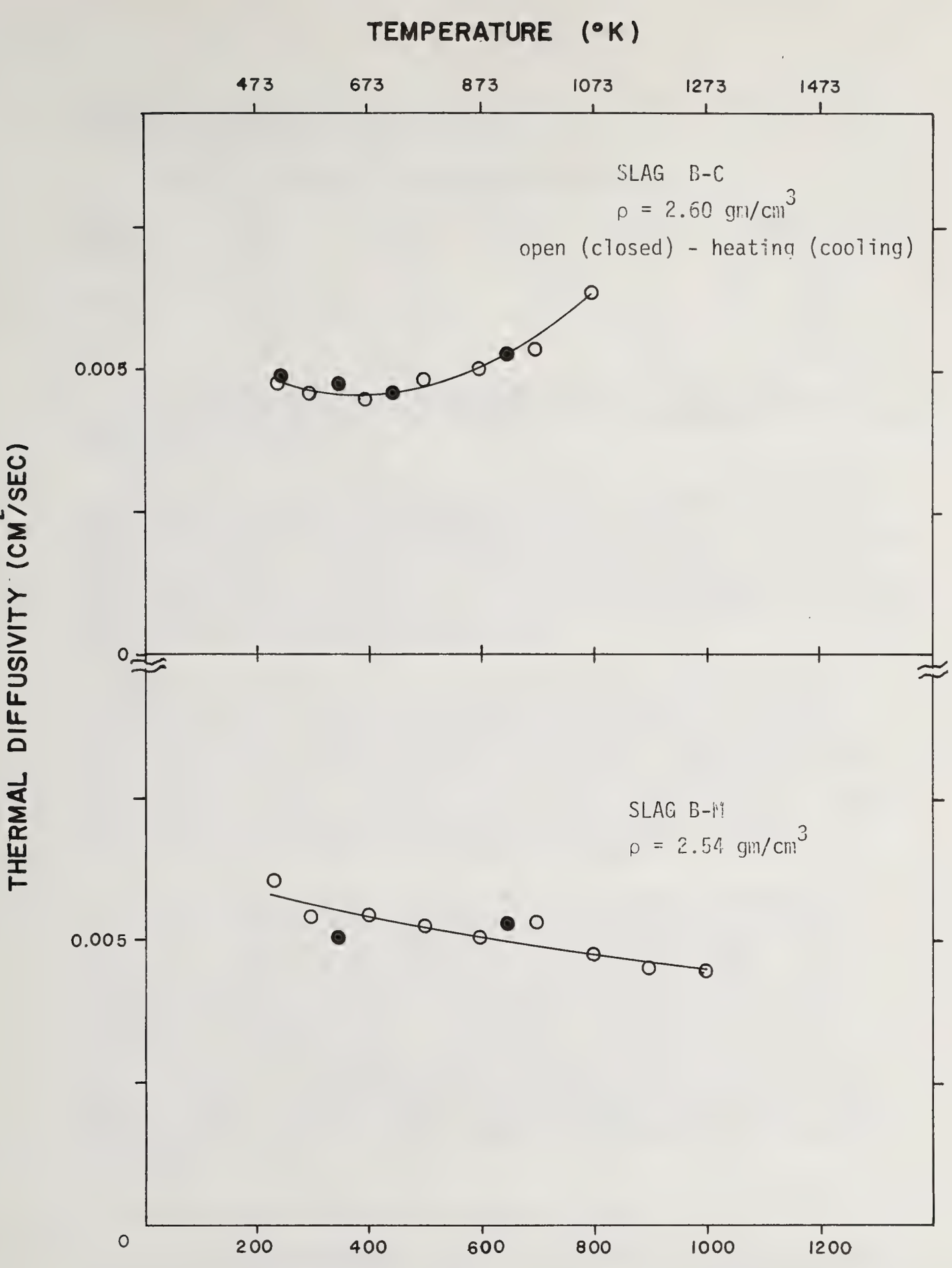

Figure 3. Thermal diffusivities of two synthetic coal slags

slags also were used in the Task B slag corrosion studies and in the wettablilty studies described later.

TABLE 1--Synthetic Slag Compositions (w/o)

Sample	SiO_2	Al_2O_3	CaO	MgO	Density (gm/cm^3)
B-C	60	15	25	-	2.60
B-M	60	15	-	25	2.54

The remelted and fused slag samples were optically transparent before and after testing. The densities are representative for dense alumina-silicate glass.

Radiation heat transfer in a partially transparent material at higher temperatures ($\gtrsim$ 500°C) depends on the absorption and reemission properties.[6,7] It also depends on scattering at boundaries and sometimes on sample thickness.[8] Radiation heat transfer through a semi-transparent material such as a solid or molten slag can be significantly larger than phonon heat transfer and therefore an important consideration in MHD thermal engineering.

Due to the complexity of the radiation mode of heat transfer, experimental measurements on semi-transparent materials are difficult to interpret. In addition, some difficulty was incurred obtaining data above 700°C on the two slag samples because the laser pulse tended to "blast off" the thin graphite coating applied to render the transparent samples opaque to the laser radiation. Hence, the positive temperature dependence of α observed in Figure 3 for slag B-C above 500°C is discounted at this time.

Using values of heat capacity for a pyroceram[+] of similar composition to the slags, the thermal conductivity was calculated to be 1.3 ± 0.2 and 1.4 ± 0.2 watts /m°K for slags B-C and B-M, respectively, with little temperature dependence to 700°C. This compares to direct thermal conductivity measurements on a sample of porous, partially crystalline natural ash (Rosebud) made at MSU which gave a temperature independent value of 1.5 ± 0.2 watts/m°K to 600°C.[10] The thermal conductivity of Corning C9606, a pyroceram with high percentage of crystalline phase within a glassy matrix, ranges from 4.0 at 25°C to 2.8 at 1000°C (watts/m°K). These values should represent an upper limit for any amorphous or crystallized slags.

4. MHD Electrode Materials--$La_{.84}Sr_{.16}CrO_3$

The thermal diffusivity of an oxide perovskite--$La_{.84}Sr_{.16}CrO_3$--was measured on heating to 1500°C and cooling; the data are displayed in Figure 4. The material was prepared by H. Anderson of

[+]Corning C9606; 54 SiO_2.21MgO.18Al_2O_3.7TiO_2, Reference 9.

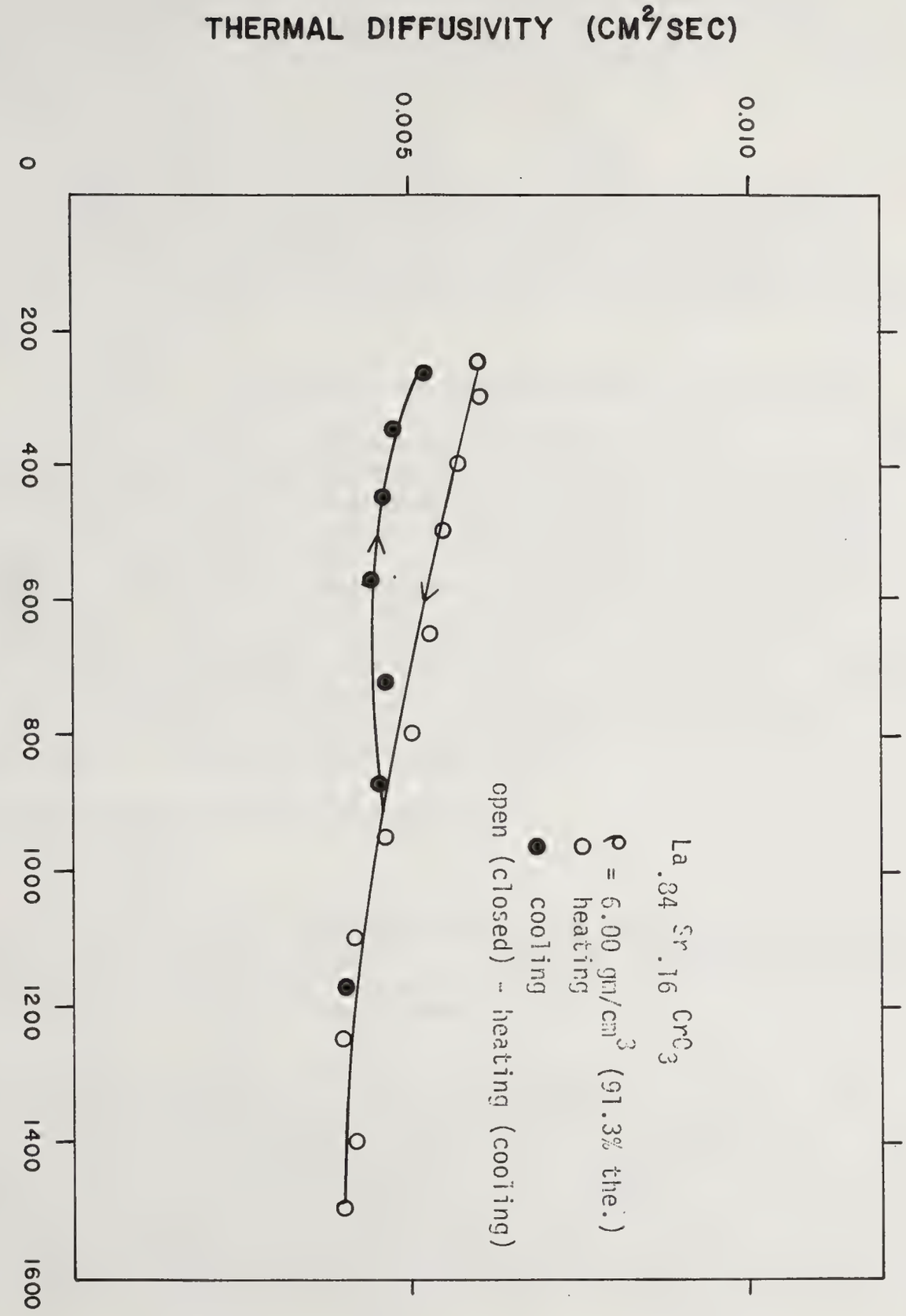

Figure 4. Thermal diffusivity of $La_{.84}Sr_{.16}CrO_3$

A.T. Research and had a density of 6.00 gm/cm^3 (91.3% theoretical). A slight hysteresis effect, perhaps attributable to chromium reduction in the N_2 atmosphere within the graphite furnace, was observed on cooling below 900°C. A 2% weight loss also was observed during the temperature cycle. Further analysis is in progress for this class of materials.

5. MHD Electrical Insulator Materials--$MgAl_2O_4$

A sample of isostatically pressed and sintered stoichiometric spinel ($MgAl_2O_4$) of 3.52 gm/cm^3 density (98.6% theoretical) was fabricated and characterized at MERDI for Task B corrosion studies. The thermal diffusivity data are depicted in Figure 5 and agree with the results of others.[12] Further analysis is in progress for this class of materials.

6. Improvements in Technique for Thermal Transport Measurements

A test was performed on an alumina reference sample to determine if a more accurate method, as described by Taylor et al.,[11] for making radiative heat loss corrections at high temperatures could be used. It was found that because of the high precision measurements required for temperature decay times, Taylor's method would require the use of a digital data acquisition system which is not available at this time. Radiation heat loss corrections can be as large as 25% at 1500°C; hence, they are important for dependable data in the operating temperature range for most MHD systems. Up to 1000°C corrections are generally less than 5% and are easily made. Excellent correlation with values of thermal diffusivity for Armco iron and pyroceram reference materials have been obtained below 1000°C.[2]

B. MHD Materials Development and Fabrication

1. Introduction

Ceramic fabrication techniques have been upgraded continuously. A total of 20 rods (1/2" diameter x 5" long) of stoichiometric spinel ($MgAl_2O_4$) have been characterized and delivered to Task B (MCMST) personnel for slag-corrosion studies.

The present technique of green forming and sintering rods has resulted in excessive taper.* Two solutions were pursued during this quarter. One, an automatic tooling tapper was designed, built, and put into operation. The tapper yields more uniform powder compaction control; hence, it yields more uniform final densities. Two, the rods are green-machined on a small, recently purchased tool lathe. For this purpose, it was necessary to grind a ceramic bit. With previous knowledge of the expected sintering shrinkage, rods now are green-machined routinely to a uniform diameter so that the end product fulfills the Task B

---

* See Reference 2 for further description of this problem.

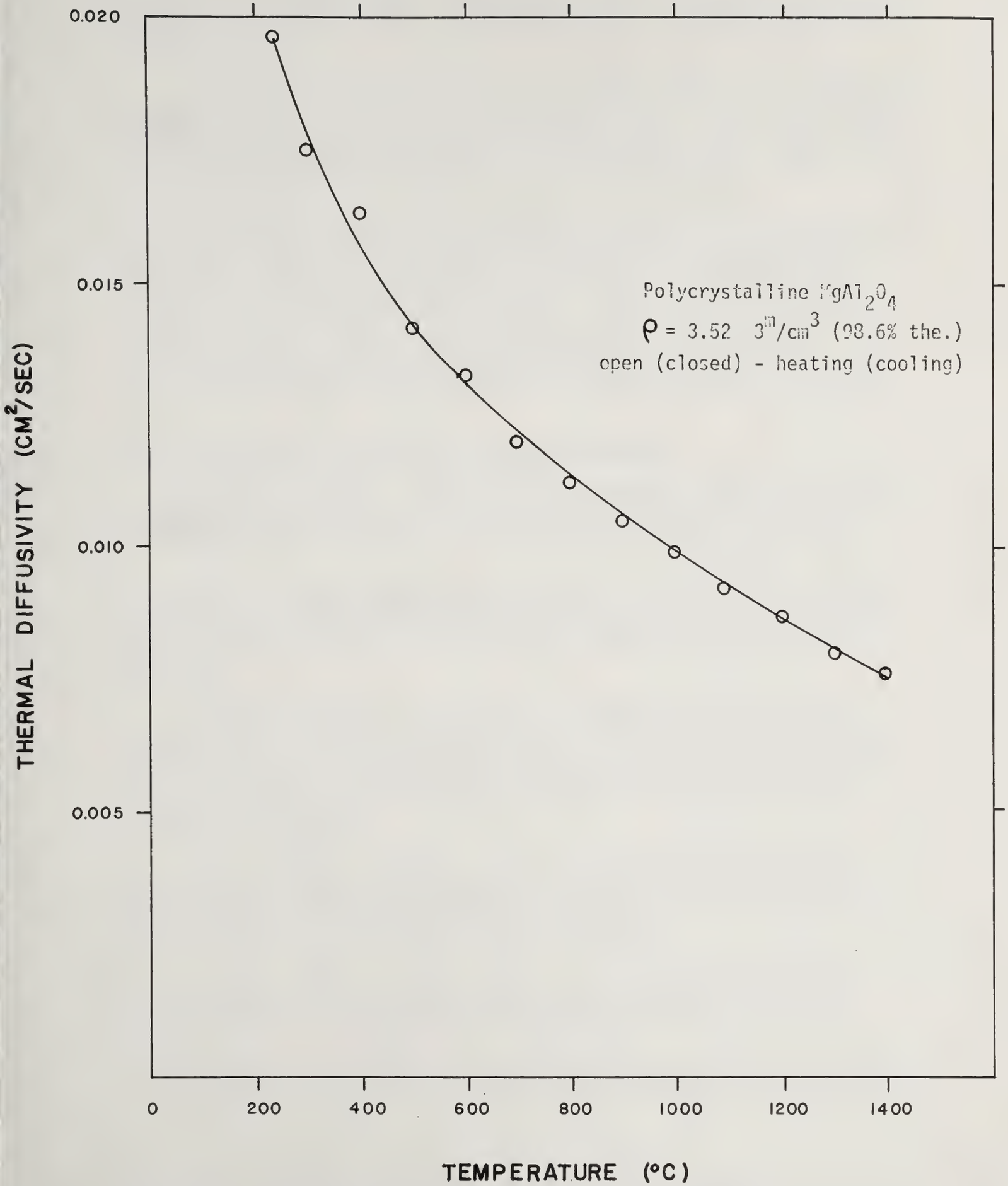

Figure 5. Thermal diffusivity of polycrystalline $MgAl_2O_4$

dimensional specifications. Utilizing these two improvements, a second batch of magnesia-rich spinel (65 $MgO.35Al_2O_3$ m/o composition) rods is in production.

Preliminary tests to produce a spray-dried powder were carried out. High-purity alumina powder was suspended in alcohol plus 3 w/o carbowax. A hand-held paint sprayer was used to obtain dispersed and dried powder agglomerates which pour and compact in a mold more easily. Sintering tests on bodies formed from these powders are in progress.

During high-temperature sintering in the Centorr furnace, hot spots developed along the graphite heating element. After several firings, this led to cracking and failure of the muffle tube. Examination of failed muffle tubes indicated that the slotted design of the heating element was responsible for this problem. After discussions with Centorr engineers, a new tapered heating element was developed. The new heating element has been received and will be installed soon. This should alleviate down-time and expensive muffle-tube replacement problems.

C. Wettability of MHD Materials by Slag-Seed Mixtures

During this quarter, wettability experiments of MHD materials by slag-seed mixtures using the sessile-drop method* have been continued. These experiments have been performed in an air atmosphere so far.

Figure 6 shows the temperature dependence of the contact angles obtained in a side-by-side comparison of the wetting of a basic synthetic slag (slag B-C in Table 1) of MgO/Al_2O_3 spinel substrates of composition ratios 50/50 and 65/35 mole percent as a function of temperature.

The wetting of the basic slag on the magnesia-rich spinel was much stronger, as evidenced by the small contact angle which decreased rapidly to almost zero at 1475°C and above. In comparison, the contact angle on the stoichiometric spinel decreased less rapidly with increasing temperature to an asymptotic value of about 10° at temperatures above 1600°C.

Curvature data of molten surfaces have been obtained; however, problems with computer programming have delayed processing. From this data, the surface tension for 12 slags and slag-seed compositions as a function of temperature will be determined.

As part of the post-test analysis to characterize the slag-substrate interaction, optical microscopy and electron microscopic examinations were initiated. The analysis is in progress.

Finally, it was determined that vibrations transmitted along the furnace stand were partially responsible for poor photographic contrast

---

+ The experimental details for the sessile drop method were described in Reference 2.

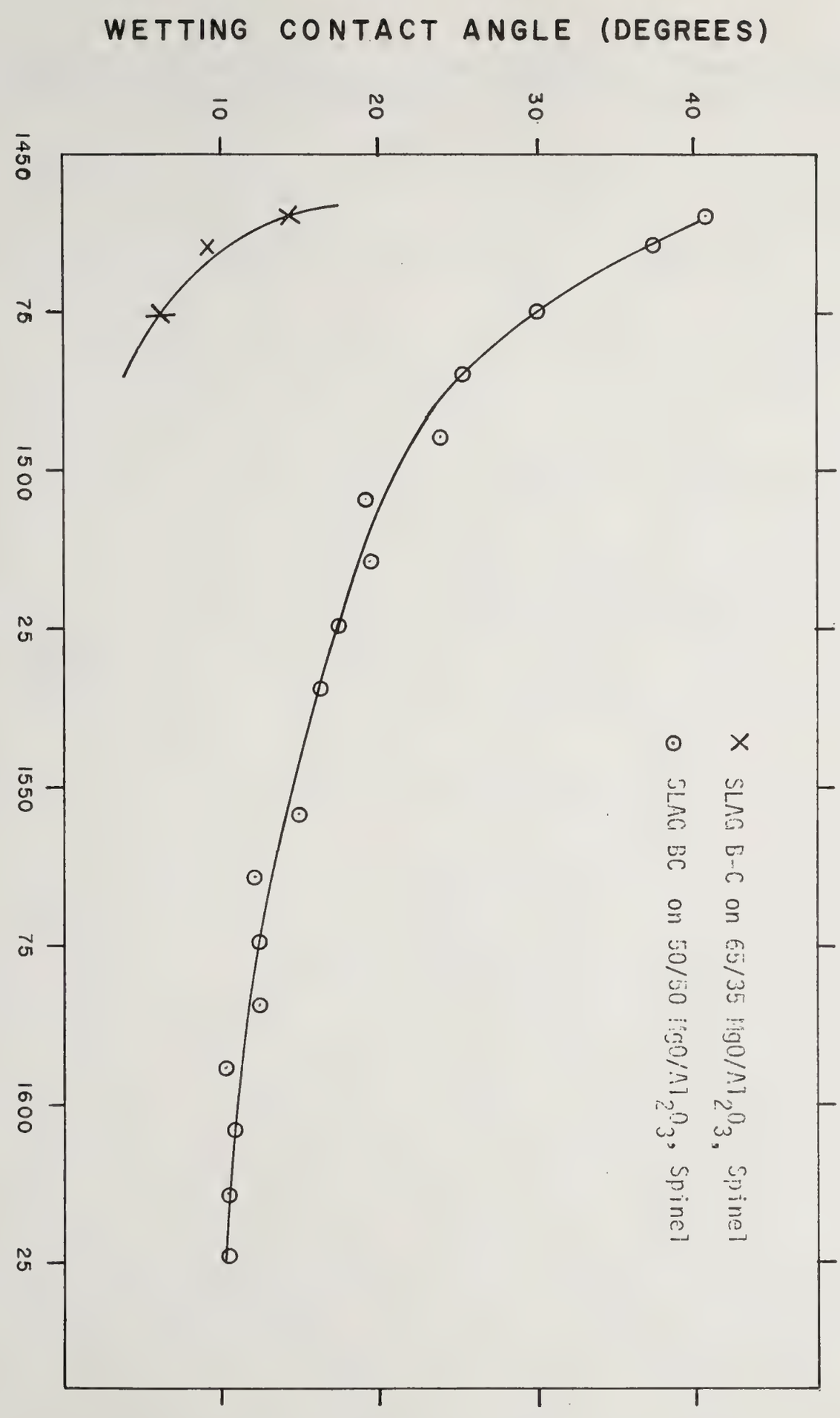

Figure 6. Wetting contact angles of a synthetic basic slag on spinel substrates

between the slag-air meniscus and the background. These vibrations were damped out, and the photographic quality was improved.

REFERENCES

1. R. R. Smyth, FluiDyne Engineering Corporation, private communication.

2. Montana Energy and MHD Research and Development Institute, MHD Power Generation: Research, Development and Engineering, Annual Report prepared for DOE, Contract EF-77-C-01-2524-12, Task N Report, October pp. 532-90, 1977.

3. H. J. Siebeneck, R. A. Penty, D. P. H. Hasselman, and G. E. Youngblood, "Thermal Diffusivity and Thermal Conductivity of a Fibrous Alumina," Ceramic Bulletin, 56 (6), p. 572, 1977.

4. D. Greve, Nils Claussen, D. P. H. Hasselman, and G. E. Youngblood, "Thermal Diffusivity/Conductivity of Alumina with a Zirconia Dispersed Phase," American Ceramic Society Bulletin, 56 (5), pp. 514-15, 1977.

5. S. L. Dole, O. Hunter, Jr., F. W. Calderwood, and O. J. Bray, "Microcracking of Monoclinic HfO_2," Department of Materials Science and Engineering, Iowa State University, private communication.

6. Y. S. Touloukian, R. W. Powell, C. Y. Ho, and P. G. Klemens, "Thermal Conductivity, Nonmetallic Solids," p. 10a, Volume 2 of Thermophysical Properties of Matter, IFI/Plenum, New York, 1970

7. A. F. Van Zee and C. L. Babcock, "A Method for the Measurement of Thermal Diffusivity of Molten Glass," Journal of American Ceramic Society, 34, pp. 244-51, 1951.

8. Robert Gardon, "A Review of Radiant Heat Transfer in Glass," Journal of American Ceramic Society, 44, p. 305, 1961.

9. Y. S. Touloukian and E. H. Buyco, "Specific Heat Nonmetallic Solids," p. 1237, Volume 5 of Thermophysical Properties of Matter, IFI/Plenum, New York, 1970.

10. R. Pollina, see "Slag Physical Properties: Electrical and Thermal Conductivity", Task G3, of this report.

11. L. M. Clark III and R. E. Taylor, "Radiation Loss in the Flash Method for Thermal Diffusivity," Journal of Applied Physics, 46, pp. 714-719, 1975.

12. R. L. Rudkin, "Thermal Diffusivity Measurements on Metals and Ceramics at High Temperatures," Report No. ASD-TDR-62-24, Part II, Air Force Materials Laboratory, Wright-Patterson Air Force Base, Ohio, 1963.

CDIF Environmental Monitoring--Air Quality/Meteorology

E. Kukay and V. Garrett

ABSTRACT

To assure the adherence of the MHD CDIF to existing environmental regulations and standards, this task involves monitoring and evaluating air quality, meteorological, and climatological data. MERDI implemented a total ambient environmental surveillance program (TAESP) to obtain necessary information for the implementation of this task. The accrued information will be used to document and compare baseline (pre-operational) and future (operational) environmental parameters.

A satellite air quality/meteorological station has been established southeast of the CDIF site. Two new pieces of equipment were installed at the permanent station at the CDIF site: a weather map facsimile machine and a Service A teletype. Other achievements of this quarter include the completion of an air quality procedures manual, the continuing development of the air quality data printout format, and cataloging of aerial photographs.

Daily forecasts indicate significant buildup of air pollutants during periods of surface-based temperature inversions. This trend will allow CDIF personnel to determine potential problem days for air pollutants and to take appropriate measures.

I. OBJECTIVE AND SCOPE OF WORK

The objective of this program is to ensure that the design, construction, and operation of the MHD Component Development and Integration Facility (CDIF) complies with the applicable environmental protection standards concerning ambient air pollution and source emission.

Meteorological and air quality investigations will be performed for the CDIF site and the surrounding area to determine the potential for air quality degradation associated with the CDIF operation. Baseline air quality data and climatological data can be used to assess the effects of the CDIF on the environment. Investigations will be implemented by designing and constructing a fixed meteorological station and several air quality monitoring stations. The system will be adequate for investigating the impact of the Engineering Test Facility (ETF), provided Butte is chosen as a potential site.

II. SUMMARY OF PROGRESS TO DATE

As part of the total ambient environmental surveillance program (TAESP), a satellite air quality/meteorological station has been established southeast of the CDIF site in addition to the permanent station at the CDIF site itself. Both sites monitor total suspended particulates, trace elements, gaseous fluoride, sulfation and nitration rates, and dustfall. A complete air quality procedures manual has been finished.

Air quality/meteorological data is entered continually into the computer for easy storage and correlation. A printout format for air quality data is being developed.

Aerial photographs of the vegetation around the CDIF site were taken during 1977. These photographs, both infrared and natural color, are being examined and documented for cataloging and future comparison studies.

A weather map facsimile machine was installed at the permanent air quality/meteorology station to obtain desired national weather maps. These maps are used to determine large-scale weather patterns and to provide a reference of weather conditions. A Service A teletype also has been installed at the permanent station to supplement information from the facsimile machine. The teletype provides more detailed, local forecasts.

Daily air quality forecasts are prepared from the data received and monitored at the two stations. These forecasts can be used by CDIF personnel to anticipate and plan for poor atmospheric conditions during MHD operation.

III. DETAILED DESCRIPTION OF TECHNICAL PROGRESS

A. Air Quality

1. Air Quality/Meteorological Stations

The first satellite air quality/meteorological station was established near Terra Verde about 2.4 kilometers southeast of the CDIF. The mobile unit which initially served the permanent air quality/meteorological site was moved the latter part of October; data collection for both air quality and meteorological parameters began at that time. Figure 1 shows the first satellite station facing northwest toward the CDIF site. All the parameters which are being measured at the permanent station also are being measured at the first satellite station, with the exception of temperature at 40 m height.

The continuous SO_2 and NO_x analyzers at the permanent station have been installed but are not operating because a portion of the air sampling train which the samplers will hook into has been back-ordered. As soon as these parts are received, the system will be placed into operation. Figures 2 and 3 show the permanent air quality/meteorological station.

2. Air Quality Data

Air quality sampling at the permanent station is continuing. Sampling at the first mobile station began during October 1977. Equipment at

both sites monitor

a) total suspended particulate and trace element analysis--24-hour samples every two days,
b) static sampling for gaseous fluoride (calcium formate), sulfation rate (lead peroxide), and nitration rate (triethanolamine)--30-day exposure, and
c) dustfall sampling for total settleable particulate and trace element analysis--30-day exposure.

A complete air quality procedures manual has been compiled. It contains data sheets and information on laboratory analytical methods, the data handling system, computer interface, etc. The manual will be updated to reflect changes as they are made.

3. Environmental Computer Data Base

Computer entry of the air quality/meteorological data is continuing. Work progressed on the development of a separate computer printout format for air quality data. The printout format for the meteorological parameters is being finalized. Once a suitable data base has been established, correlations between air quality and meteorological parameters can be established.

4. Aerial Infrared Photography

Data obtained during the 1977 aerial photography flyovers are being examined and documented. Vegetation types at all the sites examined with the infrared photographs will be identified and cataloged. This will allow ready verification of any plant destruction or damage. The photos will locate sites with possible damage, and the cataloging will provide a description of the types of any plants that are damaged.

B. Meteorology/Climatology

During the first week in October, an Alden Model 9271H weather map facsimile recorder was installed at the permanent air quality/meteorology station. The recorder automatically starts from signals received over the National Weather Service NAFAX circuit. A time clock is used to obtain the desired maps and to reject all others. The weather maps generated by the unit are used to formulate air quality forecasts and to provide a reference library of weather conditions which occurred during particular stagnation events and for correlation with standard air quality monitoring equipment information. Currently, several maps are received daily. They are as follows:

500 mb analysis 0000 and 1200 GMT
700 mb analysis 0000 and 1200 GMT
850 mb analysis 0000 and 1200 GMT
Barotropic prognosis--500 mb heights and vorticity for 12, 24, and 36 hr.
Radar summary
LFM prognosis for 24, 36, and 48 hr
Weather depiction
Surface analysis 0000, 0600, 1200, 1800 GMT
GOES Satellite, Western U.S.

12 and 24 hr clouds, precipitation and low level significant weather prognosis
36 and 48 hr surface analysis, clouds and precipitation prognosis
30 hr surface and 36 hr 1000-500 mb thickness prognosis
72 hr 500 mb prognosis.

A Service A teletype has been installed at the permanent station. National Weather Service and FAA Flight Service Station hourly weather observation data, as well as terminal and area forecasts, are available over the Service A network. This information is used as a supplement to and in conjunction with the information supplied by the facsimile machine (fax) described above. It provides more descriptive data and forecast information for the local region than does the fax. The data and forecast information provided by the fax cover the entire United States and are used to assess the general synoptic (large-scale) weather patterns that currently prevail and are expected to occur within the next couple of days. The data and forecasts provided by the Service A teletype are more detailed and apply to local areas. The terminal forecasts from the Service A teletype are assessments made by the local National Weather Station forecast office (Great Falls) of the expected weather during the next 24 hours at given cities throughout Montana.

From the area and terminal forecasts, hourly observation data, and facsimile products, a daily air quality forecast is prepared. During the past eighteen months, it has been noticed that a significant buildup of air pollutants occurs during periods when a surface-based temperature inversion exists within the Butte valley. Such inversions nearly always form during clear nights as the result of an upward flux of infrared radiation and associated surface cooling. However, during winter evenings, the inversions often formed in the presence of a cloud layer. The purpose of the air quality forecasts is to determine the likelihood that an inversion will form. Forecasts typically are prepared by 1000 MST and cover a 24-hour period. The forecasts answer two questions: 1) if an inversion currently exists, will it persist the remainder of the day (and cause a significant deterioration)? and 2) will an inversion form during the following evening (and trap effluents emitted during the night)? Regarding CDIF operation, one use of the forecasts will be to enable the people involved in assessing the environmental effects of the plant to prepare equipment, etc. in advance to test various parameters when the plant is operating under poor atmospheric dispersion periods. If adverse air quality results from operating the plant during inversion periods, the operators may want to use such forecasts as an aid to perform plant operations that will not increase air quality degradation.

C. Work Forecast

A second mobile air quality/meteorology unit will be ordered during the second quarter of FY 78. As equipment arrives, it will be placed into the system. When the parts arrive for the continuous gas analyzers, they will be readied for operation at the permanent station. A data logging system for the continuous analyzers will be ordered. This system will be compatible with the data logging systems currently in use at the permanent and satellite stations. The second satellite station will be located 1.6 kilometers north-northeast of the CDIF site.

A data reference manual will be prepared. It will contain air quality and meteorological data obtained from the permanent and satellite stations during

1977. The aerial infrared photography investigation from the summer of 1977 will be completed, and a report will be prepared. Western Telecomputing Corporation of Bozeman, Montana will conduct another communications quality survey at several locations relative to the CDIF to determine baseline noise in the 10 KHz to 1000 MHz band.

IV. CONCLUSION

Air quality and meteorological data from two stations are being collected. A third station is planned for the near future. The data are being put onto a nine-track magnetic tape for reduction and storage for later use. A computer printout for both air quality and meteorological data is near completion. When the printout is completed, a data reference manual will be compiled. Continuous SO_2 and NO_x analyzers will be put into operation with the arrival of back-ordered materials. Aerial infrared photographs obtained during the summer of 1977 are being examined. Meteorological/air quality forecasts for weather conditions near the CDIF were begun.

DIVISION OF MAGNETOHYDRODYNAMICS

MONTHLY PROJECT MANAGEMENT STATUS REPORT

REPORT DATE _____

FOSSIL ENERGY

CONTRACT/PROJECT		SCHEDULE
CONTRACT NO.	VENDOR	

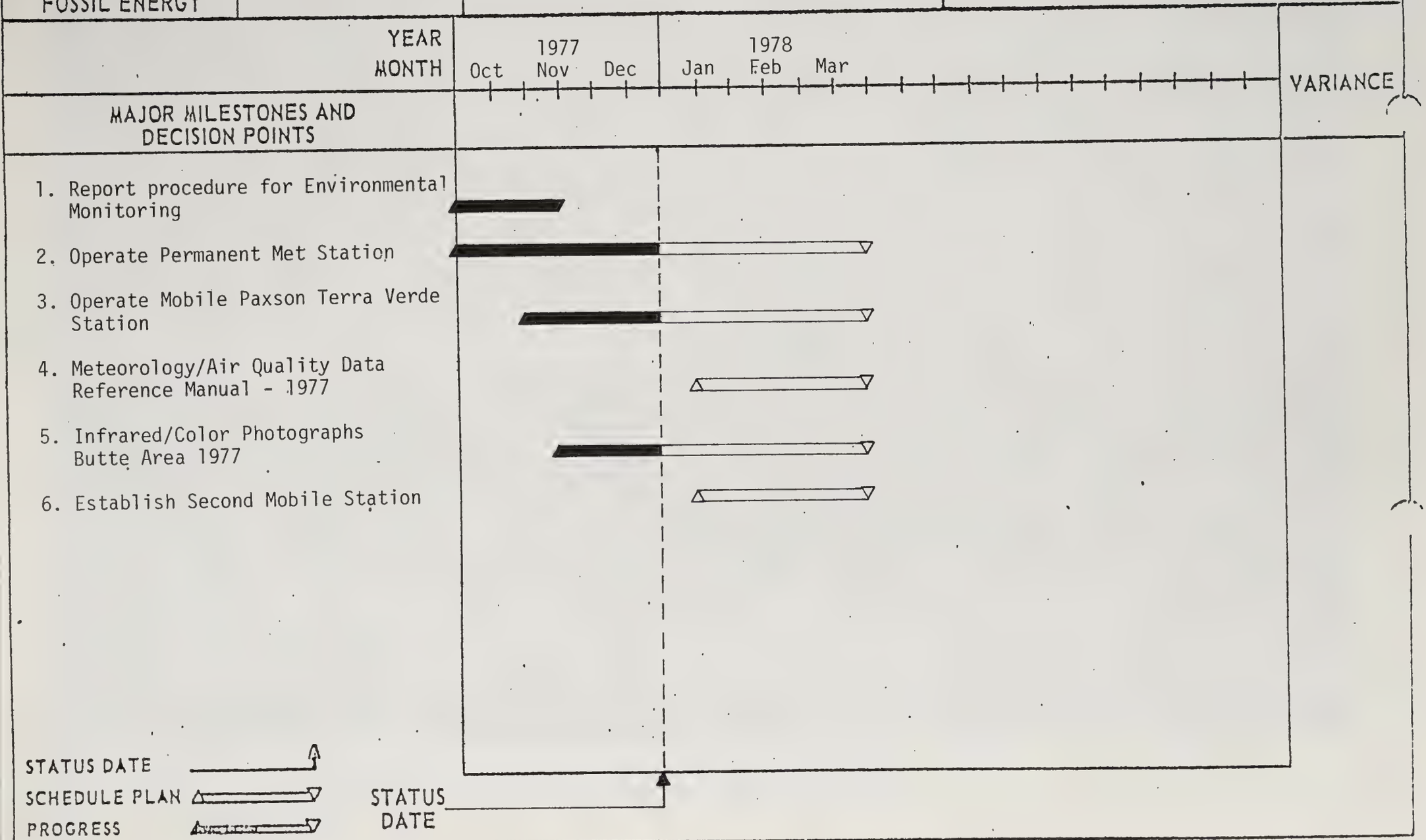

Figure 1.--Paxson Station at Terre Verde, Butte, Montana (looking northwest toward the CDIF site)
October 1977

Figure 2.--Permanent Meteorological Station at the Industrial Park, Butte, Montana (looking northwest toward the CDIF site) October 1977

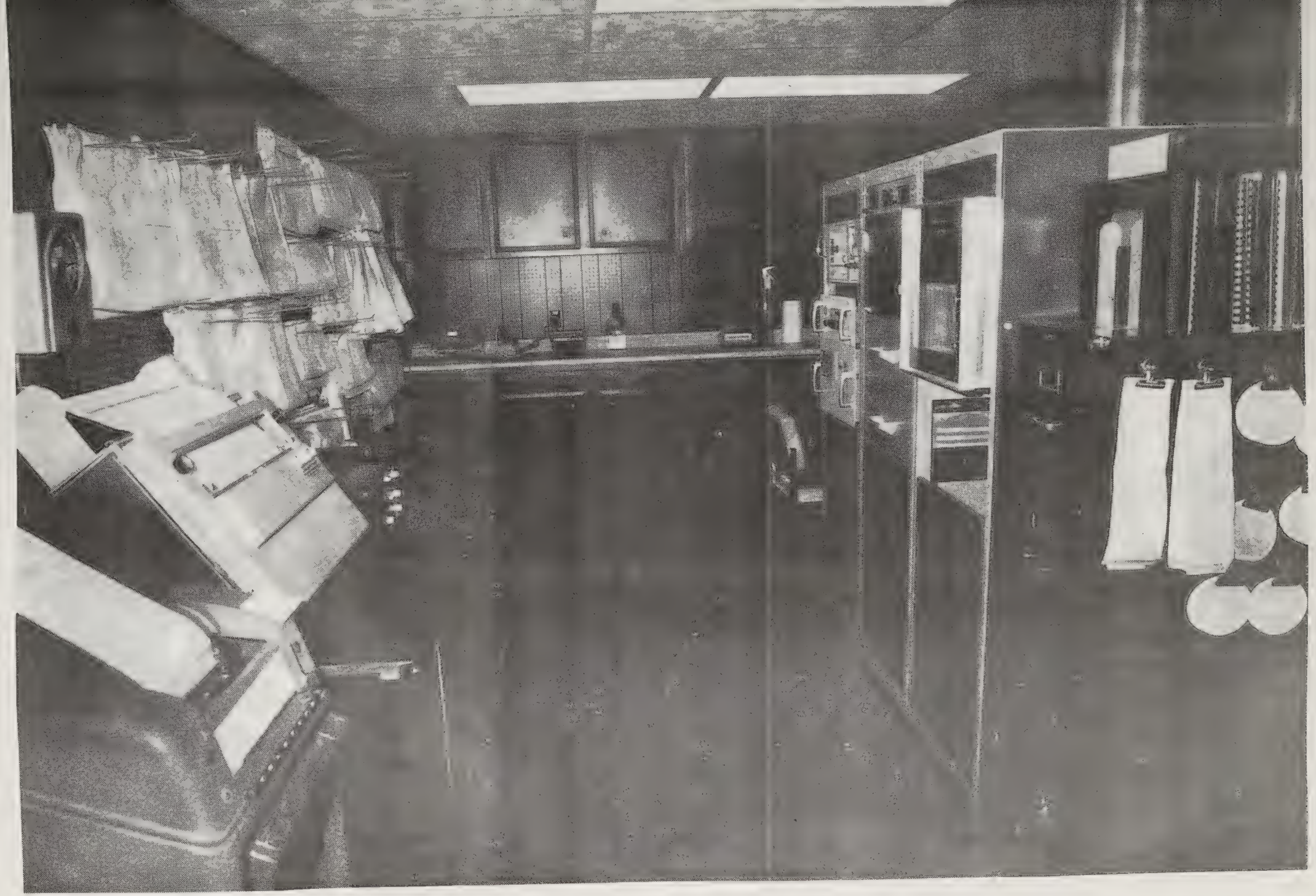

Figure 3.--Permanent Meteorological Station, Interior (looking west)
December 1977

MHD CDIF Pre-operational Biological Baseline Surveillance Program

R. Portch, J. Cornish

ABSTRACT

The biological surveillance program, implemented last quarter, progressed with the prescribed aquatic sampling and analytical (excepting trace ion) schedule plus initiation of terrestrial site acquisition/leasing from the respective land owners. Applied field and laboratory methodologies were submitted to the Department of Energy (DOE) in December 1977. A new subtask investigating the feasibility of research related to the monitoring of MHD operational effects on public/worker health was initiated. Formal work on this project should begin by mid-April 1978.

I. OBJECTIVE AND SCOPE OF WORK

The immediate surveillance program involves the identification and continued measurement of potential environmental impacts, with emphasis on trace elements, arising from CDIF activities. The major objectives are

1. The development of a valid environmental baseline for the CDIF study area,
2. The development of monitoring program design and procedures in a manner capable of distinguishing CDIF operational impacts from those produced by existing or future human activities in the Butte valley,
3. By analysis of the above data, anticipate and provide input into the resolution and mitigation of engineering problems related to the design of improved air pollution and liquid effluent control systems,
4. The identification of potential areas of concern related to public health and well-being, and
5. Contributions to the maintenance of a safe and healthful CDIF workplace environment.

Task I monitoring of primary (CDIF) impacts on terrestrial and aquatic ecosystems is organized as follows:

1. The selection of appropriate sampling areas, followed by acquisition of site access,
2. The ecological characterization of these sites will be determined through the selected biological, chemical, and physical parameters, and
3. The creation of a bioenvironmental interpretation of the study area by statistical analysis of the above data.

Secondary (non-CDIF) environmental impacts will be considered by diligent monitoring of the continued, overall development occuring in the valley. This surveillance will center around stratified soil-flora sampling and static biological (Sphagnum moss) air quality monitors.

Task II has been initiated by the preliminary public health data accruement phase. It is anticipated that preproposals in regard to public health will include the following:

1. The characterization and documentation of trace element burdens, e.g., in the local populace relative to an equivalent "control group," and
2. Participation in advanced epidemiological studies, e.g., relating past and present ambient air quality and industrial activities to historical health trends.

Additional preproposals concerned with worker-health could include

1. The effects of MHD-induced electromagnetic fields,
2. The effects of chronic and/or acute exposure to inorganic or organic pollutants released into the workplace environment (this would include fumes, vapors, gases, and ionized particulate matter), and
3. The effects of high-frequency noise and/or shock-concussion affects potentially occuring during start up or shutdown of CDIF operations.

II. SUMMARY OF PROGRESS TO DATE

The progress of the biological surveillance program for the first quarter of FY 78 can be found in the milestone chart in Table 1. An overview of each phase within the two subtasks is given below.

A. Task I

1. Terrestrial Monitoring Phase

The location and delineation of sampling sites, for both exclosures and static moss air quality samplers, are tentatively completed. Negotiations or land access inquires have been initiated with the respective land owners of the selected monitoring areas.

2. Aquatic Monitoring Phase

The sampling program continues on the prescribed schedule. Bacteriological and general chemical analysis continues on schedule, while the aliquots reserved for algal studies and trace element analysis have been back-logged until negotiations for subcontractual analytical services have been completed.

B. Task II

1. Literature Review and Consultant Acquisition Phase

This task has been initiated by the cursory review of the literature on hand in regard to public and worker health concerns. These efforts were devoted to the determination of feasible projects that could be initiated within the second quarter of FY 78.

2. Public Health Data Accruement Phase

This phase has been completed with the preliminary findings report.

III. DETAILED DESCRIPTION OF TECHNICAL PROGRESS

A. Work Accomplished (Task I)

1. Terrestrial Study

Five sites have been located for exclosure construction, with at least one site in each compass quadrant and all within two miles from the CDIF. At this time, only one exclosure area has been leased although inquires and negotiations with the other land owners is being actively pursued. A total of 20 static moss sampler units will be placed at selected sites throughout the Butte valley to monitor both "background" (non-CDIF) and CDIF emission effects once the facility becomes operational. Specifications and criteria for construction of exclosures and moss samplers have been completed; orders for materials are pending.

The draft report for environmental monitoring (field and laboratory) procedures was submitted to the Department of Energy on December 1, 1977.

2. Aquatic Study

Sample collection and analysis (excluding trace ion determinations) continues on schedule. Trace ion data through October 1977 has been received from the subcontractor and logged. Data reduction is proceeding at a slow pace due to lack of a suitable computer storage and analysis routine.

The hydrologic literature for the CDIF area has been reviewed, and potential groundwater monitoring sites have been selected within CDIF bounds. Well specifications have been drawn up and reviewed by the Department of Energy and MERDI administrative personnel. No requests for quotes or formal bids exist at this time.

B. Discussion (Task I)

1. Terrestrial Study

Efforts in the identification of the area's land ownership

patterns and site acquisition are proceeding as rapidly as possible. Site selection processes are being coordinated closely with those for air quality monitoring; this should assure effective evaluation of biological (ecological) response to any observed changes in air quality observed over the lifetime of the CDIF project.

2. Aquatic Study

The collected and reduced data volume has been judged to be insufficiently small to allow statistical analysis or comments on the study area's general water quality. Efforts related to the establishment of electronic data processing systems capable of storing and manipulating the aquatic (and eventual terrestrial) parameters continues at a moderate pace.

The aquatic flora, and especially the "water quality index species" of the cyanophyta and chlorophyta, have not been described or monitored at this date. Currently, the staff is reviewing the equipment specifications and space necessary to create a laboratory facility capable of handling this taxonomic work as well as more effectively process the chemical analysis, including trace ion determinations. These efforts are in conjunction with those allotted to the establishment of research and development oriented laboratory support for the terrestrial monitoring phase of this task.

C. Work Accomplished (Task II)

1. Literature Review and Consultant Identification

Periodic, cursory review and acquisition of literature pertinent to potential public and worker health effects, as influenced by MHD operations, has been initiated. Several consultants with expertise in the above problem areas have been identified but not contacted.

2. Public Health Data Accruement Phase

The preliminary summary report documenting efforts in the acquisition of baseline (pre-operational CDIF) data has been prepared and is being proofed by the authors.

D. Discussion (Task II)

1. Literature Review and Consultant Identification

General research problem areas have been and continue to be identified and considered superficially regarding their feasibility and relevance to the biological program's overall scope and objectives. This phase tentatively will be initiated by mid-April 1978.

2. Public Health Data Accruement Phase

This report will serve as the basis for evaluating public and, to some degree, worker health conditions as influenced by the MHD operations. Programmatic review of this phase will occur by late August 1978; the decision on whether to continue or elaborate the existing data collection will be influenced by the progress observed from existing, non-MERDI studies being conducted in the Butte-Silver Bow County area.

E. Work Forecast

1. Task I--Terrestrial Monitoring Phase

Land access lease negotiations and erection of moss sampler stations and exclosures should be completed by mid-March 1978. Barring major administrative interface of materials supply problems, the moss sampler/snow collection activities (for trace ion analysis) will be initiated by late January, while the full terrestrial field season will begin with clement weather, e.g., by mid-April. The procedures for field and analytical methods can be found in the December 1, 1977 deliverable document.

2. Task I--Aquatic Monitoring Phase

The delineated parameters will continue to be sampled on a three-week frequency as is done at present, while water and aquatic flora trace ion content will be determined every six weeks. Continued lag in processing the aquatic samples for trace ion levels and algal taxonomy should be mitigated by the end of the first quarter of CY 78 if the appropriate laboratory facilities can be created or subcontracted to existing, private analytical services.

Given the rate of analysis, the submittal of the summary report of FY 77 baseline data, scheduled for release by early May 1978, may be delayed until mid-June 1978. The programmatic review of the biological surveillance program, prior to CDIF start up, still should be initiated by, or shortly after, the end of FY 78.

3. Task II--Literature Review and Consultant Identification Phase

Negotiations for funding of a formal preproposal and/or preparation efforts in regard to matters of MHD-influenced effects on public and worker health should be initiated by late March or early April 1978.

4. Task II--Public Health Data Accruement Phase

No concerted efforts in the advancement of this project will be made during the forthcoming quarter. Evaluations of the necessity to continue this project will be determined largely by the progress and/or relevance to non-MERDI research efforts being done, or scheduled to be done, on the Butte-Silver Bow County study area.

IV. CONCLUSIONS

A. Task I

1. Terrestrial

This quarter, the creation of the necessary technical "groundwork" for the establishment of a "minimum but adequate" pre-operational biological surveillance program is nearly completed. Sites have been chosen, land access/lease negotiations have been initiated, and materials and supplies have been acquired to enable initiation of field studies by mid-April 1978. No additional data has been gathered since the release of the previous quarterly report.

2. Aquatic

The sampling program continued on schedule; however, problems with available analytical services precludes valid data reduction and statistical analysis, thus no quantitative conclusions can be made at this time.

B. Task II

1. Literature Review and Consultant Acquisition

This phase was incorporated into the surveillance program to enlarge the scope and effectiveness of the program's contribution toward an environmentally compatible MHD technology. It is anticipated that the present efforts in selecting feasible research areas will be expanded into a formal portion of the MHD CDIF Pre-operational Biological Baseline Surveillance Program by mid-April 1978.

2. Public Health Data Accruement Phase

In this phase document,it was concluded that certain pathologies occurred at elevated rates relative to the respective Montana-wide rates; however, no interpretation of the data or search for etiologies was presented. Currently, the recommendations for further research are being evaluated for possible inclusion in the general public and worker health monitoring program.

Environmental Analysis of Trace Elements and Submicron Particles from MHD Test Facilities

N. Egan, B. Moody, and K. Runnion

ABSTRACT

Major milestones for this quarter are on schedule. Chemical equilibrium, combustor, and channel programs have been obtained and incorporated into the computer. Initial testing of these programs has been conducted. Slight delays have occurred in obtaining analytical samples; however, no overall project delay is expected.

I. OBJECTIVE AND SCOPE OF WORK

Both the toxicity and essentiality to life of certain trace elements are well documented. Exhaustive studies have been performed to determine the fate of coal trace elements released during combustion in conventional power plants. More recent studies have involved analyses from coal-fired MHD facilities.

The higher temperatures generated in coal-fired MHD facilities result in 1) vaporization of more chemical species than in conventional facilities and 2) production of higher concentrations of fine particulates which are collected inefficiently by present pollution control systems. These variations will change the emission profile, thereby affecting the distribution of both toxic and essential trace elements.

The objective of this task is to characterize those trace elements and submicron particles having environmental impact which will be identified in existing MHD facilities. This task has been divided into three subtasks.

The work on Subtask A is to obtain computer programs, including data files where applicable, to analyze MHD process emissions. Process effects on the composition and concentration of emissions are to be identified, particularly trace elements and submicron particles. Emphasis is being placed on obtaining the best computer models already in use to evaluate MHD environmental effects.

Subtask B will be the modification of the programs obtained in Subtask A to evaluate potential emissions from the CDIF, including the quench process.

Subtask C will deal with selecting and sampling various MHD facilities that are deemed most appropriate to supply data with which to validate the computer models and will deal with supplying representative samples for further trace element and particulate characterization. The analytical work for characterization will be subcontracted largely to the University of Missouri at Rolla (Environmental Trace Substances Research Center--ETSRC) and Montana State University (MSU).

II. SUMMARY OF PROGRESS TO DATE

The New Hampshire chemical equilibrium program has been received. The first step in the program, thermodynamic data handling and manipulation, has been converted and successfully tested on the MERDI computer. The Montana State University combustor and channel time-temperature programs are operational, and the CDIF personnel presently are employing these programs for operational model studies.

Slight delays have occurred in obtaining analytical samples from Thompson, Rama, and Woolridge (TRW) and the University of Tennessee Space Institute (UTSI); however, analysis work is progressing on samples previously collected from the Pittsburgh Energy Research Center (PERC).

III. DETAILED DESCRIPTION OF TECHNICAL PROGRESS

A. Subtask A: Emission Modeling

The accurate, reliable prediction of MHD emissions is required for appropriate review, analysis, and approval of various MHD facilities required for the technology development program. Models exist for the gaseous emission, NO_x and SO_2, but trace element and particulate models for MHD have not been developed. The object of this subtask is to obtain existing computer models to be used as building blocks for development of the emission model. Characterization of the growth and formation of particles is part of the model development.

Computer models that have been identified with the above objective are discussed in the following sections. Model development also is presented. Trips were made to two organizations that are conducting MHD computer modeling work.

1. Model Selection and Acquisition

Rather than developing all new computer programs, emphasis has been placed on obtaining existing models and using them as building blocks. The models will be kept as simple as possible and still be consistent with reasonable accuracy as operational models. Selection of a model does not mean it is the best available but that it has characteristics adaptable to our emission model.

Due to the high temperatures in an MHD system, the composition of the gases is assumed to be in equilibrium. A chemical equilibrium program will be used to predict the trace elements and trace-element compounds that will be gaseous upon leaving the combustor. Thermodynamic data for trace elements at high temperatures is fragmentary. A chemical equilibrium program developed by the University of New Hampshire (UNH) has been acquired. This program, written at the Naval Ordinance Test Station (NOTS) to evaluate propellant systems, was modified by the UNH. This modified version of the NOTS propellant evaluation program (PEP) is used to determine the composition and temperature of flames in a study of particle formation in flames. The program is simple, has good documentation, and consists of a large data file on trace elements.

The time-temperature history of the gases as they travel through the MHD system is an important operating parameter. Several combustor and channel models exist. It has been decided to use the programs developed at MSU for MERDI because the programs are already on the MERDI computer, documentation is available, the originators are close for consultation, and the CDIF staff is using the programs for operational models.

Downstream of the combustor and channel, fewer models are available to determine the time-temperature history of the effluents. A mathematical model for the quench was developed during the last contract period by MERDI. A program has not been selected or developed to model radiant cooling.

Models for NO_x emission from MHD systems have been developed by STD Research Corporation, Energy and Environmental Research, and Stanford University. These organizations are reluctant to give MERDI their computer programs because thorough documentation is not available. They would prefer to run the programs for MERDI under any conditions desired and to include integration with a quench model. An evaluation to select an NO_x model has not been completed.

The formation and growth of particulates is very important in characterizing trace elements and submicron particles. Research on nucleation and growth of particles is being conducted by several organizations. Massachusetts Institute of Technology (MIT) and Aerodyne Research Corporation have done paper studies of the homogeneous nucleation of SiO_2. Experimental work is just beginning to verify and expand these simple models that use classical nucleation theory. Battelle Pacific Northwest Laboratory and the University of New Hampshire are looking at nucleation and growth of ash. Model development is in the preliminary stages. Most research in this area looks at well-ordered and well-defined systems. Selection of a model for nucleation of trace elements will depend on more information. Work is being initiated at MERDI to study the theory and survey the research of the nucleation phenomena.

2. Model Description

a. Chemical equilibrium program

The University of New Hampshire has modified the NOTS propellant evaluation program to determine the composition and temperature of flames. There are two main steps in the equilibrium computation. The first is the preparation of a thermodynamic data file for the system under consideration and involves only data handling. The second step is the actual computation, which proceeds in three stages. The first stage is concerned with the input of data and control options, system stiochiometry, and labeling information. The second stage provides the initial estimate of the system composition. The actual temperature-equilibrium interaction is performed in the third stage.

Documentation: Computer Techniques for Determining Flame Temperature and Composition, Raymond E. Desrosiers, Interim Report, ERDA Contract (E49-18)-2205, March 20, 1977, Department of Chemical Engineering, University of New Hampshire, Durham, New Hampshire.

b. Combustor program

The combustor program was developed originally at Montana State University to predict the thermodynamic state of the combustion plasma entering the nozzle, based on the physical configuration of the combustor. It assumes that the coal particles are devolatilized instantly but that carbon burnout from the coal particles is governed by chemical kinetics and diffusion of O_2 and CO_2. Steady state is assumed, and the gaseous species are assumed in chemical equilibrium at all times. Twenty-one reactions are considered among 29 reacting species, including NO_x, SO_2, and various potassium compounds. The program assumes that the ash fuses and that the slag does not vaporize. Either one- or two-stage combustion can be handled.

Documentation: A Digital Computer Model and Simulator for Pulverized Coal-Fired MHD Combustors, Donald A. Rudberg, ERL Report No. 677, August 1977, Electronics Research Laboratory, Montana State University, Bozeman, Montana.

c. Steady-state MHD channel flow program

The steady-state MHD channel flow program was developed originally at Montana State University. It solves the one-dimensional equations of motion for the MHD nozzle, channel, and diffuser. Boundary layers are accounted for by overall heat transfer and skin friction terms.

It can be run with either area or temperature specified down the channel.

Documentation: Fortran IV Computer Programs for the Analysis of Quasi One-Dimensional MHD Flow Problems, T. D. Robles and R. M. Johnson, ERL Report No. 277, June 1977, Electronics Research Laboratory, Montana State University, Bozeman, Montana.

d. Model development

All the programs from the University of New Hampshire chemical equilibrium program are on the computer. The first step, thermodynamic data handling and manipulation, has been converted and successfully tested on the MERDI computer. A copy of the complete raw data file was supplied with the computer program. Arrangements are being made to obtain computer punch cards of this data from the University of New Hampshire to accelerate data placement in the

computer. The second step of the program, the calculation of the equilibrium composition, needs to be converted and tested. The user's manual will have to be modified so it is compatible with the MERDI computer.

The combustor and channel programs are operational at steady-state on the MERDI computer. The modification and use of these programs for trace-element emission modeling was discussed with the program originators from MSU. They foresee no problem in adding trace element data to the combustor program; however, the program (as presently written) considers only gaseous species. The equilibrium calculation is already the slowest part of the combustor program; additional data will increase the run time. Rather than incorporating the equilibrium program into the combustor program, it seems more advantageous to use the time-temperature output of the combustor program as input to the equilibrium program. The channel program also can supply a steady-state, time-temperature history for the equilibrium computation.

Development of computer models for the quench, radiant cooling, and formation and growth of particles has not been started. Mathematical analysis of the quench was completed during the last contract period; a computer program will be written during this contract period; and a nucleation phenomena study is being initiated.

3. Trips

Visits were made by MERDI personnel to STD Research Corporation (STD) and Energy and Environmental Research (EER) to discuss their modeling work.

a. STD Research Corporation

STD has computer programs for a complete MHD system and chemical equilibrium and NO_x programs. High-temperature thermodynamic data is needed to expand the equilibrium program. Much of the data is hard to find, nonexistent, or suspect. STD is willing to run any programs MERDI desires but is reluctant to give MERDI any codes.

b. Energy and Environmental Research (EER)

EER is doing the NO_x computer modeling for Exxon's "Environmental Assessment of Advanced Energy Systems." They would like to run the program for MERDI because they feel it would be too time-consuming for MERDI to learn the workings of the program. Integrating the program with a quench model would pose no foreseeable problems.

B. Subtask B: CDIF Emission Modeling

The quench model discussed under Subtask A is applicable directly to the CDIF. The combuster and channel programs are being developed as operational programs for the CDIF. Development and modification of the computer

models will be concerned with ensuring that the programs are flexible enough to apply to the CDIF.

C. Subtask C: Sampling and Analysis

Experimental work on trace elements and submicron particles is covered under Subtask C. The University of Tennessee Space Institute (UTSI) and Thompson, Rama, Woolridge (TRW) have been selected as sampling sites. The scopes of work and milestones for analysis of trace elements are presented for the Environmental Trace Substances Research Center (ETSRC) and Montana State University (MSU). Subcontractors will be under contract in January and November, respectively. Trips by MERDI personnel to organizations that are conducting research on measurement techniques also will be discussed.

1. Site Selection and Sampling

There are two main requirements which a facility must meet to qualify for particulate and trace-element emission sampling: 1) coal must be the primary fuel and 2) MHD temperatures must be attained. UTSI and TRW facilities meet these criteria and have been selected as sampling sites for trace element and submicron particle emissions. Both facilities will conduct their own sampling, but representatives from MERDI will be on hand to monitor the sampling.

The UTSI facility is fairly flexible and includes a combustor, a channel with magnet, a diffuser/radiant boiler, and water-jacketed hot gas cyclones. The combustor is designed for 100 percent slag carry-over, which makes the facility somewhat atypical. UTSI will make three runs with seed injection. Samples of the coal, the slag, and the total particulates will be collected. The hot exhaust gases from the cyclones will be sampled with a probe connected to a modified Brinks sampler for total particulate determination. High exhaust gas temperatures limit sample probe times, and only microgram quantities are obtainable.

The TRW facility also is fairly flexible. The exhaust is cooled with a water quench similar to the CDIF design. Particulate sampling of the water-laden exhaust stream is very difficult. TRW has suggested designing a special instrumented sampling section before the water quench. This section would be designed and built during the next contract period.

TRW will make two runs, one seeded and one unseeded. Samples of the coal, the slag, the water from the slag tank, and the quench water will be collected. A water-cooled probe also will be inserted into the second-stage of the combustor to collect a condensed gas sample.

Samples will be sent to ETSRC and MSU for analysis. Samples previously collected from the Pittsburgh Energy Research Center (PERC) also will be analyzed by ETSRC.

a. Scope of work for the Environmental Trace Substances Research Center (ETSRC)

The intent in this contract period is for ETSRC to analyze samples collected at three facilities to determine trace and major

element partitioning and enrichment.* Development of new analytical techniques is encouraged. Samples will be collected by TRW and UTSI and sent to ETSRC for analysis. Previously collected PERC samples also will be analyzed.

Trace elements of known toxicity or those essential to living systems, plus certain major elemental constituents, are of special importance and are detailed in Table I. ETSRC will perform analyses on each sample for these specified elements and for any other elements which are deemed appropriate.

Table I.--Specific Trace and Major Elements Requested for Analysis

Trace Elements		Major Constituents
Toxic	Essential	
Lead (Pb)	Chromium (Cr)	Silicon (Si)
Cadmium (Cd)	Manganese (Mn)	Aluminum (Al)
Nickel (Ni)	Cobalt (Co)	Iron (Fe)
Magnesium (Mg)	Copper (Cu)	Calcium (Ca)
Beryllium (Be)	Zinc (Zn)	Sodium (Na)
Bismuth (Bi)	Selenium (Se)	Potassium (K)
Arsenic (As)	Molybdenum (Mo)	
Antimony (Sb)	Boron (B)	
Tin (Sn)	Vanadium (V)	

The samples and desired analysis to be performed by ETSRC include the following:

1) Coal--Samples from PERC, TRW, and UTSI will be analyzed to determine percent ash content and to quantitatively analyze for the previously detailed trace and major elements. Dual analyses should be performed on one sample to determine reproducibility of the analysis procedure.

2) Slag--Samples from PERC, TRW, and UTSI will be analyzed for bulk trace and major element concentrations with the intent of determining partitioning effects. Dual analyses should be performed on representative samples to determine slag homogeneity. Analyses will be performed on samples from potassium seeded and non-seeded runs.

---

*During coal combustion, certain elements tend to become concentrated in various ashes. The tendency to concentrate according to location in the facility is called element partitioning, and the tendency to concentrate in particles of a certain size is called particle enrichment.

3) Slag Dump Tank Water--TRW and PERC will supply water samples from their slag tanks. Analyses will determine the water-soluble trace and major element fraction of the slag. Samples from seeded and non-seeded runs will be analyzed.

4) In-Stream Samples--Total particulate and cascade impactor samples from PERC will be analyzed. TRW will supply total particulate samples. Seeded and non-seeded runs will be analyzed, and Cascade impactor samples will be measured for particle size vs. element concentration.

5) Baghouse Sample--Bulk trace and major element analyses will be performed on a PERC sample for a partitioning determination.

6) Quench Water--Seeded and non-seeded samples will be supplied by TRW. Dual analyses will be performed on these samples. Non-seeded samples from PERC also will be studied. Ponding of CDIF quench water requires a knowledge of trace and major element concentrations and, therefore, a method of analysis. While all problems with analysis of quench water may not be solved this contract period, work must continue in this area. Studies should proceed on overcoming the adverse effects of potassium seed on analytical sensitivity.

Milestones for ETSRC's subcontract include the following:

Preparation of PERC Samples	
Begin	January 1, 1978
Finish	January 31, 1978
Arrival of TRW and UTSI Samples	January 21, 1978
Preparation of TRW and UTSI Samples	
Begin	January 21, 1978
Finish	January 31, 1978
Analytical Period	
Begin	February 1, 1978
Finish	March 15, 1978
Reports	
1st Interim	February 15, 1978
2nd Interim	March 15, 1978
Final	April 15, 1978

b. Scope of work for Montana State University (MSU)

Studies from conventional facilities have shown that many trace elements tend to concentrate in the smaller particulate and that the majority of the concentration occurs on the particle surface. This means that the particle surface indeed may expose living tissue to considerably higher levels of toxic trace elements than a bulk analysis would seem to indicate.

At present, only bulk trace element analyses have been performed on MHD emissions. If the surface deposition phenomena does occur in effluents from MHD facilities as it does from conventional plants, early detection and characterization of these emissions are needed so that effective means of control can be developed. The effort required to provide initial information in this area is discussed in the following section.

The intent in this contract period is to analyze particulate samples collected at three facilities in order to determine particle size, particle density, surface particle composition and concentration by size, and bulk particle composition and concentration by size. Work will continue on improving methods of analysis using techniques developed during the previous contract period. New methodologies will be explored for areas applicable to improving trace element analysis.

MSU will analyze two PERC samples collected by ETSRC. MSU also will perform analyses on samples collected by TRW and UTSI.*

Trace elements of known toxicity or those essential to living systems, plus certain major elemental constituents, are of special importance and are detailed in Table I.

Montana State University will perform analyses on samples as specified for these elements and for any other elements which are deemed appropriate.

Samples to be analyzed by MSU include the following:

1) Total Particulate--Two total particulate samples will be analyzed. The PERC sample was collected before the baghouse and effectively collects particulates down to 0.8 microns. The second sample is to be collected from the cyclone exhaust at UTSI.* High-exhaust gas temperatures limit sample probe times, and only microgram quantities are obtainable.

2) Cascade Impactor Sample--MSU will obtain a PERC cascade impactor sample from ETSRC. The sample to be analyzed was collected before the baghouse.

3) Condensed Gas Stream Sample--Two condensed gas stream samples collected from the second stage of the TRW combustor also will be analyzed by MSU.

Desired analyses of these samples include the following:

1) Particle Size--Knowledge of particle size aids in determining possible problems to be encountered in developing effective pollution control systems. Both the PERC and UTSI*

---

*This assumes that sufficient samples are available.

total particulate samples will be analyzed to determine the overall range of particulate sizes. The lower three stages (<1 micron) of the PERC cascade impactor sample also will be studied to obtain a better estimate of submicron particle sizes.

2) Particle Density (Particle Concentration by Size)--Particle density, as well as particle size, is important in determining necessary pollution control devices. The PERC cascade impactor sample will be used for this study. Four particle size ranges will be measured to determine the particle density. The desired ranges are nine to ten microns, three to four microns, one to 0.8 microns, and $\leq$0.5 microns. Assuming the particles falling in this region equal 100 percent, the approximate percent in each range will be calculated.

3) Surface Particle Composition and Concentration by Size--Three size ranges of particulates from each PERC and UTSI* total particulate sample plus three sizes from the PERC cascade impactor sample will be analyzed for the aforementioned trace and major elements. Two particles of approximately the same size will be chosen from each range for analysis to aid in determining particle surface chemical homogeneity. Desired ranges for the total particulate samples are nine to ten microns, three to four microns, and one to 0.8 microns. For the cascade impactor sample, the desired ranges are three to four microns, one to 0.8 microns, and $\leq$0.5 microns. Determination of the limits of detection may be possible only for certain trace elements.

4) Bulk Particle Composition and Concentration by Size--This allows a comparison of bulk versus surface trace and major element composition and concentration. Bulk trace and major element analyses should be performed on the same samples (PERC and UTSI)* and in the same particle ranges as in 3 above. Two TRW condensed gas stream samples (one potassium-seeded and the other non-seeded) of any size also will be measured for the previously mentioned trace and major elements.

Milestones for MSU's subcontract include the following:

Development of Methods of Analysis	
Begin	November 1, 1977
Finish	March 31, 1978
Arrival of PERC Samples	December 22, 1977
Arrival of UTSI and TRW Samples	January 23, 1978
Analysis Period	
Begin	December 22, 1977
Finish	March 15, 1978

*This assumes that sufficient samples are available.

Reports

1st Interim	January 15, 1978
2nd Interim	March 1, 1978
Final	April 15, 1978

2. Trips

Due to the high temperatures in MHD exhaust streams, new and innovative sampling and measurement techniques may be needed to provide better samples.

Ensuring that analytical techniques will give good experimental data also is necessary. Representatives from MERDI visited several organizations in these areas of research. A brief discussion of the information obtained is presented in the following sections.

a. Thompson, Rama, Woolridge, Incorporated (TRW)

TRW has been selected as one of the sampling sites for the trace element study, and MERDI personnel toured and discussed the MHD combustor facility. TRW has achieved three successes in their combustor development: 1) temperatures above 4000°F, 2) slag rejection of 70 percent in the combustor, and 3) significant carbon burn out.

In situ methods of temperature and velocity measurements in the MHD combustor and channel are being investigated by TRW; however, no significant achievements have been accomplished to date. Water-cooled probes have been somewhat successful in high-temperature sampling.

TRW would like a proposal to develop a sampling train after the combustor and before the quench. Trace-element emission studies then could buy dedicated time to perform experiments.

b. Spectron Development Laboratories, Incorporated

Spectron's interest and expertise is in the development of laser measurement techniques and instrumentation. Laser anemometery is used to measure velocity, particle size, and number density. In situ measurement of gas composition is in the development stages. The feasibility of laser measurements in MHD emission work needs to be assessed.

c. Montana State University (MSU)

MSU has a subcontract with MERDI to examine intraparticle compositions. A representative from MERDI visited MSU to assess capabilities for particle analysis. The scanning electron microscope (SEM) with an X-ray fluorescence attachment will be used as the main analytical tool in determining size and physical characteristics and giving qualitative chemical analysis. Proton-induced X-ray analysis (PIX) will be used for bulk chemical analysis. Delivery of the scanning auger microprobe will be delayed for six months. Lack of funding for the quadrupole system eliminates the secondary ion mass spectrometry (SIMS) from consideration during this contract period.

d. Northern Testing Laboratory

Northern Testing Laboratory at Billings, Montana was visited to assess its analytical capabilities. The laboratory presently is performing coal, slag, and fly ash trace and major element analyses plus particle sizing studies for several area companies (Decker Coal Company, The Montana Power Company--Colstrip, and Burlington Northern Energy and Minerals Department).

D. Work Forecast

1. Subtask A

Gathering of computer programs, including data files where applicable, to analyze MHD process emissions will continue. Process effects on the composition and concentration of emissions, particularly trace elements and submicron particles, will be identified.

2. Subtask B

Programs obtained in Subtask A will continue to be expanded and modified to evaluate potential emissions from the CDIF.

3. Subtask C

Data collected from UTSI, PERC, and TRW will be analyzed for trace element and particle characterization by the University of Missouri at Rolla (Environmental Trace Substances Research Center) and Montana State University. Development of new analytical techniques will be encouraged with application of these techniques to CDIF and ETF a primary goal.

IV. CONCLUSIONS

Characterization of trace element profiles from small MHD plants and development of computer models enable the anticipation of future difficulties at an early enough stage to prevent costly and time-consuming changes in major MHD facilities. Therefore, it is important to the overall environmental engineering program to provide predictive initial information through the use of the available small-scale MHD facilities presently in operation. The analyses of samples to be collected at these facilities will 1) allow development of new analytical techniques, 2) allow assessment of emission profiles, and 3) offer material with which to evaluate presently developed computer models.

Socioeconomic Impact Study of the MHD CDIF Project in Butte, Montana

Thomas H. Pelletier

ABSTRACT

The Component Development and Integration Facility (CDIF), a 50 MW_t coal-fired, open-cycle MHD facility, currently is under construction in the Industrial Park at Butte, Montana.

In assessing the environmental impacts of the CDIF, it is necessary to analyze the social and economic impact on the community of Butte. It is our objective to identify, monitor, and appraise the socioeconomic conditions of a community affected by a large-scale application of high technology. This project includes the evaluation of the socioeconomic impact during three phases of project evolution.

MERDI scheduling corresponds to the construction schedule submitted by Kaiser Engineers of Oakland, California--the CDIF construction contractors.

Phase I	Pre-construction Baseline Data	6/1/77 -10/1/77
Phase II	Construction Phase	10/1/77 - 1/1/79
Phase III	Post-construction Operation	10/1/77 - 8/1/79

I. OBJECTIVE AND SCOPE OF WORK

This project will monitor the socioeconomic impacts of an advanced technology project on an economically depressed community during three phases of construction. Additionally, the study will provide detailed information which will be useful in determining the socioeconomic impact of other potential MHD facilities on a Montana community.

Phase II of the project coincides with the construction of the CDIF and encompasses the following tasks:

A. Complete and refine the economic profile which began in Phase I,

B. Administer a construction worker profile which will gather and present data concerning the construction worker's characteristics,

C. Develop and administer a community studies survey which will determine the social acceptability of the community toward MHD developments in and around the Butte area,

D. Determine the direct economic impacts of the CDIF construction, and

E. Determine the indirect impacts of the CDIF construction.

II. SUMMARY OF PROGRESS TO DATE

Phase I of the project, the pre-construction baseline data, has been assembled and includes the following tasks:

A. The Community Profile

1. An up-to-date demographic picture of Butte describing existing circumstances of the community

2. The physical and social infrastructure of the Butte-Silver Bow urban area

3. The economic baseline of the Butte-Silver Bow urban area

B. The Construction Project Profile

1. The Component Development and Integration Facility (CDIF) specifications report

2. The direct site improvement of the CDIF

3. The CDIF construction schedule.

The pre-construction baseline information accumulation and assessment phase of this three-phase project was initiated on June 1, 1977. It has been necessary to gather the baseline data in order to monitor and assess changes and impacts on the Butte-Silver Bow area as they relate to the CDIF construction.

Phase II, the construction phase of the project, will monitor and assess direct and indirect impacts of the construction of the CDIF on the Butte-Silver Bow area.

Phase II was initiated on October 1, 1977 and has involved completing and refining the economic profile. A questionnaire has been developed, and a time frame has been established for the construction worker profile. The revised scope of work and a report entitled Procedures for Socioeconomic Monitoring have been completed.

III. DETAILED DESCRIPTION OF TECHNICAL PROGRESS

A detailed description of the technical progress of Phase I, pre-construction baseline data, has been presented in the annual report of Task S_3--Socioeconomic Impact Study of the MHD-CDIF Project in Butte, Montana which is included under the title MHD Power Generation Research, Development, and Engineering. A detailed description of Phase II is presented in the following sections.

A. Economic Profile

To carry out the proposed assessment satisfactorily, it is imperative to refine the Phase 1 economic profile of Butte-Silver Bow.

The economic profile is made up of two main sections: employment and income. The employment data will be presented both by occupation and by industry as far as can be determined. The unemployment situation will be analyzed as it relates to the occupation areas affected. Information obtained in the Butte household survey, done by Dr. Paul Miller of the University of Montana Sociology Department, will further explain the extent of under-utilized human resources in the study area.

The income data will be disaggregated by source. Labor income will be broken down by industrial sector. Per capita personal income, gross annual income, net annual income, household income, and fixed income data will be presented by census tracts and fire districts. Census tracts have been established by the U.S. Bureau of Census for the city of Butte. Fire districts have been established by the county and the local citizens in order to provide fire protection for those areas not covered by the city of Butte operations. The fire districts have become definite areas of political, social, cultural, and economic distinction. The economic profile also will include pertinent information on the mining industry, agriculture, wholesale and retail activity, welfare, and taxation. It is important to include these various economic indicators because they are capable of describing certain aspects of the community.

Further analysis of the economic profile will take place to accurately assess the MHD CDIF impacts. The economic profile is of primary importance to the validity of this study. Therefore, it has been necessary to continue to monitor and analyze the economic data available for Butte-Silver Bow. There are many factors that are worth evaluating which Phase I did not address completely. Further evaluation of the economic profile has been continuing in order to provide the clear, complete picture that is vitally necessary to the success of this study.

In addition to the economic profile, the following tasks are being pursued and will continue through the next quarter. Phase II of this project is expected to coincide with the CDIF construction, with an estimated completion date of January 1, 1979.

B. Construction Worker Profile

The project survey will consist of distributing and collecting short self-administered questionnaires to construction workers at the CDIF site. This questionnaire will be administered three times (once in mid-February, again in mid-July, and again in late November) in order to take into account the maximum and minimum construction force.

The survey will gather data on the construction workers' characteristics: former and present residences, family and housing situations, and occupations. The completed survey will present assimilated data that describes the construction worker profile.

This profile is modeled after the Construction Worker Profile for the Old West Regional Commission, 1975. On the next page is a sample of the questionnaire to be used.

C. Community Studies Survey

The community survey is being developed and defined. The purpose of this survey is to determine the attitudinal impacts of the Butte-Silver Bow community toward the MHD CDIF and related activities. An attempt will be made to observe individual and group responses to the construction phase impacts. Responses also will be observed in relation to the overall MHD CDIF impacts on the community. The survey will determine the social acceptability of the community toward MHD developments in and around Butte.

Additional information concerning the institutions and groups established in the Butte area, due to the MHD CDIF, directly and indirectly will be included and described. These groups include MERDI, the National Center for Appropriate Technology, Department of Energy, and Kaiser Engineers. They owe their existence in Butte to the MHD developments and must be included in order to completely understand the impacts.

D. Direct Economic Impact of CDIF Construction

The construction cost budget shall be determined in this phase. Information will be compiled on employment and income levels of both construction and operations personnel associated with the CDIF. Information will be obtained on payroll and major purchases of CDIF materials in the local area.

Data will be collected directly from project planners, engineers, contractors, and subcontractors.

E. Indirect Impact of CDIF Construction

Monitoring and assessing the indirect impact of the CDIF is being analyzed. Some areas of concern include the service sector, local contractors, the demand on existing infrastructure, and the introduction into the community of other industries because of MHD. A multiplier will be used to determine the impacts on the community. Additional developments in this study area will be identified and assessed as they relate to the MHD CDIF.

Sample questionnaire

1. What is your occupation (job title)?_____

2. What is your local place of residence?_____
(town or place)

(NOTE: Your local place of residence is the place from which you commute daily to your job and may not be your permanent address or the address at which your family is located).

3. In what kind of housing unit do you live at your local place of residence? (circle one)

single family housing | apartment or townhouse | mobile home | travel trailer or camper | sleeping room

4. a. Is this where you lived before you started working on this project? (Circle one) YES NO

b. If no, where did you live previously?_____
town state

5. When did you first start working on this project?_____
month year

6. a. During the six weeks prior to the time you began work on this project, were you unemployed at any time? (circle one) YES NO

b. If yes, for about how many work days were you unemployed during the six week period?_____
days

7. What is your age?_____years

8. What is your marital status? (circle one) MARRIED SINGLE

WIDOWED SEPARATED DIVORCED

IF YOU DO NOT HAVE A WIFE OR CHILDREN, PLEASE DO NOT ANSWER ANY FURTHER QUESTIONS. THANK YOU.

9. a. If you do have a wife and/or children, do they live with you at the local place of residence indicated in question 2 above? (circle one) YES NO

b. If no, where do your wife and/or children live?_____
town state

10. How many children age 18 or under do you have?_____children

Thank you very much for your cooperation.

Sample questionnaire

1. What is your occupation (job title)?_____

2. What is your local place of residence?_____

(NOTE: Your local place of residence is the place from which you commute daily to your job and may not be your permanent address or the address at which your family is located).

3. In what kind of housing unit do you live at your local place of residence? (circle one)

single family housing | apartment or townhouse | mobile home or camper | travel trailer | sleeping room

4. a. Is this where you lived before you started working on this project? (Circle one) YES NO

b. If no, where did you live previously?_____

5. When did you first start working on this project?_____

6. a. During the six weeks prior to the time you began work on this project, were you employed at any time? (circle one) YES NO

b. If yes, for about how many work days were you employed during the six week period?_____

7. What is your age?_____years

8. What is your marital status? (circle one) MARRIED SINGLE

IF YOU DO NOT HAVE A WIFE OR CHILDREN, PLEASE DO NOT ANSWER ANY FURTHER QUESTIONS. THANK YOU.

9 a. If you do have a wife and/or children, do they live with you at the local place of residence indicated in question 2 above? (circle one) YES NO

b. _____

10. How many children age 18 or under do you have?_____

Thank you very much for your cooperation.

IV. CONCLUSIONS

In monitoring and assessing the socioeconomic impacts of the MHD CDIF on Butte-Silver Bow, there are many factors to take into consideration. The pre-construction baseline data (Phase I) has been assembled and presented. It is very important to establish accurate and complete pre-operational baseline data to properly assess the socioeconomic impacts. The completion of the economic profile is vitally important to the reliability of the baseline data and, therefore, must be accomplished satisfactorily.

The development in Butte-Silver Bow of the MHD CDIF has indicated a positive effect on the local economy. In the areas of employment and economic stimulus, the MHD CDIF and related activities have assumed an increasingly important role in the local community.

After careful examination of the baseline data, including the demographic picture, physical and social infrastructure, and the economic profile of the community, it is apparent that the urban growth typical of other Montana cities has not occurred in Butte. A major reason for this appears to be due to the decline in mining activity in the area.

The unstable condition of Butte's economy reflects its dependency on the unstable conditions of the copper mining industry. Traditionally, employment and economic conditions fluctuate in relation to mining activity. Butte is in a process of industrial and economic diversification, which is highly important to the future of the area. Diversification of the economic base is needed to provide stability and opportunity for growth and progress. The MHD CDIF and related activities have been contributing to that diversification and shall continue to contribute.

There are more new businesses located in the study area in 1977 than in the previous years. In 1975, there were 90 new businesses; in 1976, there were 134 new businesses; and in seven months of 1977 (January through July), there were 119 new businesses according to the Montana Department of Labor. Population appears to be stablizing and perhaps even increasing after many years of decline, which (in turn) will affect all areas of the local social and economic conditions.

This study is designed to identify and assess the direct and indirect impacts, both negative and positive, of the MHD CDIF upon the Butte-Silver Bow area. To properly identify the direct and indirect impacts of the CDIF construction, it was necessary first to assess the study area without the CDIF development. The investigation and analysis of the baseline data presents the information and trends, over a period of time, for Butte-Silver Bow although changes in the information and trends cannot be attributed automatically to CDIF developments. The changes and impacts must be dealt with separately and individually with direct and indirect causes being presented and analyzed. Therefore, a close watch must be kept on mining activity and other influential factors of the community that also have significant impacts.

The construction worker profile and the community studies survey will aid in identifying the impacts of the CDIF. It is necessary to find out exactly how many local and non-local workers are employed on the CDIF, and the characteristics of the labor force that are pertinent to the community. It also is important to find out the attitudes and ideas of the citizens of the community in order to understand how the MHD CDIF and related activities affects the people of the Butte-Silver Bow area.

DIVISION OF MAGNETOHYDRODYNAMICS

MONTHLY PROJECT MANAGEMENT STATUS REPORT

REPORT DATE December 31, 1977

FOSSIL ENERGY

CONTRACT/PROJECT		SCHEDULE
CDIF Project Management Support and Related MHD Dev. Efforts		BASE SUPPORT - SUPPORT SERVICES
CONTRACT NO.	**VENDOR**	CDIF
EF-77-C-01-2524-3	MERDI	

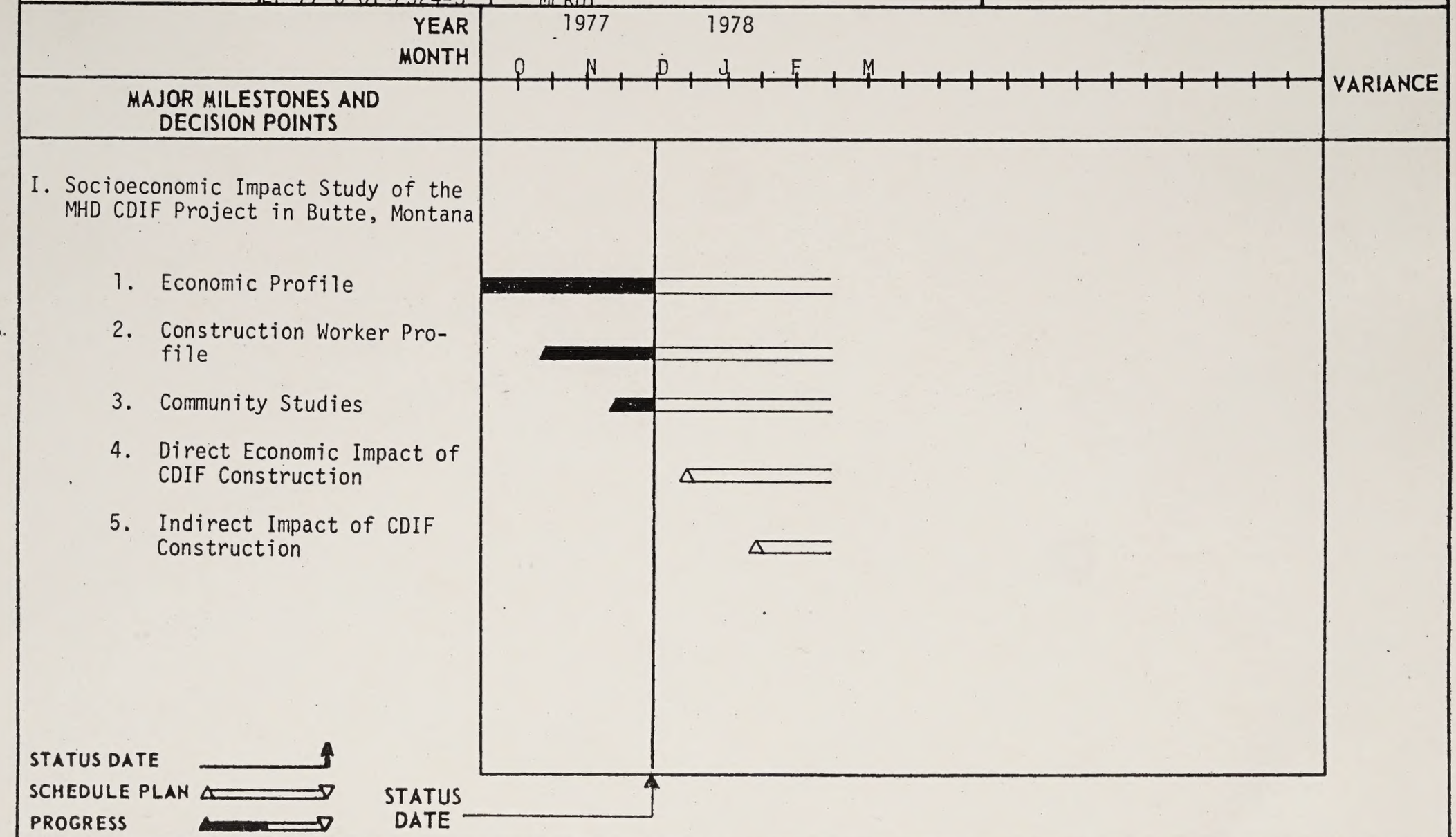

ADMINISTRATIVELY CONFIDENTIAL

VARIANCE OR PROBLEM FLAG IN RIGHT COLUMN ◇1